Stable Isotope Fractionations of Chlorinated Ethenes Associated with Physical Processes

by

Fatemeh Vakili

A thesis
presented to the University of Waterloo
in fulfillment of the
thesis requirement for the degree of
Doctor of Philosophy
in
Earth Sciences

Waterloo, Ontario, Canada, 2017

Examining Committee Membership

The following served on the Examining Committee for this thesis. The decision of the Examining Committee is by majority vote.

External Examiner	NAME: Dr. Richelle Allen-King Title: Professor
Supervisor(s)	NAME: Dr. Walter Illman, Dr. Orfan Shouakar-Stash Title: Professor, Adjunct Professor
Internal Member	NAME: Dr. Shaun Frape, Dr. Edward Sudicky Title: Professor, Professor
Internal-external Member	NAME: Dr. William Annable Title: Associate Professor

AUTHOR'S DECLARATION

I hereby declare that I am the sole author of this thesis. This is a true copy of the thesis, including any required final revisions, as accepted by my examiners.

I understand that my thesis may be made electronically available to the public.

Abstract

Chlorinated ethenes are the widespread source of groundwater contamination, which mostly originate from industrial and dry-cleaning facilities. Since chlorinated ethenes are denser than water, they sink below the water table if spilled in large quantities and accumulate on top of low-permeability zones and bedrocks. In the subsurface, these contaminants undergo different processes such as advection, dispersion, diffusion, sorption and biodegradation. The knowledge of the processes affecting the movement of contaminant plume is beneficial to develop efficient remediation strategies. During the last two decades, compound-specific isotope analysis (CSIA) has become a powerful tool in identifying contamination sources and mechanism affecting the fate and transport of contaminants. There is a general acceptance that only transformation processes (i.e. degradation) contribute to stable isotope fractionation of organic compounds, while physical processes such as dissolution, volatilization, sorption, and diffusion have negligible effects on stable isotope fractionation. Most of the studies on the effect of physical processes on stable isotope fractionation of chlorinated ethenes have focused on stable carbon isotopes. In this study, controlled laboratory batch and column experiments were performed using different materials to evaluate the effect of sorption, desorption, diffusion, and back-diffusion on C, Cl, and H isotope fractionation of TCE and *cis*-DCE under static and dynamic conditions.

The shift in H isotope fractionation during sorption batch experiments were significant and toward depletion of heavy isotopologues in the aqueous phase which was a counterintuitive phenomenon. The enrichment factors (ε_H) estimated for the sorption batch experiments were in the range of +32 ± 2.7 ‰ and +149 ± 31 ‰. Chlorine isotope data showed small enrichment in the aqueous phase. The enrichment factors (ε_{Cl}) estimated for the sorption batch experiments ranged between -0.2 ± 0.06 ‰ and -0.8 ± 0.11 ‰ which were very small compared with the reported enrichment factors due to transformation processes. Carbon isotope results showed that sorption had a very small effect on isotope fractionation, which can be neglected when compared with isotope fractionations due to degradation process. The results from column experiments showed that sorption and desorption have a small effect on C and Cl isotope ratios of TCE even in the presence of a strong sorbent such as granular activated carbon (GAC). The isotope fractionations can be neglected compared with the ones during transformation processes. However, the shift in H isotope ratios was significant and showed a maximum isotope separation (Δ^2H) of -360 ‰ by the end of the experiment.

As for the diffusion batch experiment, chlorine isotope separation of TCE and *cis*-DCE was observable and H isotope separation was significant. The H isotope separation ranged between -35 ‰ and -286 ‰. The Cl isotope separation ranged between -0.28 ‰ and -1.33 ‰. Results from the diffusion box experiment also showed significant H isotope separation of TCE and *cis*-DCE and observable chlorine isotope separation. The results from the current study showed that the effect of physical processes such as sorption, diffusion, and back-diffusion on H isotope fractionation of TCE and *cis*-DCE was significant. The reported value for H isotope fractionation of TCE due to biodegradation was small compared to H isotope fractionation values obtained in this study for physical processes. Therefore, compound-specific hydrogen isotope analysis is a promising tool to identify physical processes that affect the movement of chlorinated ethenes in the subsurface. Chlorine and carbon isotope fractionations due to physical processes were small compared with the isotope fractionations due to biodegradation.

Acknowledgements

I would like to express my sincere appreciation to my supervisors Dr. Orfan Shouakar-Stash and Dr. Walter Illman for their invaluable guidance and support throughout my doctoral study. My gratitude is extended to my committee, Dr. Shaun Frape, Dr. Ramon Aravena, and Dr. Ed Sudicky for their constructive feedback and guidance. I acknowledge my external examiners, Dr. Richelle Allen-King and Dr. William Annable for their time to review my thesis.

This thesis would not have been completed without the support of Isotope Tracer Technologies Inc. (IT^2). I am grateful to Dr. Orfan Shouakar-Stash, Mirna Stas, and Bob Drimmie for allowing me to use their lab equipment and supplies to analyze enormous number of samples. I would also like to thank Joanna Niemi for her contribution to this work. She provided assistance in performing the column experiments and analyzing the VOC samples. I have conducted part of my experiments at the Environmental Isotopes Lab (EIL) at the University of Waterloo. Throughout my PhD work, I had constructive discussions with Dr. Jordi Palau, Christopher Neville, Jeff Roberts, and Dr. Steven Berg. Their time and useful comments are much appreciated. I would like to thank the EIL staff especially Oya Albak, Humam El-Magammar, and Rhys Gwynne for their technical expertise. I would also like to thank Wayne Noble and Shirley Chatten for analyzing my VOC samples.

Thanks to all my fellow students and friends at the University of Waterloo who made my student life a great experience. In particular, I would like to thank Negar Ghahramani, Orin Regier, Justin Clark, Rubaiat Sharmeen, Mike Makahnouk, Elahe Talaei, Mahsa Shayan, Mona Mojdeh, and Rana Tehrani Yekta. Thanks to my amazing roommates Maddy Rosamond and Geertje Pronk for their friendship and support.

Lastly, I would like to convey my deepest gratitude to my parents for their unconditional love and support throughout my life. Dad, it hurts to think that you are not here anymore, but my love for you will live forever. I thank my sisters and brothers who are always there to support me. I am grateful beyond words to my sister, Tahereh, and her love, Farhad, for the encouragement and generous support during the journey of writing my dissertation.

Dedication

To my parents

Table of Contents

List of Figures

List of Tables

Chapter 1
Introduction

1.1 Background

Chlorinated solvents are prevalent and persistent groundwater contaminants that mostly arise from industrial contamination (Squillace, et al. 1999). Chlorinated solvents have lower viscosity and higher density than water (known as Dense Non-Aqueous Phase Liquids, DNAPL) and once released into the subsurface, they migrate through the vadose zone and move below the water table and accumulate on top of the low hydraulic conductivity zones and create the source of contamination. Part of the DNAPL source is dissolved in groundwater, transported through advection and dispersion (Freeze and Cherry. 1979) and creates a contaminant plume in the aquifer. Furthermore, some of the DNAPL source diffuses into the low hydraulic conductivity zones and act as secondary sources of contamination. Once the contaminant concentration in the aquifer is decreased, previously diffused contaminants diffuse back into the groundwater flow. The contaminant plume also undergoes transformation processes such as biotic and abiotic degradation; and phase transfer processes such as sorption that cause the retardation of the contaminant plume.

The application of stable isotopes as a source verification tool was established by pioneering studies (vanWarmerdam, et al. 1995; Beneteau, et al. 1999), which reported that chlorinated solvents from different manufacturing plants have characteristic isotopic signatures. These exciting findings encouraged researchers to successfully utilize compound-specific isotope analysis (CSIA) to trace contaminants back to their sources (Palau, et al. 2014; Hunkeler, et al. 2011b; Schmidt, et al. 2004; Hunkeler, et al. 2004; Jendrzejewski, et al. 2001). In the subsurface, there are other processes such as degradation, sorption, diffusion, and volatilization that might cause isotopic fractionations. Nonetheless, the fact that various processes can cause isotopic fractionations does not totally eliminate the usefulness of CSIA as a source determination tool in the presence of those processes. Thorough understanding of the isotopic behaviors associated with various processes enables the user to utilize CSIA as a fingerprinting tool, since the isotopic shifts are typically predictable and characteristic of individual processes. Therefore, it is highly important to establish a comprehensive knowledge of isotopic behaviors associated with different processes in order to better assess contaminant plumes.

During the last two decades, a vast number of studies conducted on the effect of transformation processes such as biotic and abiotic degradation on stable isotopes of chlorinated ethenes. Table 1-1

summarizes the experiments on degradation of trichloroethene (TCE) and *cis*-dichloroethene (*cis*-DCE) and estimated enrichment factors (ε). As can be seen from the table, most of the studies focused on carbon stable isotope fractionation of TCE and *cis*-DCE and a few data are available on chlorine and hydrogen isotopes fractionation.

The effect of phase transfer processes such as vaporization, dissolution, and sorption on stable isotopes fractionation of different organic compounds was also examined by several researchers. For example, Huang, et al. 1999, evaluated the effect of evaporation on carbon and chlorine isotopic fractionation of trichloroethene and dichloromethane at room temperature (24 ± 1°C). Their results showed that the vapor phase became depleted in chlorine isotopes with respect to the liquid phase, while it became enriched in carbon isotopes. The enrichment factors obtained from the experimental results were +0.31‰ for carbon and -1.82‰ for chlorine in TCE. Poulson and Drever. 1999 studied carbon, chlorine, and hydrogen stable isotopes fractionation of trichloroethylene during progressive evaporation at room temperature (22 ± 2°C). Their experimental results yielded enrichment factors of ε_C = +0.24 ‰ and ε_{Cl} = -1.64 ‰ for carbon and chlorine isotopes of TCE, respectively, which are similar to the enrichment factors obtained by Huang, et al. 1999. Hydrogen isotopes results showed a slight enrichment in vapor phase similar to carbon isotope results (ε_H = +8.9 ‰). Moreover, Jeannottat and Hunkeler. 2012 investigated carbon and chlorine isotopes fractionation of TCE during NAPL – vapor equilibration, air – water partitioning, and diffusive transport. Their results for NAPL – vapor equilibration experiments showed an inverse carbon isotope fractionation, which is in agreement with studies by Poulson and Drever, 1999, and Huang, et al. 1999. The authors reported a negligible carbon isotope fractionation (ε_C = +1.0 ± 0.05 ‰) and a significant chlorine isotope fractionation (ε_{Cl} = -1.39 ± 0.06 ‰) during diffusion-controlled vaporization experiment.

The behavior of carbon and chlorine ratios of chlorinated ethenes during the diffusion of the contaminant vapor through a thick unsaturated sandy layer was studied by Hunkeler, et al. 2011. Their results indicated that carbon and chlorine isotopic signatures of chlorinated ethenes remained constant during the migration of vapor phase through the unsaturated zone. Jin, et al. 2014, conducted laboratory experiments using gel diffusion tubes to investigate the diffusive hydrogen isotope fractionation of toluene and ethylbenzene, and chlorine isotope fractionation of TCE and *cis*-DCE. Their results revealed a significant isotope fractionation for the examined organic compounds. Wanner and Hunkeler. 2015 investigated carbon and chlorine isotope fractionation of TCE and 1,2-

dichloroethane (1,2-DCA) during diffusion in aqueous phase and reported small isotope fractionations.

In general, previous studies have concluded that dissolution and sorption mechanisms do not change the carbon stable isotope signature of chlorinated ethenes. For example, Hunkeler, et al. 2004, investigated the effect of dissolution on carbon stable isotopes of TCE and PCE through laboratory and field experiments and reported that negligible carbon isotope fractionation occurred during dissolution. Slater, et al. 2000, examined stable carbon isotope fractionation during the equilibrium sorption of PCE, TCE, benzene, and toluene onto graphite and activated carbon. These authors conducted several sorption batch experiments over a sorption range of 10 to 90 percent and concluded that sorption does not alter the carbon isotopic signature of the contaminants. Schuth, et al. 2003, studied the effect of sorption on carbon isotope ratios of chlorinated ethenes (TCE, *cis*-DCE, VC), and carbon and hydrogen isotopes of BTEX compounds (benzene, toluene, and p-xylene) onto carbonaceous minerals (lignite and activated carbon). They also reported that sorption does not affect the isotopic ratios of the aforementioned VOCs. Kopinke, et al. 2005, performed multi-step batch experiments and chromatographic experiments to investigate carbon isotope fractionation of benzene, toluene, 2,4-dimethylphenol, and o-xylene due to sorption to humic acids. They estimated enrichment factors of ε_C = 0.44 ‰ for benzene and ε_C = 0.6 ‰ for toluene from the multi-step batch experiments; and ε_C = 0.17 ‰ for benzene, ε_C = 0.35 ‰ for 2,4-dimethlphenol, and ε_C = 0.92 ‰ for o-xylene from chromatographic experiments. Furthermore, Imfeld, et al. 2014, performed multi-step batch experiments using different sorbents to assess carbon and hydrogen isotope fractionations of benzene and toluene. Their results showed that consecutive sorption steps in an aquifer had a negligible effect on isotope fractionations of benzene and toluene. Poulson, et al. 1997, estimated K_{oc} values of deuterated benzene, toluene, and ethylbenzene through an HPLC experiment and reported that the deuterated compounds have lower K_{oc} values compare to the non-deuterated compounds. Therefore, they indicate that the heavy isotopologues have a lower retardation factor. Carbon isotope fractionation of benzene and toluene due to adsorption in HPLC columns was also examined by Harrington, et al. 1999, and was reported to be negligible. They also examined the effect of vaporization on carbon isotopes of BTEX and found a small positive isotope fractionation similar to those reported by other studies Poulson and Drever. 1999; Huang, et al. 1999.

The current study focuses on assessing the behavior of chlorine and hydrogen stable isotopes of TCE and *cis*-DCE during sorption, desorption, diffusion, and back-diffusion processes as most of the previous studies focused on carbon isotopes. To our knowledge, Cl and H isotope fractionation of chlorinated solvents during physical processes has not been fully investigated to date. In addition, there are a limited data available on Cl and H isotopes of chlorinated solvents during biodegradation of chlorinated solvents.

Table 1-1 Overview of enrichment factors during abiotic and biotic degradation processes

Compound	Experiment	ε_C (‰)	ε_{Cl} (‰)	ε_H (‰)	Reference
TCE, PCE	Equilibrium Sorption on Graphite and Activated Carbon	<±0.5	-	-	(Slater, et al. 2000)
TCE, *cis*-DCE, VC	Equilibrium Sorption on Lignite, Lignite coke, and Activated Carbon	<±0.5	-	-	(Schuth, et al. 2003b)
TCE	Reductive dechlorination (Anaerobic, Pinellas culture)	-7.1	-	-	(Lollar, et al. 1999a)
TCE	Reductive dechlorination (Anaerobic, KB-1 culture)	-2.5 -6.6	-	-	(Bloom, et al. 2000a)
TCE	Reductive dechlorination (Anaerobic, KB-1 culture)	-14.3 -13.4 -13.9 -15.2	-	-	(Slater, et al. 2001)
TCE	Reductive dechlorination (Anaerobic, Dehalococcoides ethenogenes 195)	-9.6	-	-	(Lee, et al. 2007)
TCE	Reductive dechlorination (Anaerobic, Sulfurospirillum multivorans)	-16.4	-	-	(Lee, et al. 2007)
TCE	Reductive dechlorination (Anaerobic, Dehalobacterrestrictus PER-K23)	-3.3	-	-	(Lee, et al. 2007)
TCE	Reductive dechlorination (Anaerobic, Dehalococcoides-containing enrichment culture ANAS)	-16	-	-	(Lee, et al. 2007)
TCE	Reductive dechlorination (Anaerobic, Sulfurospirillum halorespirans)	-18.5	-	-	(Cichocka, et al. 2007)
TCE	Reductive dechlorination (Anaerobic, Sulfurospirillum multivorans)	-18.4	-	-	(Cichocka, et al. 2007)
TCE	Reductive dechlorination (Anaerobic, Desulfitobacterium sp. PCE-S)	-12.1	-	-	(Cichocka, et al. 2007)
TCE	Reductive dechlorination (Anaerobic, Geobacterlovleyi SZ)	-8.4	-	-	(Cichocka, et al. 2008)

TCE	Reductive dechlorination (Anaerobic, Dehalobacter restrictus PER-K23)	-3.3	-	-	(Cichocka, et al. 2008)
TCE	Reductive dechlorination (Anaerobic, Dehalococcoides ethenogenes 195)	-13.5	-	-	(Cichocka, et al. 2008)
TCE	Reductive dechlorination (Anaerobic, Geobacter lovleyi strain SZ)	-12.2	-3.6	-	(Cretnik, et al. 2013)
TCE	Reductive dechlorination (Anaerobic, Desulfitobacterium hafniense Y5)	-9.1	-2.7	-	(Cretnik, et al. 2013)
TCE	Reductive dechlorination (Anaerobic, Bio-Dechlor Inoculum culture)	-16.4	-3.6	+34	(Kuder, et al. 2013)
TCE	Reduction by cyanocobalamin (Abiotic)	-16.1	-4	-	(Cretnik, et al. 2013)
TCE	Reduction by cobaloxime (Abiotic)	-21.3	-3.5	-	(Cretnik, et al. 2013)
TCE	Oxidation by permanganate (Abiotic)	-25.1 -26.8	-	-	(Hunkeler, et al. 2003)
TCE	Oxidation (Aerobic, Burkholderiacepacia G4)	-18.2	-	-	(Barth, et al. 2002)
TCE	Cometabolic oxidation (Aerobic, Methylosinus trichosporium OB3b)	-1.1	-	-	(Chu, et al. 2004)
TCE	Reduction by cyanocobalamin (Abiotic)	-15.2	-	-	(Nijenhuis, et al. 2005)
TCE	Oxidation by permanganate (Abiotic)	-21.4	-	-	(Poulson and Naraoka. 2002)
TCE	Dechlorination by Fe(0) (Abiotic)	-8.6	-	-	(Dayan, et al. 1999)
TCE	Dechlorination by Fe(0) (Abiotic)	-10.1	-	-	(Schuth, et al. 2003a)
TCE	Dechlorination by Peerless iron (Abiotic)	-13.9 -13.0	-	-	(VanStone, et al. 2004)
cis-DCE	Reductive dechlorination (Anaerobic, KB-1 culture)	-14.1 -16.1	-	-	(Bloom, et al. 2000a)
cis-DCE	Reductive dechlorination (Anaerobic, lab microcosm)	-19.2	-	-	(Hunkeler, et al. 2002)
cis-DCE	Reductive dechlorination (Anaerobic, KB-1 culture)	-21.9 -25.5 -18.8 -18.9	-	-	(Slater, et al. 2001)
cis-DCE	Reductive dechlorination(Anaerobic, Dehalococcoidesethenogenes 195)	-21.1	-	-	(Lee, et al. 2007)
cis-DCE	Reductive dechlorination (Anaerobic, Dehalococcoides sp. BAV1)	-21.9 -25.5 -18.8 -18.9	-	-	(Slater, et al. 2001)

cis-DCE	Reductive dechlorination (Anaerobic, Dehalococcoides-containing enrichment culture ANAS)	-29.7	-	-	(Lee, et al. 2007)
cis-DCE	Aerobic, enrichment culture, 12 – 14 °C	-9.8	-	-	(Tiehm, et al. 2008)
cis-DCE	Aerobic, enrichment culture, 22 – 24 °C	-8.8 -7.1 -8.2	-	-	(Tiehm, et al. 2008)
cis-DCE	Oxidation (Aerobic, β-Proteobacterium JS666)	-8.5	-0.3		(Abe, et al. 2009)
cis-DCE	Reductive dechlorination (Anaerobic KB-1 culture)	-18.5	-1.5		(Abe, et al. 2009)
cis-DCE	Reductive dechlorination (Anaerobic, Bio-Dechlor Inoculum culture)	-26.8	-1.7		(Kuder, et al. 2013)
cis-DCE	Oxidation by permangenate	-21.1	-	-	(Poulson and Naraoka. 2002)
cis-DCE	Dechlorination by Fe(0) (Abiotic)	-14.4	-	-	(Dayan, et al. 1999)
cis-DCE	Dechlorination by Peerless iron (Abiotic)	-15.9 -16.0	-	-	(VanStone, et al. 2004)
cis-DCE	Dechlorination by Connelly iron (Abiotic)	-11.9 -6.9	-	-	(VanStone, et al. 2004)

1.2 Research Objectives

The aim of this research is to investigate the evolution of Cl and H isotopic ratios for:

- Sorption of TCE and *cis*-DCE under static conditions (laboratory batch experiments)
- Sorption and desorption of TCE under dynamic conditions (laboratory column experiments)
- Back-diffusion of TCE and *cis*-DCE from a low permeability zone (laboratory batch experiments)
- Diffusion and back-diffusion of TCE and *cis*-DCE in a simulated aquifer-aquitard system (laboratory box experiment)

The stable isotope results from this research can help to identify the processes that chlorinated ethenes undergo in the subsurface. Once the processes affecting the contaminant plumes are identified, appropriate remediation techniques can be applied to the contaminated field sites.

1.3 Thesis Scope

This thesis is organized in four chapters. Chapter 1 provides the literature review on stable isotope fractionations during various processes that organic contaminants undergo in the subsurface. Chapter 2 includes the sorption experiments and chapter 3 includes the diffusion and back-diffusion experiment. Chapter 4 summarizes the major conclusions and discusses potential future work.

To evaluate the effect of sorption on Cl and H stable isotope fractionation of TCE and *cis*-DCE, a series of controlled batch and column experiments were conducted using different materials with different amounts of organic carbon content. Materials used for the batch experiments include shale, dolostone, and a mixture of Borden sand and granular activated carbon (GAC). Materials used for the column experiments include US Ottawa silica sand, Borden sand, and a mixture of Borden sand and GAC. Aqueous samples were collected from the experiments and were submitted to the Environmental Isotope Lab (EIL) of the University of Waterloo, Waterloo, Ontario, Canada and Isotope Tracer Technologies Inc. (IT^2), Waterloo, ON, Canada for C, Cl, and H isotope analyses. The majority of chlorine and all of the hydrogen stable analyses were conducted at IT^2.

Isotope fractionations of TCE and *cis*-DCE during back-diffusion process were investigated by performing a series of controlled laboratory batch experiments using different materials including shale and dolostone. The behavior of stable isotopes of TCE and *cis*-DCE during diffusion and back-diffusion processes was investigated through a laboratory box experiment over a period of 23 months. For this study, a thin layer of sand, resembling an aquifer, was placed between two layers of kaolin clay, resembling overlying and underlying aquitards. The collected aqueous samples were analyzed for H and Cl stable isotope ratios at IT^2.

Chapter 2

The Effect of Sorption on Stable Isotopes of TCE and *cis*-DCE

2.1 Introduction

As DNAPLs such as chlorinated solvents sink under the water table and accumulate on top of low conductivity zones, contaminant plumes are transported in the aquifer throughout various processes such as advection, dispersion and diffusion. Although these processes play a large role in determining the shape and size of a plume, additional processes such as sorption and degradation can also control the shape and size of a plume by slowing down the velocity of the solutes (Schwartz and Zhang. 2003).

The identification of trichloroethene (TCE) and its degradation products as possible carcinogens (Yeh and Kastenberg. 1991) had led the scientific community to focus on developing tools that can aid in better determining and characterizing the contamination sources as well as understanding the fate of these contaminants in the subsurface in order to develop best remediation strategies. During the last decade, compound-specific isotope analysis (CSIA) has emerged as one of the most useful techniques in fingerprinting organic contaminant sources (Hunkeler, et al. 2011c; Hunkeler, et al. 2004; Blessing, et al. 2009) as well as understanding the transformation mechanisms (i.e. biotic and abiotic degradation) of these contaminants in the subsurface (Hunkeler, et al. 1999; Lollar, et al. 1999a; Lollar, et al. 2001; Slater, et al. 2001; Barth, et al. 2002; Poulson and Naraoka. 2002; Vieth, et al. 2003; VanStone, et al. 2004; Chartrand, et al. 2005; Elsner, et al. 2005; Hirschorn, et al. 2007; Elsner, et al. 2007; Elsner, et al. 2010; Cichocka, et al. 2008; Abe, et al. 2009; Fletcher, et al. 2011; Hunkeler, et al. 2011a; Lojkasek-Lima, et al. 2012; Wiegert, et al. 2012; Cretnik, et al. 2013; Schmidt, et al. 2004; Liu, et al. 2014).

There is a general acceptance that small isotopic fractionation occurs during phase transfer processes such as sorption (Hunkeler, et al. 2004; Harrington, et al. 1999; Schuth, et al. 2003b; Slater, et al. 2000) and can be neglected when compared to uncertainties of the current analytical methodologies.

The main objective of this study is to evaluate the effects of sorption and desorption on chlorine, carbon, and hydrogen stable isotopic ratios of TCE and *cis*-DCE under static and dynamic situations.

These investigations were conducted by carrying out a series of controlled laboratory batch and column experiments that will be explained in the next section.

2.2 Method and Materials

2.2.1 Laboratory Batch Experiments

Laboratory batch experiments have been performed using different materials including shale from the Rochester Formation (Smithville, ON), dolostone from the Eramosa Formation (Smithville, ON), and a mixture of Borden sand and granular activated carbon (GAC). The GAC was purchased from Alfa Aesar, A Johnson Matthey Company, Ward Hill, MA, USA. Samples of the shale, dolostone, and Borden sand were submitted to Agriculture and Food Laboratory of University of Guelph, Guelph, Ontario, Canada, for organic carbon analysis. Organic carbon content of the shale, dolostone, and Borden sand are measured to be 0.6 % dry, 0.4 % dry, and 0.038 % dry, respectively. Based on the study by Langer, et al. 1999, stylolites that are present in the fractures of dolostone are responsible for sorption of TCE. Stylolites form under pressure dissolution and contain high organic carbon content. Organic matter and other insoluble phases are removed from carbonates when they are under high pressure, concentrate in the fractures, and form stylolites. The batch experiments with shale and dolostone were conducted to examine isotope fractionation of TCE and *cis*-DCE during a single-step sorption process. Control vials were prepared using the same bottles and filled with the solution without the sorbents to quantify VOC losses through the septa caps. The batch experiment with Borden sand and GAC mixture was conducted to investigate isotope fractionation of TCE during both sorption and desorption processes.

For shale and dolostone batch experiments, the rocks were ground using Planetary Ball Mill Pulverisette 5 (Fritsch manufacturer). 120±1 g of ground rock was poured into a 250 mL screw-cap amber glass bottle and then filled with TCE/*cis*-DCE solution (aqueous concentration of 2 mg/L) without head space (Figure 2-1). The batch experiments with TCE and cis-DCE were conducted individually. One bottle was dedicated for each sampling time and liquid samples were collected for VOC concentration as well as isotope analyses during a 60-day period. In total four sets of bottles were prepared which contained shale and TCE, shale and cis-DCE, dolostone and TCE, and dolostone and cis-DCE. After preparing all the bottles, they were wrapped in bubble wrap and were placed on a rotary shaker until the sampling time arrived. Two more sets of batch experiments were conducted

using the same procedure described above and the same materials (ground shale and dolostone), but at a higher TCE concentration of ~ 11 mg/L to investigate the behavior of stable isotopes at different concentrations.

For Borden sand and GAC batch experiments, 187 ± 0.5g of Borden sand and 0.48 ± 0.01g of GAC were mixed and poured into a 250 mL screw-cap amber glass bottle to make a medium with 0.2 % dry (by weight) activated carbon. The bottles were filled with TCE solution (aqueous concentration of 270 mg/L) without headspace and capped with PTFE-lined septa. Bottles were shaken by hand every day. The sorption part of the experiment took place in eight days and liquid samples were collected for VOC and isotope analysis during that time period. A bottle was sacrificed for each sampling time. For the desorption part, all the liquid in the last bottle that was used for the sorption part of the experiment was removed as much as possible and the bottle was filled with ultra-pure water. For the desorption part, we followed the procedure described in OECD Guidelines for the Testing of Chemicals: Adsorption-desorption using a Batch Equilibrium Method (2000). However, we did not centrifuge the bottles prior to removing the liquid since the glass bottles were not safe for centrifuging. The collected liquid samples were analyzed for C, Cl, and H isotope analysis at Isotope Tracer Technologies Inc. (IT^2), Waterloo, Ontario, Canada.

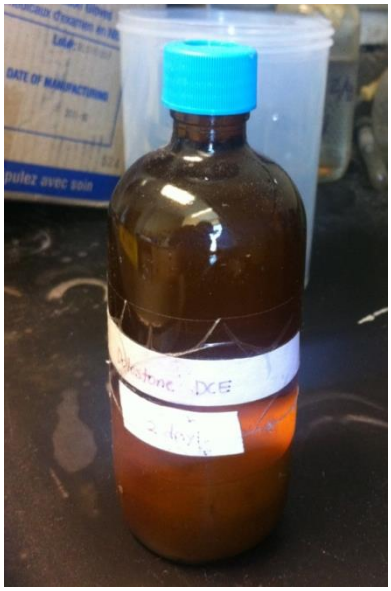

Figure 2-1 A sample of bottle prepared for sorption batch experiment

2.2.2 Laboratory Column Experiments

The sorption of TCE depends on the amount of the organic carbon (f_{oc}) that is present in the soil (Karickhoff, et al. 1979; Schwarzenbach and Westall. 1981; Allen-King, et al. 1997). Therefore, three column experiments using different media with different organic carbon content were performed to investigate the stable isotope fractionation of TCE during sorption and desorption processes. The first column (C2) contained commercially sieved silica sand (20/30). A sample of the sand was sent to Agriculture and Food Laboratory at the University of Guelph, Guelph, Ontario, Canada for organic carbon analysis. The total carbon (inorganic + organic carbon) was <0.5% dry; hence, the organic carbon content is very low. The second column (C3) consisted of Borden sand (fine-to medium-grained sand) with an average organic carbon content of 0.038% dry (Agriculture and Food Laboratory, University of Guelph, Guelph, Ontario, Canada). The third column (C6) contained a mixture of Borden sand and 1% (by volume) granular activated carbon (GAC). The organic carbon content for column C6 was calculated to be 0.28 % dry.

The C2 and C3 columns were constructed of Plexiglas which is resistant to TCE at low concentrations, and C6 column was constructed of stainless steel which is resistant to TCE at high concentrations. The Plexiglas columns had a diameter of 5 cm and a length of 50 cm. The stainless steel column had a diameter of 10.3 cm and a length of 15.4 cm. Sampling ports were placed vertically along the column with 2.54 cm intervals. In order to sample the column at the center, 16 gauge airtight needles were placed into the column halfway through nylon Swagelok fittings that were installed on the columns wall (Figure 2-2). The needles were filled with silica fibre which acted as a filter.

The physical properties of the columns were calculated by measuring the mass of the columns in three steps: 1) mass of the empty column; 2) mass of the column plus dry soil; and 3) mass of the column plus saturated soil (Table 2-1). Two stainless steel screens were placed at either end of each column (1 mm and 0.2 mm mesh sizes) to contain the porous medium. All columns were flushed with CO_2 gas for 90 minutes to remove the air inside the pores. Subsequently, the columns were slowly wetted from the bottom with ultra-pure water using a peristaltic pump. Once a steady outflow rate was achieved, columns were flushed with sodium azide solution (2 g/L) for a few days to maintain abiotic conditions in the columns. Eh, pH, and dissolved oxygen (DO) of the effluent were monitored

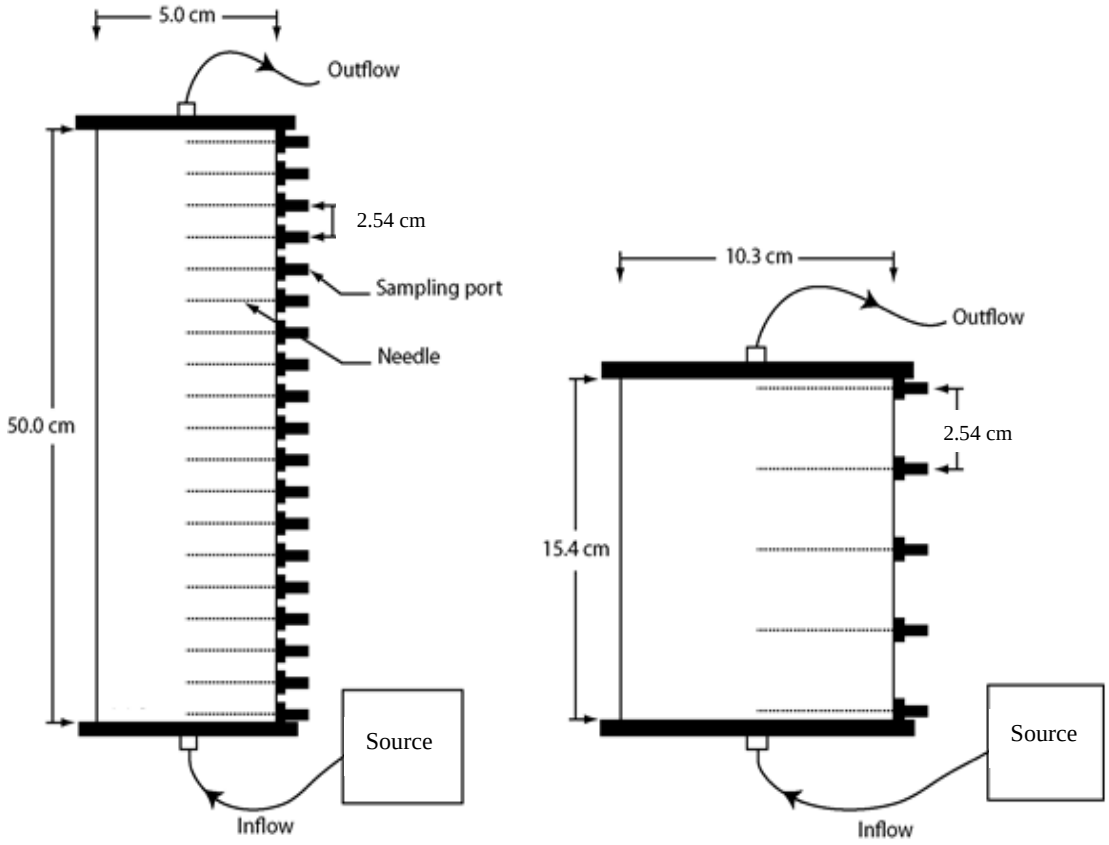

Figure 2-2 Schematic of the Plexiglas columns (C2 and C3) setup on the left, and stainless steel column (C6) setup on the right.

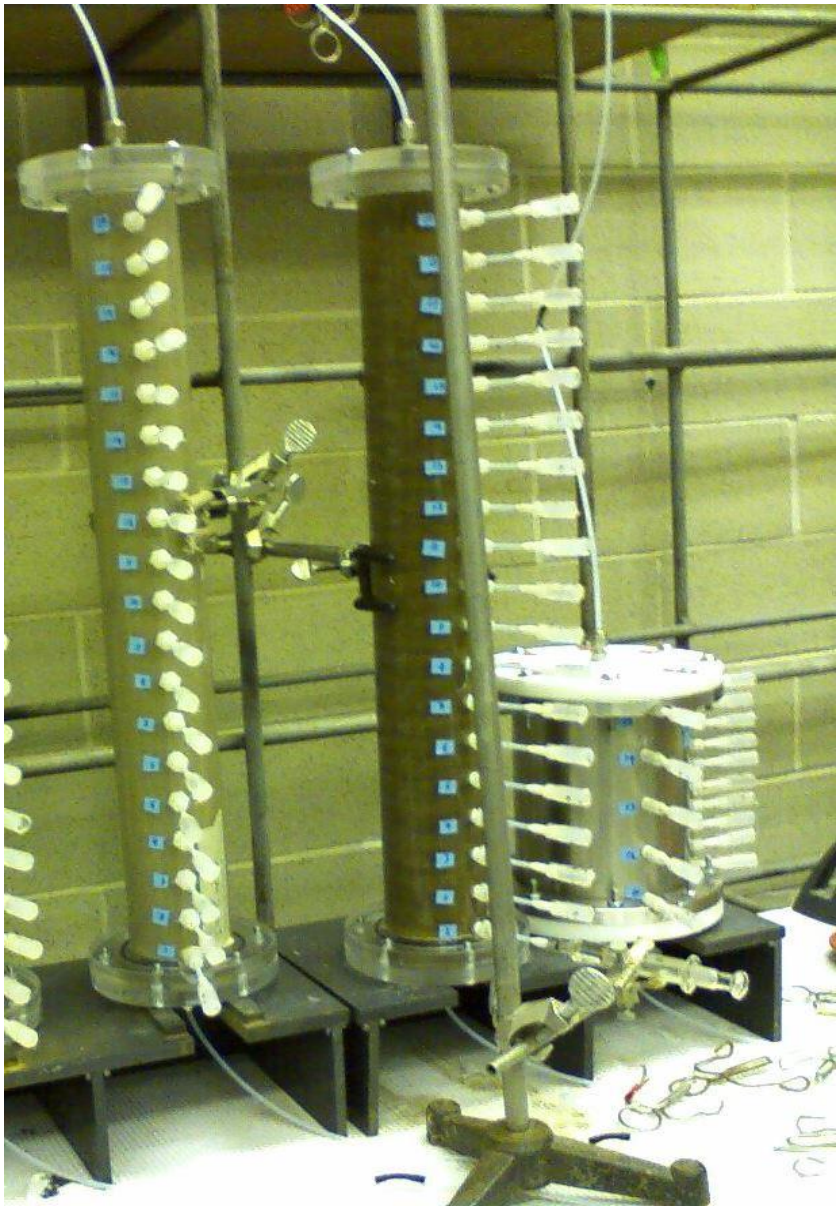

Figure 2-3 From left to right: Ottawa Sand Column (C2), Borden Sand Column (C3), and Borden Sand and GAC Column (C6); the picture shows the method of sampling using a glass syringe from port 1 of C3

to ensure that stable oxic conditions were maintained. Experiments were conducted at room temperature (22 ±1˚C).

A TCE solution was prepared at 5 mg/L for C2 and C3, and at saturation (1.1 g/L) for C6 since GAC is a strong sorbent (stainless steel was used for C6 as it is more resistant to higher concentrations of TCE). The injection solution was contained in a collapsible Teflon bag to minimize headspace. The TCE solution was injected into the columns C2 and C3 at a rate of 400 ± 20 mL/day, and into C6 at a rate of 450 ± 20 mL/day. Liquid samples were obtained from the bag and three sampling ports along the column, one near the column influent, one at the middle of the column, and the column effluent, using a glass syringe (Figure 2-3). Once TCE concentration of the effluent reached the initial TCE concentration of the source solution, the contaminant source was disconnected and ultra-pure water was injected into the columns to flush out the contaminant inside the pores and desorb the previously sorbed contaminants. Liquid samples were collected from the selected sampling ports and submitted to Environmental Isotope Laboratory (EIL) at the University of Waterloo, Waterloo, Ontario, Canada for C and Cl stable isotopes analysis. Samples collected from Borden sand and GAC column (C6) were additionally analyzed for H stable isotopes at Isotope Tracer Technologies Inc. (IT^2), Waterloo, Ontario, Canada.

Table 2-1 Physical properties of the columns

Column ID	Type of Medium	Porosity	Dry Bulk Density g/cm^3	Volume of pores (ml)
C2	Silica sand	0.385	1.77	378
C3	Borden Sand	0.395	1.76	388
C6	Borden Sand + GAC	0.336	1.77	432

2.2.3 Analytical Procedure

The analytical procedures for chemical concentration and stable isotope analyses are described in Appendix A.

2.3 Results and Discussion

Chlorine, carbon, and hydrogen isotopic ratios are reported in delta (δ) notation and calculated from:

$$\boldsymbol{\delta R_{sample}} = \left(\frac{\boldsymbol{R_{sample} - R_{reference}}}{\boldsymbol{R_{reference}}}\right) \cdot \mathbf{1000}\ ‰ \qquad 2\text{-}1$$

where R is the $^{13}C/^{12}C$-ratio, or $^{37}Cl/^{35}Cl$-ratio, or $^{2}H/^{1}H$-ratio. The reference for chlorine isotope is Standard Mean Ocean Chloride (SMOC); for hydrogen isotope is a hydrogen gas calibrated to Vienna Standard Mean Ocean Water (VSMOW); and for carbon isotopes is the international standard Vienna Pee Dee Belemnite (VPDB). The δ-values are expressed as parts per thousand or permil (‰).

For all of the experiments, the isotope results are plotted based on the isotope separation (Δ) which is the difference between the δ-values of the isotopes of the contaminant at time zero and δ-values after a certain time has elapsed. The lines labeled as "analytical uncertainty" on the plots indicate the upper and lower limits for uncertainty of the analytical methods for stable isotopes. For example, on the plots with three vertical axes of $\Delta^{2}H$, $\Delta^{37}Cl$, and $\Delta^{13}C$, the lines intercept the $\Delta^{2}H$ vertical axis at +10 and -10; the $\Delta^{37}Cl$ vertical axis at +0.1 and -0.1; the $\Delta^{13}C$ vertical axis at +0.5 and -0.5.

2.3.1 Laboratory Batch Experiments

2.3.1.1 Shale with TCE / *cis*-DCE Batch Experiment Results

The control and batch experiments for TCE and *cis*-DCE were conducted separately (four individual experiments in total); however, the concentration and isotope analyses results of TCE and *cis*-DCE for control vials are shown on the same plot. The initial concentrations of TCE and *cis*-DCE used for the experiments were 2 mg/L.

The results from the control experiments show that concentration and isotopic ratios of TCE and *cis*-DCE did not change significantly during the experiment (Figure 2-4 and Figure 2-5) indicating that no VOC loss or other processes contributing to isotope fractionation (e.g. biodegradation) was present.

The TCE concentration results from the batch experiments (Figure 2-6) revealed that concentration decreased at a relatively high rate within the first 240 hours of the experiment, and subsequently the

rate decreased around t = 240 h onward. Overall, 53% of TCE was sorbed during the experiment. The concentration results of *cis*-DCE from the batch experiments (Figure 2-8) also showed that concentration dropped rapidly within the first 24 hours followed by a slow decrease to the end of experiment. In total, 36% of *cis*-DCE was sorbed during the experiment. The concentration results from both sets of batch experiments imply that sorption of TCE and *cis*-DCE to the soil appear to be a bi-phasic process as there is an initial stage of fast sorption followed by a second stage of slow sorption.

Chlorine isotope results for shale and TCE batch experiments showed that the solution became enriched gradually in heavier isotopes and reached a maximum isotope separation ($\Delta^{37}Cl$) of 0.85 ‰ by the end of the experiment (Figure 2-7). The results for shale and *cis*-DCE batch experiment (Figure 2-9) showed that the solution became enriched in ^{37}Cl at the beginning of the experiment when the rate of sorption was rapid. The isotopic ratios shifted toward the original Cl isotopic ratios of *cis*-DCE once the rate of sorption became slow. The maximum Cl isotope separation observed for this experiment was +0.19 ‰.

Carbon isotope ratios for shale and TCE batch experiment showed a minor enrichment of ^{13}C in the solution (Figure 2-7) which was slightly above the uncertainty of the analytical method (maximum $\Delta^{13}C$=1.7 ‰).

Carbon isotope ratios for shale and *cis*-DCE experiment indicated negligible fractionation as the results were within the uncertainty of the analytical method (Figure 2-9). Other researchers have also reported negligible carbon isotope fractionation of chlorinated solvents due to sorption process (Slater, et al. 2000; Schuth, et al. 2003b). Therefore, for the rest of the experiments, only chlorine and hydrogen isotopes were analyzed. The reason behind adsorption of light isotopologues of Cl and C could be that heavy isotopologues form weaker van der Waals bonds with organic carbon (Caimi and Brenna. 1997; Kopinke, et al. 2005). Moreover, Aelion, et al. 2009, discussed that heavy isotopologues prefer to stay in the solution, since they have smaller volumes compared with their lighter counterparts (the bonds to heavy isotopes are slightly shorter).

Hydrogen isotope ratios of TCE and *cis*-DCE, however, indicated that the solution was depleted in heavier isotopes over time indicating that molecules with heavy H isotopes were adsorbed. The maximum H isotope separations of -91 ‰ and -23 ‰ were observed for TCE and *cis*-DCE, respectively, by the end of experiment. This is a counterintuitive phenomenon and might be related to

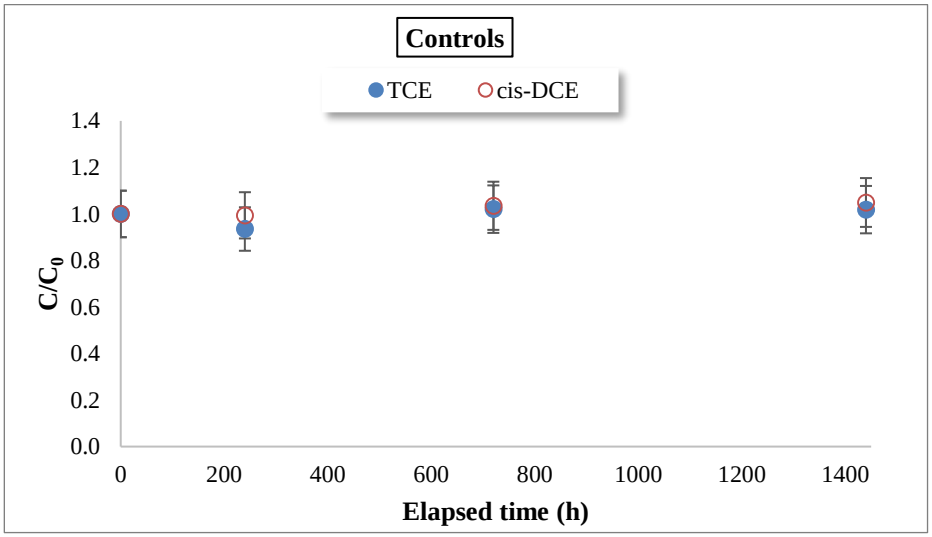

Figure 2-4 Relative concentrations of TCE and *cis*-DCE for controls; the uncertainty of the analytical method is ±10 %

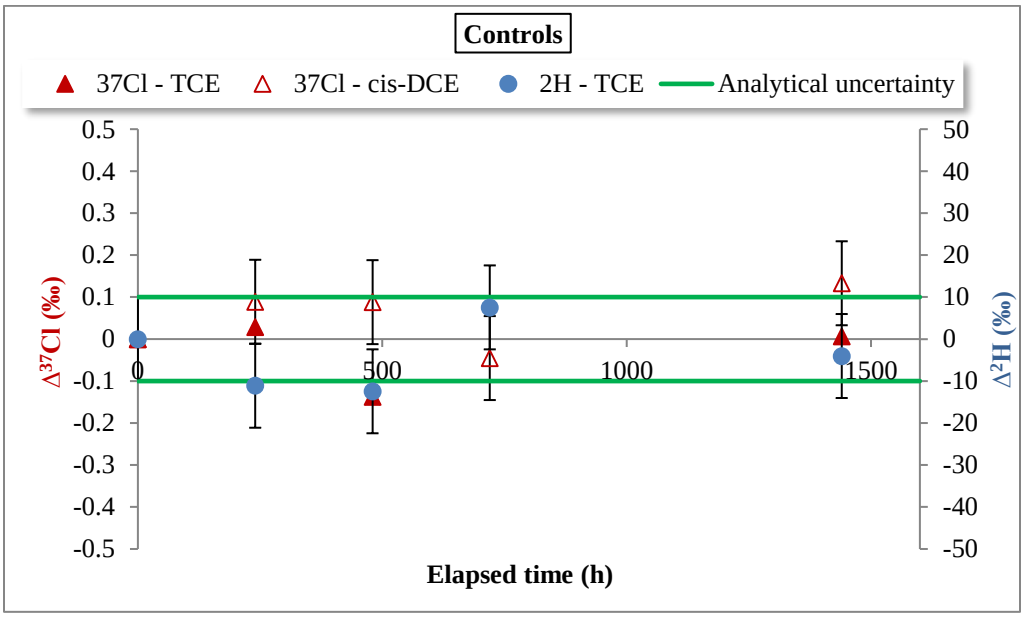

Figure 2-5 Stable chlorine and hydrogen isotope fractionations for controls; the uncertainty of the analytical methods for Cl and H isotope ratios are ±0.1 ‰ and ±10 ‰, respectively

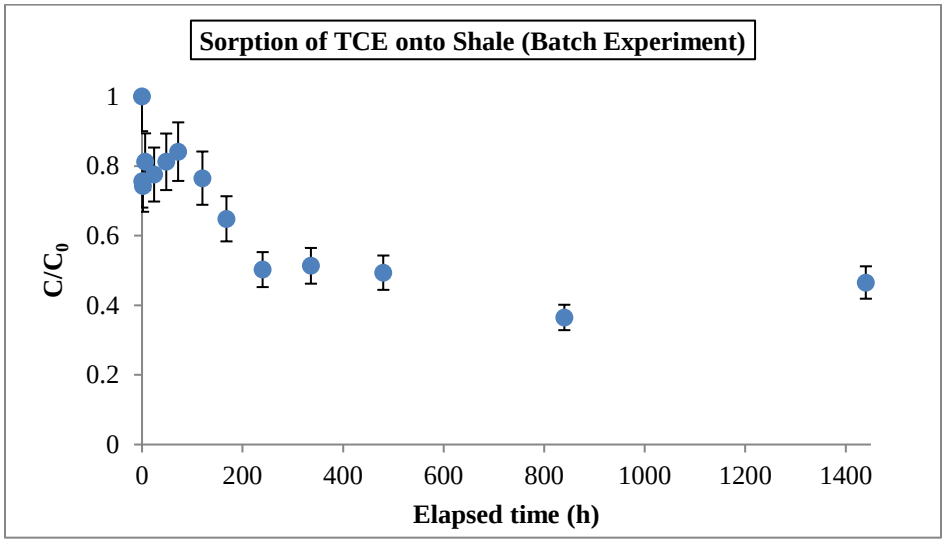

Figure 2-6 Relative concentrations of TCE for sorption batch experiments using shale; the uncertainty of the analytical method is ±10 %

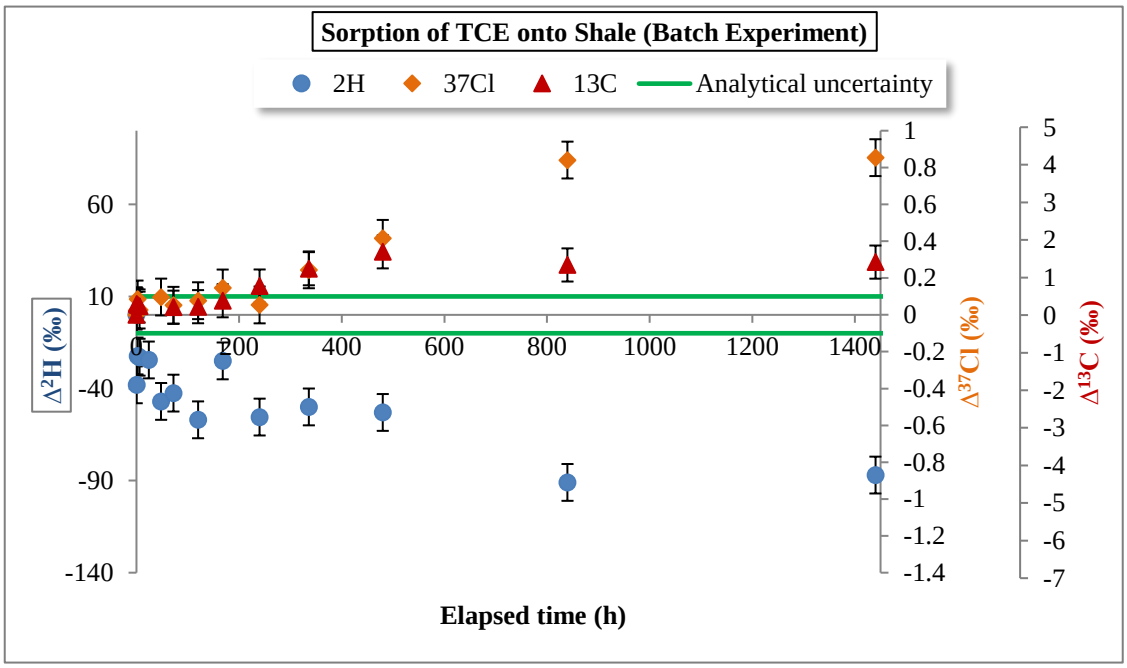

Figure 2-7 Stable carbon, chlorine and hydrogen isotope fractionations of TCE for sorption batch experiments using shale; the uncertainty of the analytical methods for C, Cl, and H isotope ratios are ±0.5 ‰, ±0.1 ‰, and ±10 ‰, respectively

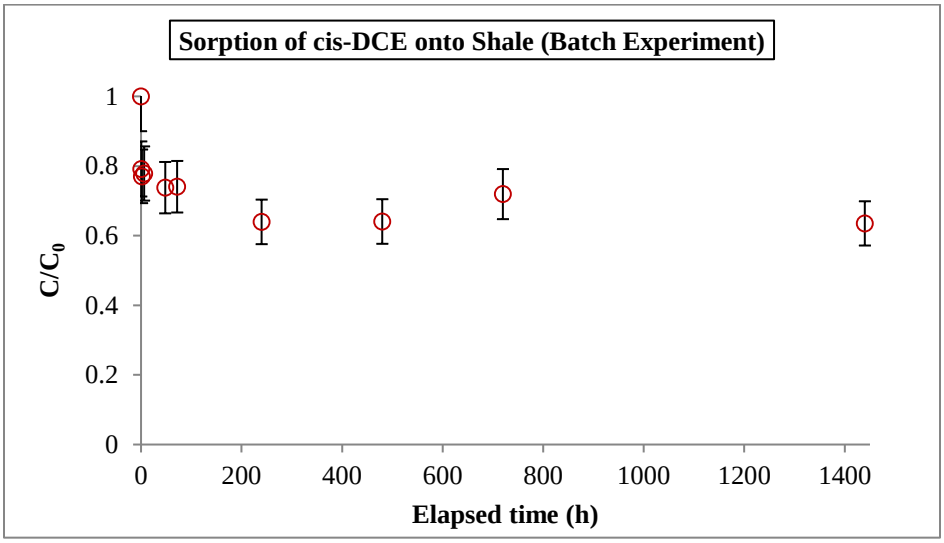

Figure 2-8 Relative concentrations of *cis*-DCE for the sorption batch experiments using shale; the uncertainty of the analytical method is ±10 %

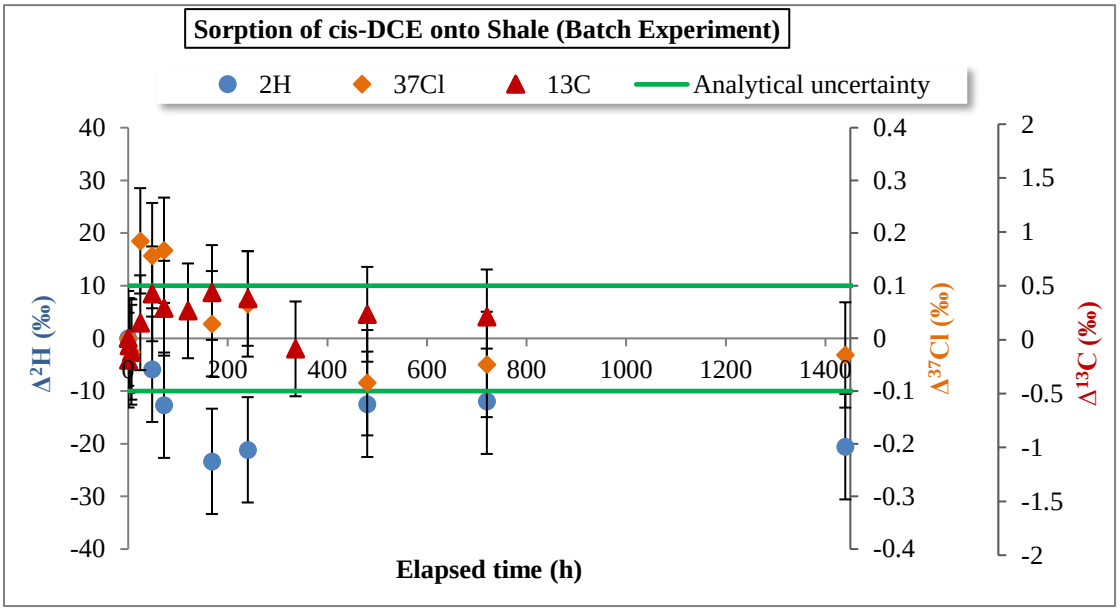

Figure 2-9 Stable carbon, chlorine, and hydrogen isotope fractionations of *cis*-DCE for the sorption batch experiment using shale; the uncertainty of the analytical methods for C, Cl, and H isotope ratios are ±0.5 ‰, ±0.1 ‰, and ±10 ‰, respectively

different vibrational energies for molecules with different isotopes (Schauble, et al. 2001; Schauble, et al. 2004; Black, et al. 2011, as well as personal communication with Dr. Tadeusz Gorecki and Dr. Marcel Nooijen, 2016, Department of Chemistry, University of Waterloo, Waterloo, Ontario, Canada). Further investigations and modeling tools using theoretical and computational chemistry are required to fully understand this behavior. Isotope modeling requires the knowledge of the exact molecular shape of the compounds and the thermodynamics of adsorption. Calculation of sorption energies for different isotopologues of chlorinated ethenes can be an interesting topic for future research.

The comparison of the concentration results of TCE and *cis*-DCE in the same media (i.e. shale; Figure 2-6 and Figure 2-8) indicated that higher amounts of TCE were sorbed (53 %) compared with *cis*-DCE (36 %). Stable isotopes results (Figure 2-7 and Figure 2-9) also showed that the isotopicseparations of *cis*-DCE is smaller than TCE. The maximum C, Cl, and H isotopic separations of TCE were 1.7 ‰, 0.85 ‰, and -91 ‰, respectively, while the separation values for *cis*-DCE were 0.44 ‰, 0.19 ‰, and -23 ‰. The reason for the lower sorption of *cis*-DCE than TCE may be due to its lower organic carbon-water partition coefficient (K_{oc}). K_{oc} values of TCE can be calculated based on their octanol-water partition coefficient (K_{ow}) values using the following equation (Schwarzenbach and Westall. 1981):

$$\boldsymbol{logK_{oc} = 0.49 + 0.72 logK_{ow}} \qquad 2\text{-}2$$

cis-DCE has a $logK_{ow}$ of 2.13, while TCE has a $logK_{ow}$ of 2.42 (Sangster. 1997). Calculated $logK_{oc}$ for *cis*-DCE is 2.024 and for TCE is 2.232. Therefore, *cis*-DCE with a lower K_{oc} value has a higher tendency to stay in solution.

2.3.1.2 Dolostone and TCE/*cis*-DCE Sorption Batch Experiments Results

Aqueous samples of TCE and *cis*-DCE from the batch experiments were analyzed for VOC concentration (Figure 2-10 and Figure 2-12); and chlorine and hydrogen isotope ratios (Figure 2-11 and Figure 2-13). Similar to the batch experiments with shale, TCE concentration results from dolostone batch experiment (Figure 2-10) showed a two-stage pattern; a first stage of fast sorption in which about 50% of TCE was adsorbed during the first 6 hours; and a second stage of slow sorption which lasted to the end of experiment. Stable isotope results of TCE (Figure 2-11) showed that the

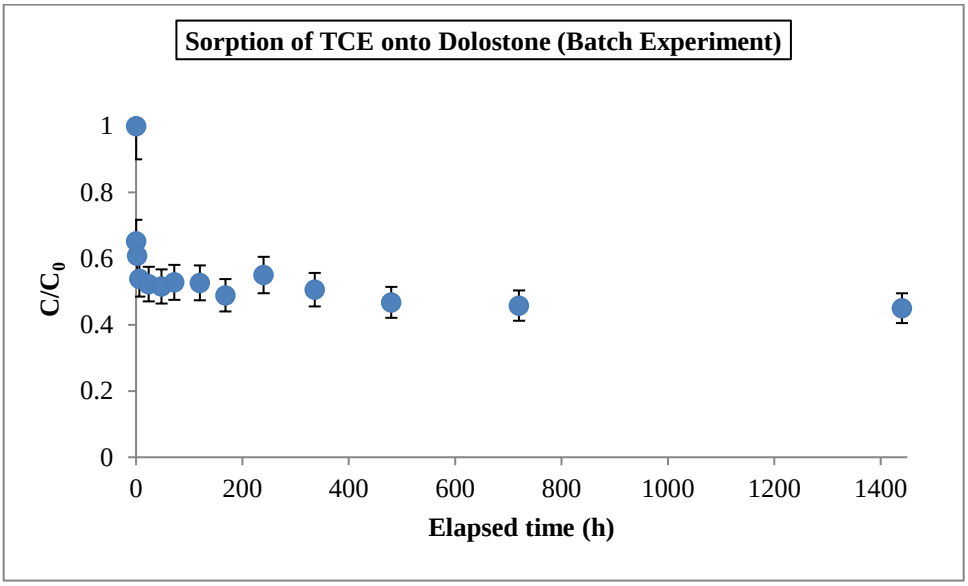

Figure 2-10 Relative concentrations of TCE and for sorption batch experiments using dolostone; the uncertainty of the analytical method is ±10 %

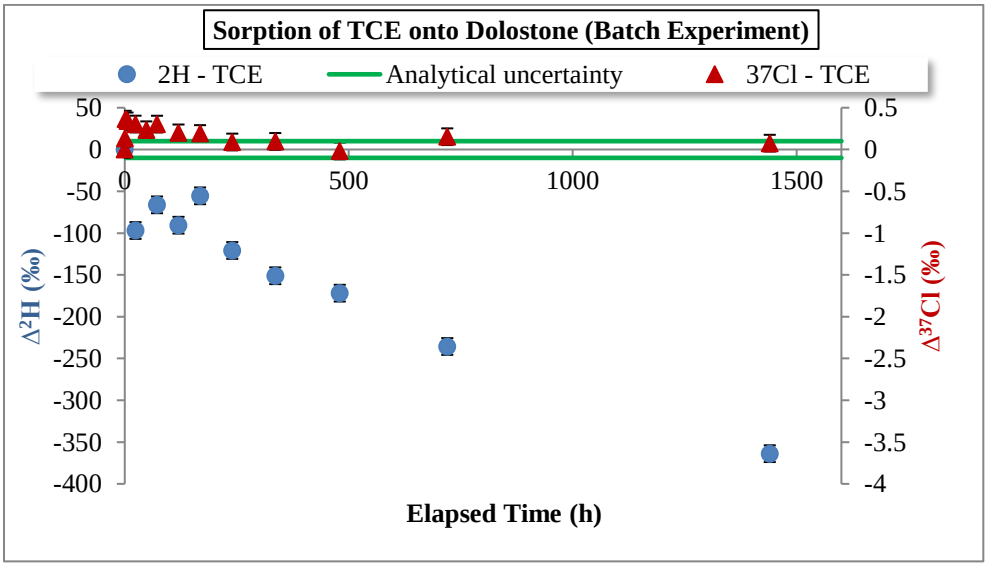

Figure 2-11 Stable hydrogen and chlorine isotope fractionations of TCE for sorption batch experiment using dolostone; the uncertainty of the analytical methods for Cl and H isotopes are ±0.1 ‰ and ±10 ‰, respectively

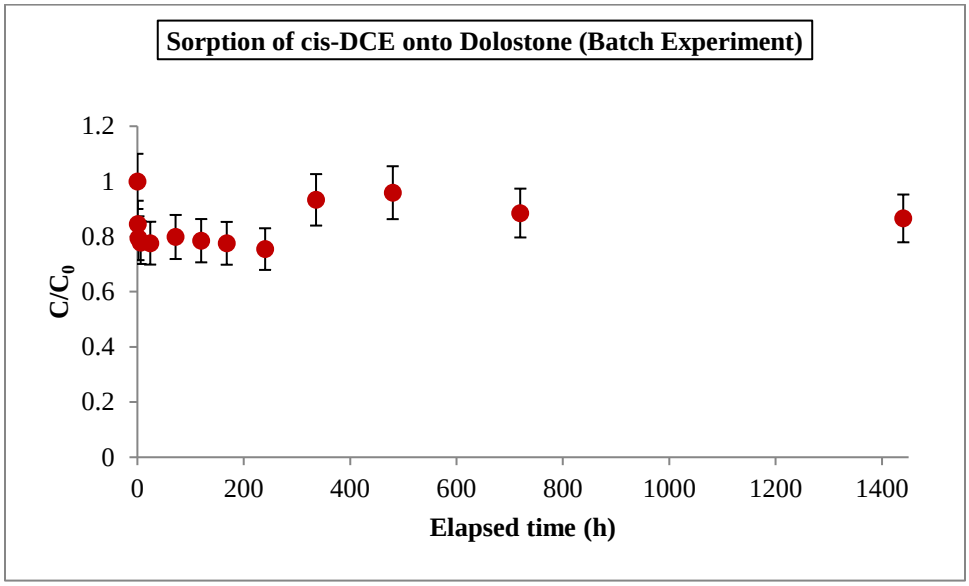

Figure 2-12 Relative concentrations of *cis*-DCE and for sorption batch experiments using dolostone; the uncertainty of the analytical method is ±10 %

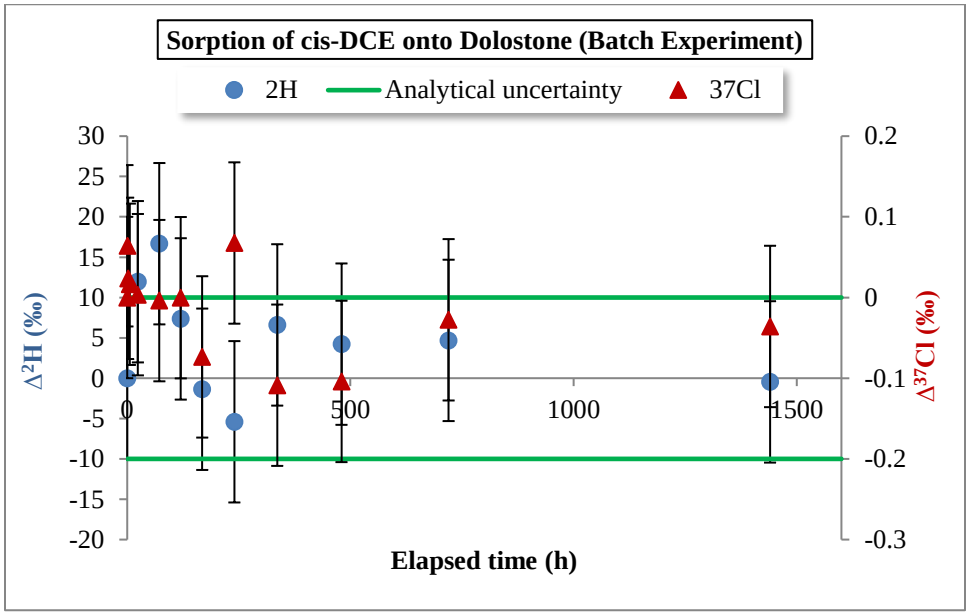

Figure 2-13 Stable hydrogen and chlorine isotope fractionations of *cis*-DCE for sorption batch experiment using dolostone; the uncertainty of the analytical methods for Cl and H isotopes are ±0.1 ‰ and ±10 ‰, respectively

solution became slightly enriched in Cl isotopes with a maximum isotopic separation ($\Delta^{37}Cl$) of +0.36 ‰ at t = 2h when the rate of sorption was high. The Cl isotope ratio of the solution started to drop and remained close to the isotopic signature of the original TCE solution during the slow stage of sorption. However, the solution became increasingly depleted in ^{2}H during the sorption experiment with a maximum isotope separation ($\Delta^{2}H$) of -364 ‰ by the end of the experiment.

The concentration results for *cis*-DCE (Figure 2-12) showed that the concentration dropped about 20% within the first 6 hours of the experiment and remained constant up to 240 hours, the aqueous concentrations started to rise after 240 hours which was an indication of desorption of previously sorbed *cis*-DCE molecules. Overall and after accounting for the uncertainty of the analytical method, the observed sorption in the system was small. The results of chlorine and hydrogen stable isotope analysis of *cis*-DCE samples (Figure 2-13) revealed that the isotopic ratios did not change throughout the experiment and remained within the uncertainty of the analytical methods (±0.1 ‰ for Cl and ±10 ‰ for H). As discussed in previous section, the reason for sorption of less amount of *cis*-DCE compared with TCE in the same media (dolostone) is the lower K_{oc} value of *cis*-DCE.

2.3.1.3 Shale/dolostone and TCE Sorption Batch Experiment Results (Higher VOC Concentration Case)

The batch experiments with shale and dolostone were repeated with a higher initial concentration of TCE (11 mg/L) to evaluate the effect of contaminant aqueous concentration on chlorine and hydrogen stable isotope ratios during sorption. A series of control bottles with TCE solution and without soil were also prepared and analyzed for TCE concentration, and Cl and H stable isotopes.

Concentration results for batch experiments with shale and dolostone (Figure 2-14 and Figure 2-16) showed a two-stage pattern of TCE sorption; a first stage of rapid sorption followed by a stage of slow sorption to the end of the experiments. Chlorine isotope results of TCE for batch experiments with shale showed that there was a slight enrichment of ^{37}Cl in the solution with a maximum $\Delta^{37}Cl$ = 0.36 ‰ during the fast stage of sorption. Hydrogen isotope results (Figure 2-15) showed a progressive significant depletion of ^{2}H in the solution and reached a maximum $\Delta^{2}H$ of -136 ‰. VOC concentrations and stable isotopes results from controls showed that there is no VOC loss in the system (Figure 2-14 to Figure 2-17).

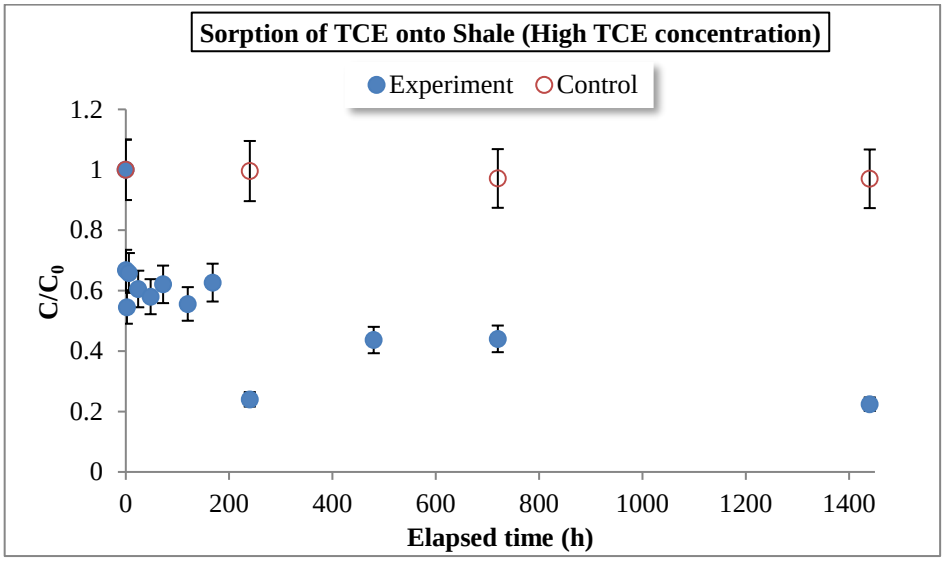

Figure 2-14 Relative concentration of TCE for controls and sorption batch experiment using shale (high TCE concentration); the uncertainty of the analytical method is ±10 %

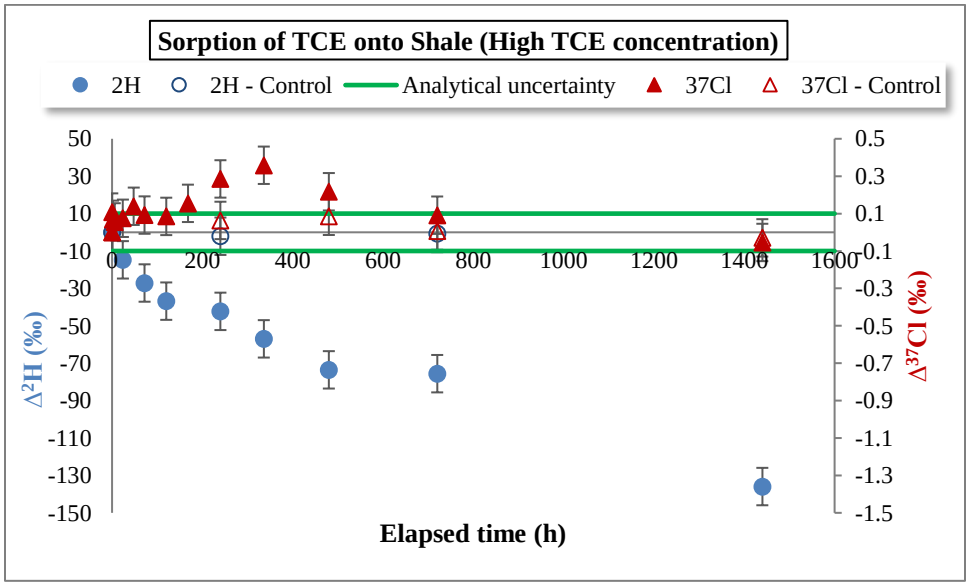

Figure 2-15 Stable hydrogen and chlorine isotope fractionations for controls and sorption batch experiment using shale (high TCE concentration); the uncertainty of the analytical methods for Cl and H isotopes are ±0.1 ‰ and ±10 ‰, respectively

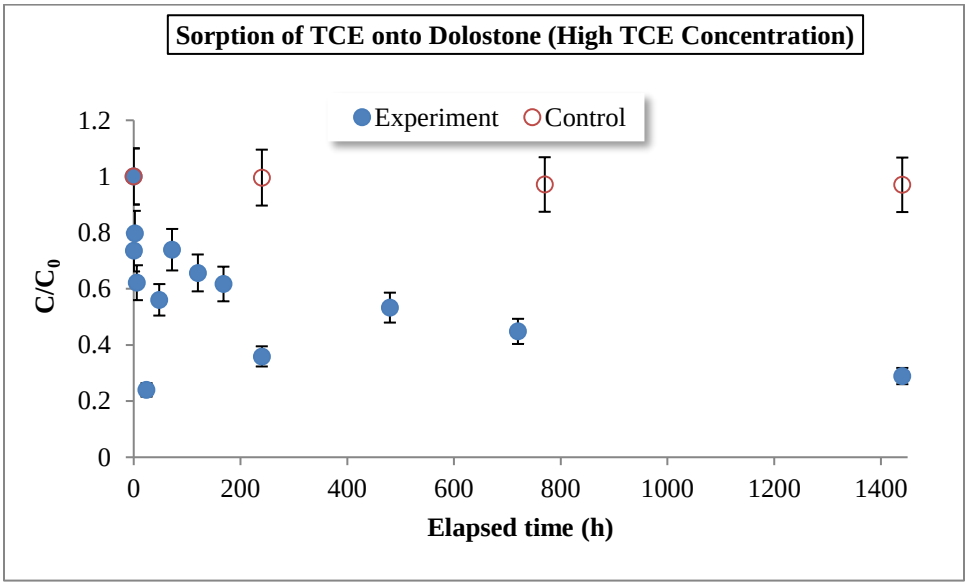

Figure 2-16 Relative concentration of TCE for controls and sorption batch experiment using dolostone (high TCE concentration); the uncertainty of the analytical method is ±10 %

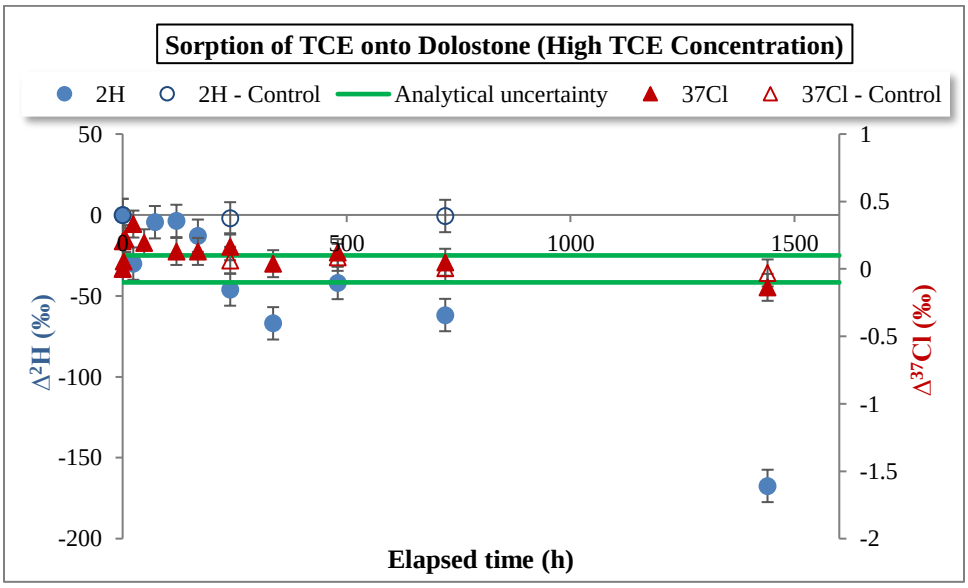

Figure 2-17 Stable chlorine and hydrogen isotope fractionations of TCE for controls and sorption batch experiment using dolostone (high TCE concentration); the uncertainty of the analytical methods for Cl and H isotopes are ±0.1 ‰ and ±10 ‰, respectively

The isotope ratios at the higher concentration of TCE showed a similar behavior as the experiments with lower TCE concentration. The isotope results from all of the TCE sorption batch experiments indicated that during the sorption of TCE, the solution became slightly enriched in ^{37}Cl and significantly depleted in ^{2}H. Also from the isotope results, it is noticeable that enrichment of Cl isotope was happening at the beginning of the experiment when the rate of sorption was rapid. At the later time through the experiment, the Cl isotope signature of the solution shifted toward the initial isotopic signature. However, H isotope ratios in the solution showed a continuous depletion throughout the experiment. This phenomenon was clearly an indication of a non-equilibrium isotopic sorption.

The results from all of the batch experiments showed similar trends for Cl and H isotopic ratios except for shale and TCE batch experiment which showed a continuous enrichment of ^{37}Cl in the solution up to t = 720 h and reached a plateau after that time. The samples from this experiment might have been defective (i.e. diffusive loss of the molecules with light isotopes during the experiment or while the samples were stored before being analyzed).

2.3.1.4 Dual Chlorine – Hydrogen Isotope Plots

In order to better illustrate the evolution of H and Cl isotopic ratios of TCE and *cis*-DCE during sorption batch experiments, the results of both isotopes of each compound were plotted on the same graph (Figure 2-18 and Figure 2-19). As seen in Figure 2-18, for all of the batch experiments (shale/dolostone and TCE with 2 mg/L and 11 mg/L concentrations, total of 4 experiments), the shift in H isotopic ratios was significantly larger than the Cl isotopic ratios considering the analytical uncertainty of ±10 ‰ for H and ±0.1 ‰ for Cl isotope analysis. The shift in Cl isotopic ratios for shale and TCE (2 mg/L) batch experiment were significantly large. As mentioned previously, this could be an indication that the samples from this experiment were defective.

Figure 2-19 shows the dual isotope plot for shale/dolostone and *cis*-DCE batch experiments. Considering the analytical uncertainty of ±10 ‰ for H and ±0.1 ‰ for Cl isotope analysis, Cl and H isotopic ratios of *cis*-DCE did not change significantly during the experiment. As we discussed earlier, *cis*-DCE concentration results from the experiments also showed that in the same media,

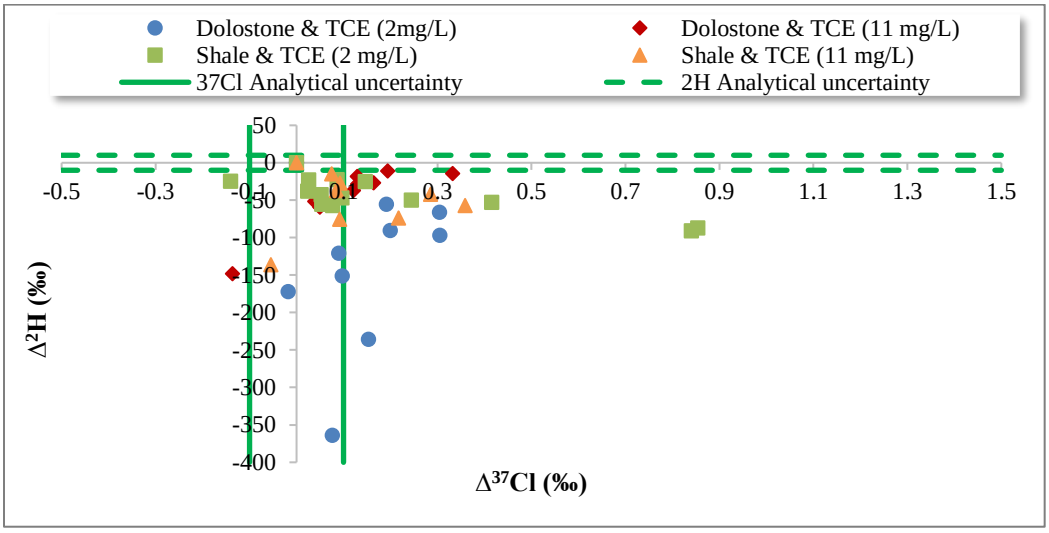

Figure 2-18 Dual isotope plot of TCE and sorption batch experiments using shale/dolostone; the uncertainty of the analytical methods for Cl and H isotopes are ±0.1 ‰ and ±10 ‰, respectively

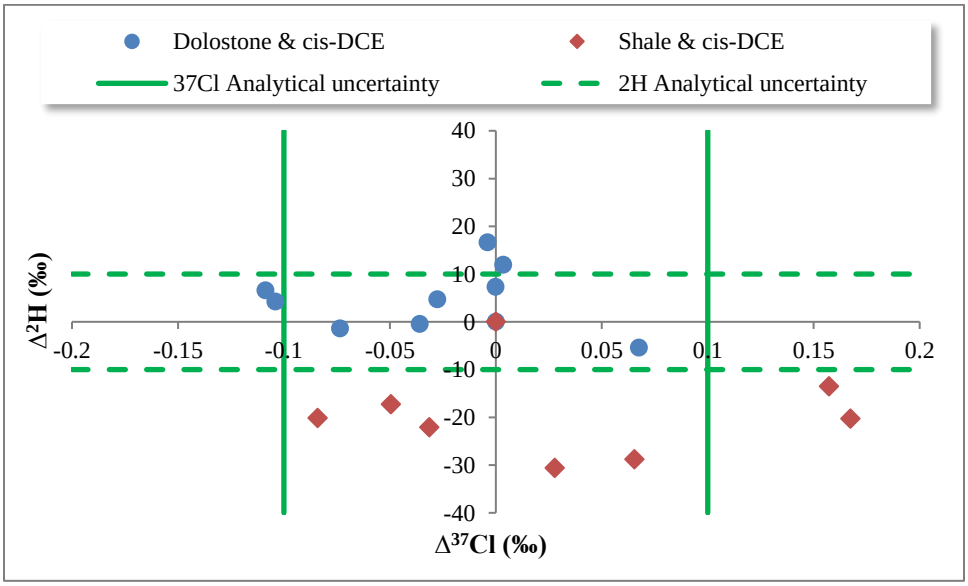

Figure 2-19 Dual isotope plot of *cis*-DCE and sorption batch experiments using shale/dolostone; the uncertainty of the analytical methods for Cl and H isotopes are ±0.1 ‰ and ±10 ‰, respectively

smaller amounts of *cis*-DCE were sorbed compared with TCE. This can explain why isotopic ratios of *cis*-DCE did not change during the sorption experiments.

2.3.1.5 Calculation of Enrichment factors from Sorption Batch Experiment Isotope Results

The Rayleigh equation (Equation 2-3) was used in order to quantify isotope fractionation (α) from the experimental data.

$$\boldsymbol{ln}[(\boldsymbol{\delta}+\mathbf{1000})/(\boldsymbol{\delta_i}+\mathbf{1000})] = (\boldsymbol{\alpha}-\mathbf{1})\boldsymbol{lnf} \qquad 2\text{-}3$$

where δ is the isotopic composition of the compounds, δ_i is the initial isotopic composition of the compounds, *f* is the remaining fraction of the compounds in the solution. The isotopic enrichment factor (ε) can be calculated from the isotope fractionation factor using Equation 2-4:

$$\boldsymbol{\varepsilon} = (\boldsymbol{\alpha}-\mathbf{1}) \times \mathbf{1000} \qquad 2\text{-}4$$

In our experiments, Cl isotopes showed an enrichment in the solution at the early stages of the experiments and then the isotopic ratios shift toward the original isotopic ratios and reach a steady state. H isotopes, on the other hand, showed a continuous depletion to the end of the experiment meaning that the system is in a kinetic state in terms of H isotopes. Therefore, for the Rayleigh plots, we use Cl isotope results to the point that they show a kinetic state and for the H isotope, we use the entire experimental results. Samples of the Rayleigh plots for Cl, C, and H isotopes of TCE are shown in Figure 2-20 and Figure 2-21. The remaining plots are shown in Appendix B. Chlorine and Hydrogen isotopes ratios of *cis*-DCE in the sorption batch experiment with dolostone did not change and the Rayleigh plots had poor correlation factors; therefore, the plots are not shown. The isotope enrichment values are listed in Table 2-2. Samples from only two sets of batch experiments (shale and TCE, and shale and *cis*-DCE) were analyzed for C isotopes. The calculated enrichment factors were -1.9 ‰ for the shale and TCE experiment and <0.5 ‰ for the shale and *cis*-DCE experiment, which are insignificant compared with the isotopic enrichment factors reported for degradation processes (Slater, et al. 2001; Hunkeler, et al. 2002; Schuth, et al. 2003a; Lee, et al. 2007; Cretnik, et al. 2013). The enrichment factors calculated for ^{37}Cl were in the range of -0.2 ‰ to -0.8 ‰, which are negligible compared with the isotope enrichment values obtained for biodegradation (Abe, et al. 2009; Cretnik, et al. 2013; Kuder, et al. 2013). The enrichment factors for H isotope of TCE were significant (in the range of +45 ‰ to +149 ‰) for both shale and dolostone. The H enrichment factor

of *cis*-DCE for the batch experiment with shale (+32 ‰) was smaller than the enrichment factor of TCE for the batch experiment with shale (+52 ‰). The sorption batch experiments on dolostone and *cis*-DCE showed very small sorption and as a result, very small isotope fractionation (the isotope results were within the range of uncertainty of the analytical methods).

Table 2-2 Isotope enrichment factors for the sorption batch experiments. The values are reported with ±95% confidence interval of the linear regression slope. NA denotes not available.

Medium	Compound	Initial Concentration (mg/L)	ε_{Cl} (‰)	ε_{H} (‰)	ε_{C} (‰)
Shale	TCE	2	-0.8 ± 0.11	+52 ± 6.5	-1.9 ± 0.16
Shale	*cis*-DCE	2	<0.1	+32 ± 2.7	<0.5
Dolostone	TCE	2	-0.5 ± 0.12	+149 ± 31.0	NA
Dolostone	*cis*-DCE	2	<0.1	<10	NA
Shale	TCE	11	-0.2 ± 0.03	+46 ± 17.9	NA
Dolostone	TCE	11	-0.2 ± 0.06	+53 ± 22.5	NA

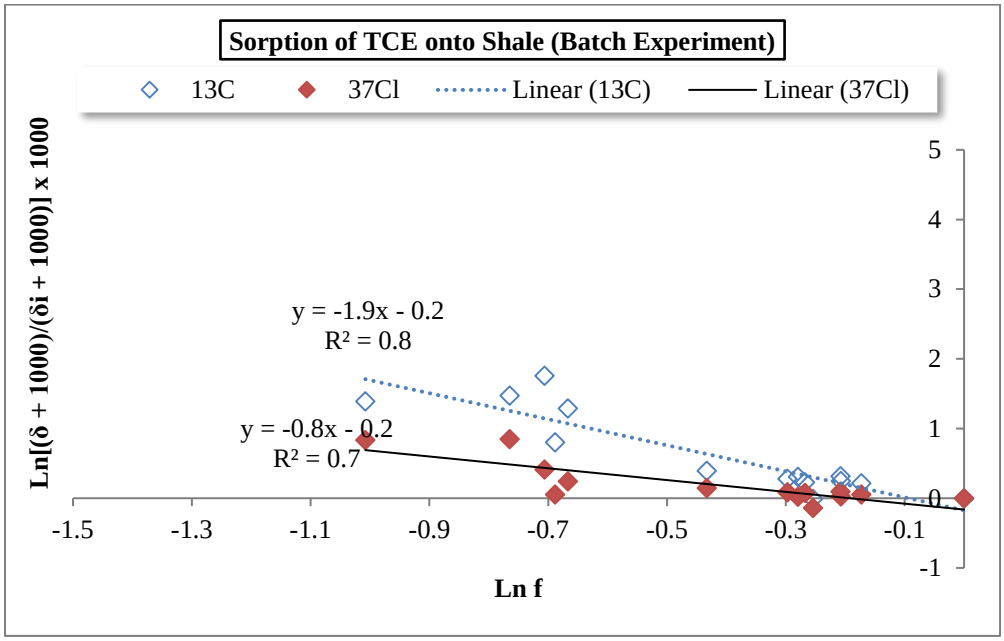

Figure 2-20 Rayleigh plot for C and Cl isotopes of TCE remained in the solution during sorption batch experiment using shale (TCE concentration of 2 mg/L)

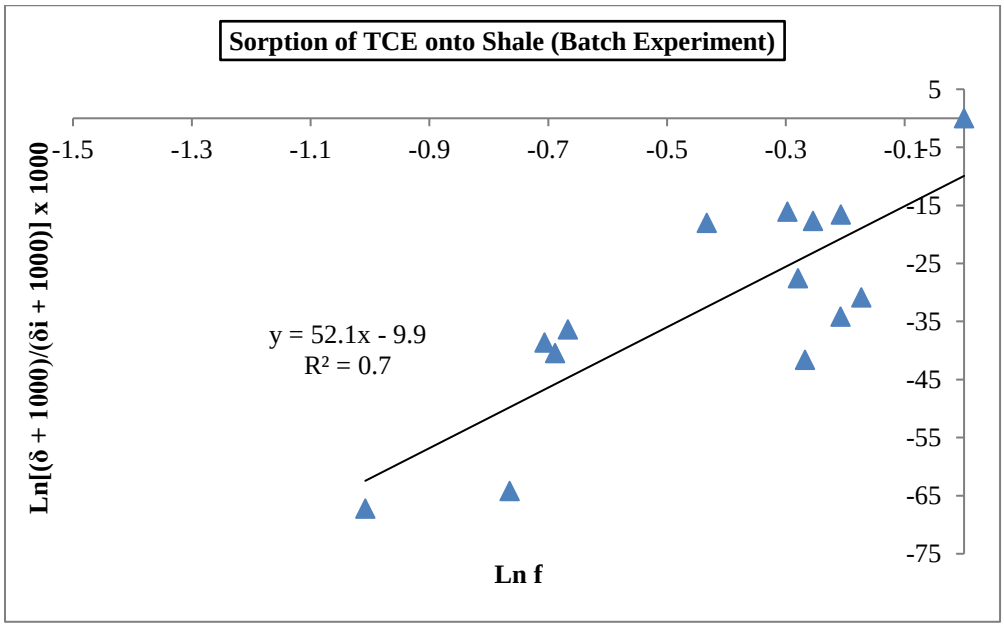

Figure 2-21 Rayleigh plot for H isotope of TCE remained in the solution during sorption batch experiment using shale (TCE concentration of 2 mg/L)

2.3.1.6 Borden Sand and Granular Activated Carbon

The concentration and stable isotope results for the batch experiments are shown in Figure 2-22 and Figure 2-23. An initial aqueous TCE concentration of 270 mg/L was used for the experiment. As can be seen in Figure 2-22, TCE concentration dropped rapidly during the sorption period and continued to drop during the desorption. This is an indication that desorbed TCE molecules were being sorbed again and sorption was still a dominant process up to t = 300 h. Aqueous TCE concentration started to rise slightly after t = 300 h indicating that TCE molecules were strongly attached to GAC (Figure 2-22). Cl isotope results (Figure 2-23) showed that the solution became slightly enriched in ^{37}Cl isotope (with a maximum $\Delta^{37}Cl = +0.74‰$ at t = 45 h) at the early stages of the experiment. The solution became slightly depleted in ^{37}Cl isotopes during the desorption part of the experiment. Chlorine isotope fractionations were very small even in the presence of GAC which is a strong sorbent.

Stable H isotope results (Figure 2-23) showed a small enrichment throughout the experiment (except for a large enrichment at t = 311 h). The H isotope results are in contrast with the results from shale and dolostone batch experiments, which were explained in previous sections. The reason for small fractionations of H isotopes might be the rapid uptake of TCE molecules by GAC since Granular activated carbon is a highly porous material which provides a very large surface area and makes a strong sorbent. The Borden sand used for this experiment also contained natural organic carbon ($f_{oc} = 0.00038$); however, the sorption was dominated by GAC in this experiment.

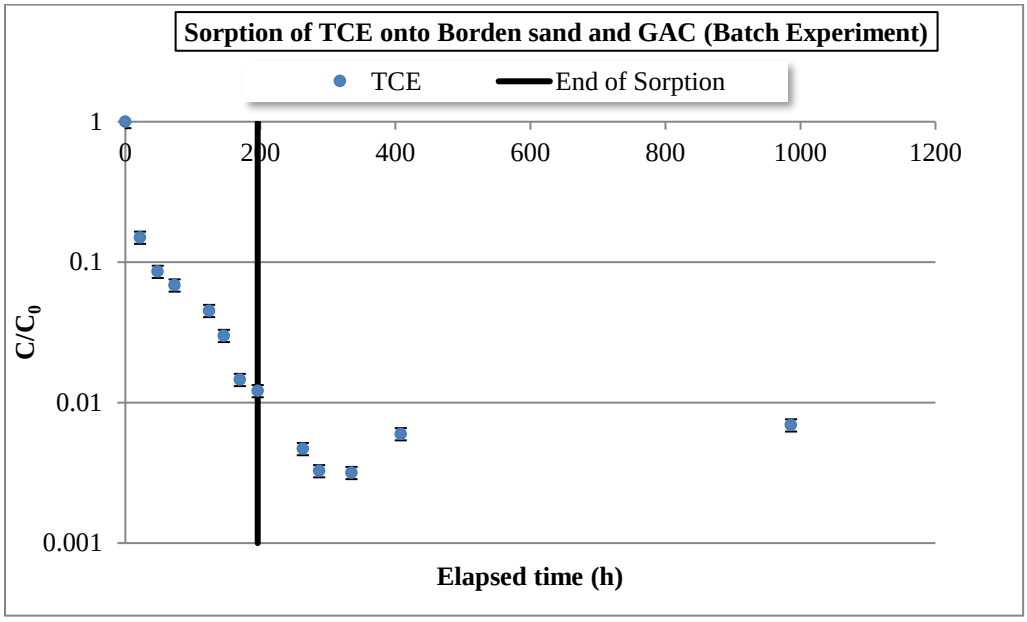

Figure 2-22 Relative concentration of TCE for sorption batch experiment using a mixture of Borden sand and GAC; the uncertainty of the analytical method is ±10 %

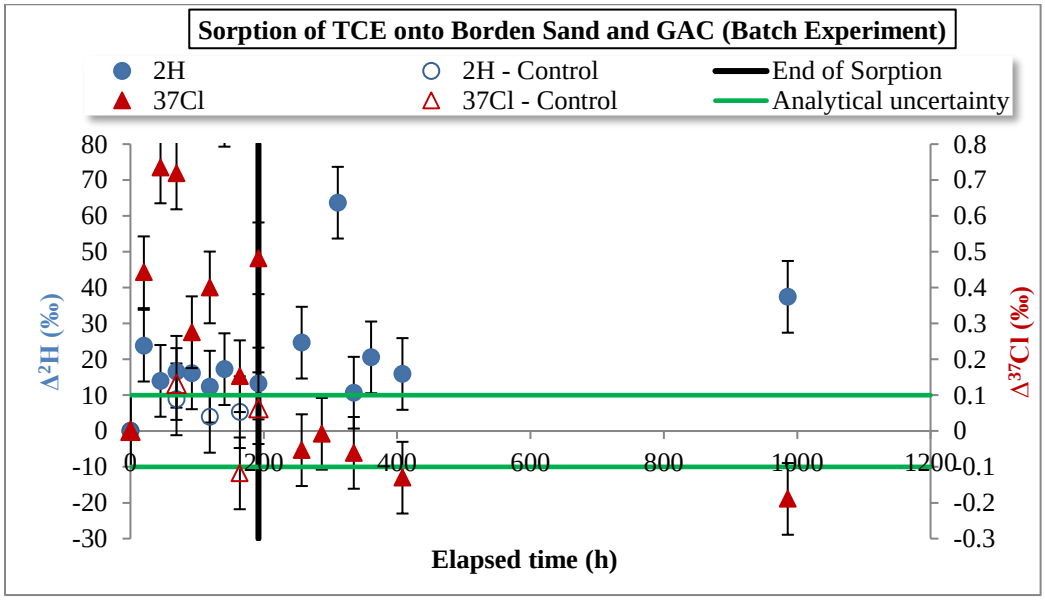

Figure 2-23 Stable chlorine and hydrogen isotope fractionations of TCE for sorption batch experiment using a mixture of Borden sand and GAC; the uncertainty of the analytical methods for Cl and H isotopes are ±0.1 ‰ and ±10 ‰, respectively

2.3.2 Laboratory Column Experiments

2.3.2.1 Ottawa Silica Sand Column (C2) and Borden sand Column (C3)

The column experiments were conducted using two different porous media with different organic carbon content to investigate the effect of sorption on C and Cl stable isotopes fractionation of TCE. The source contaminant solution was transferred into a collapsible Teflon bag and both columns were connected to the same bag. The concentration of TCE solution used for the experiments was 5 mg/L. The flow rate was set at about one pore volume per day and samples were collected from the source solution and at three different ports along the columns. Port 1 is the closest port to the source solution and port 20 is the effluent, which is the furthest (Figure 2-2). Samples of Ottawa silica sand and Borden sand were analyzed for organic carbon content at the Agriculture and Food Laboratory at the University of Guelph, Guelph, Ontario, Canada. Ottawa silica sand had a total carbon of less than 0.5 % dry and hence a very low organic carbon content. Borden sand had a total carbon content of 0.0724 % dry from which 0.038 % dry was considered to be organic carbon (f_{oc} = 0.00038). As seen from Figure 2-24 and Figure 2-27, a concentration plateau (in which the inflow TCE concentration became equal to the effluent concentration) for both columns was reached at t = 37 h, after injecting about 1.5 pore volumes of TCE solution. Desorption occurred rapidly initially and then slowed down around after 4 days of flushing the columns with clean water (t = 200 h), but still occurred at low rates after 17 days of flushing with clean water.

The Cl and C isotopic ratios of the source solution did not change during the experiment; hence, the isotope results are plotted based on isotope separation values ($\Delta = \delta_{sample} - \delta_{source}$). Part of the collected samples during desorption was not analyzed for isotopes due to the low concentrations and/or small volumes of the collected samples. The Cl stable isotope results of C2 (Figure 2-25) shows that isotope separations of the samples from ports 1 are negligible during sorption part of the experiment. Port 1 was the closest to the source solution and TCE samples collected from this port had the same isotopic signature as the TCE source solution. Isotope separation of the TCE samples from port 11 were also insignificant. Samples from port 20 showed small fractionations during the sorption part of the experiment as the solution traveled a longer distance relative to the samples collected from ports 1 and 11. The trend for effluent samples was slight enrichment at the early time followed by small depletion. Since Ottawa silica sand contained negligible amount of organic carbon, there was a possibility that TCE molecules with light Cl isotopes were being temporarily sorbed to the sand

surface at the early stages and desorbed later on. The isotopic signature of the effluent shifted toward the original isotopic signature of the source solution after flushing the system with clean water for about 20 hours.

The results from carbon isotope analysis (Figure 2-26) show that isotopic ratios of the samples collected from all three ports did not change during sorption and desorption. The isotopic ratios were mostly within the uncertainty of the analytical method for $\delta^{13}C$ analyses. Therefore, C isotopes fractionations due to sorption can be neglected when interpreting the isotope data from the field sites where transformation processes are dominant.

The Cl isotope ratios of TCE from C3 (Figure 2-28) showed a slight enrichment over time during the sorption part of the experiment, meaning that molecules with light Cl isotopes were being sorbed. A maximum $\Delta^{37}Cl$ of 0.3 ‰ was observed for the sorption part of the experiment which is small compared with the uncertainty of the analytical method for $\delta^{37}Cl$ analysis (±0.1 ‰). The contaminant source was switched with ultra-pure water after 107 hours. The heavy Cl isotopes showed up at the effluent at time t = 127 h which was 20 hours after the contaminant source was switched with ultra-pure water. It should be noted that 20 hours was the time for displacement of one pore volume from the column. Once clean water passed through the column and previously sorbed light isotopologues desorbed and re-entered the solution, isotope ratios of the samples became negative relative to the initial TCE solution (depletion). The carbon isotope results (Figure 2-29) showed small enrichments throughout the experiment. However, the shift is very small compared with the total analytical uncertainty for $\delta^{13}C$ analysis which is ±0.5 ‰. The U.S. EPA guide for field application of CSIA (Hunkeler, et al. 2008) recommends a criterion of 2 ‰ for carbon isotope fractionation in order to recognize biodegradation in the field. Therefore, the shift in C isotope ratios of TCE due to sorption can be neglected where biodegradation of TCE is taking place.

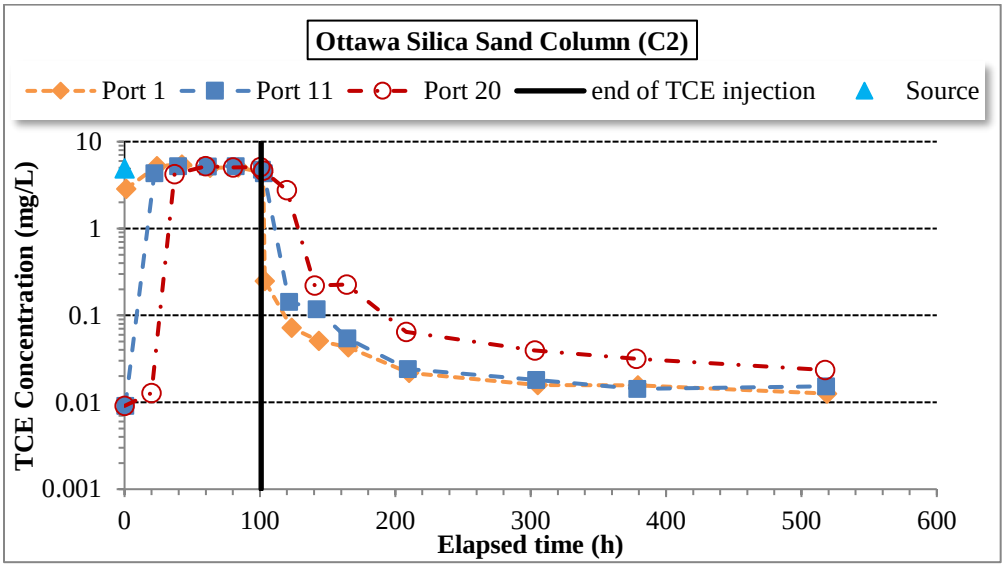

Figure 2-24 TCE concentration of the samples taken from different ports on Ottawa silica sand column (port 1 is the closest to the source and port 20 is the furthest); the uncertainty of the analytical method is ±10 %

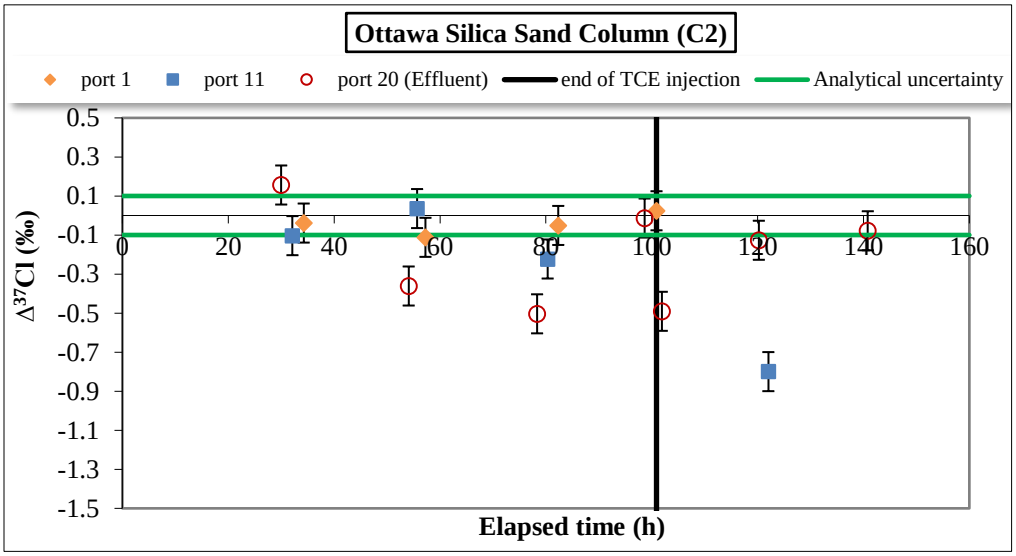

Figure 2-25 Stable chlorine isotope separations of TCE in the samples collected from different ports on Ottawa silica sand column (port 1 is the closest to the source and port 20 is the furthest); the uncertainty of the analytical methods for Cl isotope is ±0.1 ‰

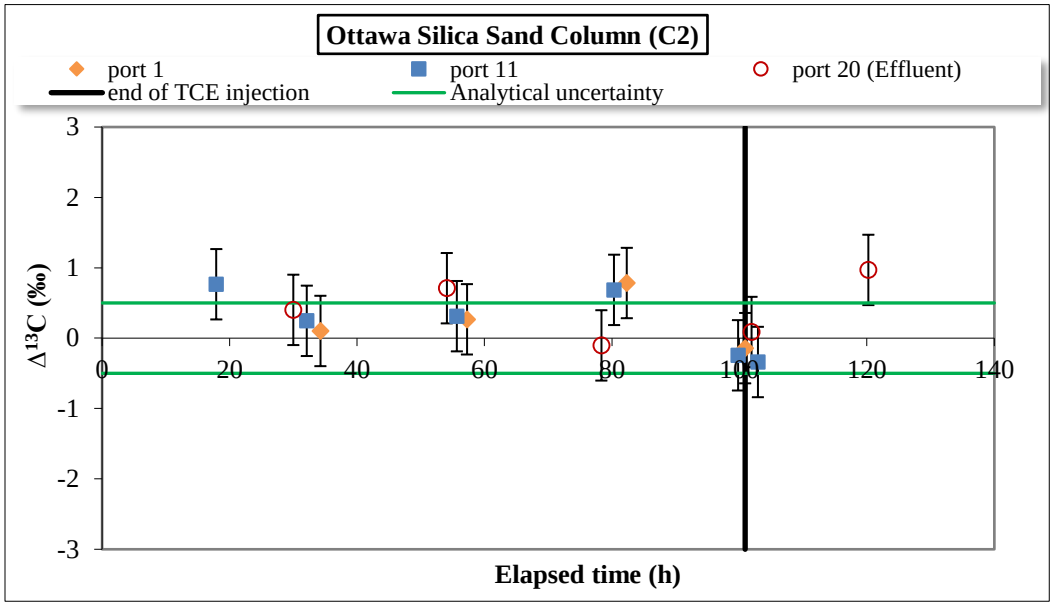

Figure 2-26 Stable carbon isotope separations of TCE in the samples collected from different ports on Ottawa silica sand column (port 1 is the closest to the source and port 20 is the furthest); the uncertainty of the analytical methods for C isotope is ±0.5 ‰

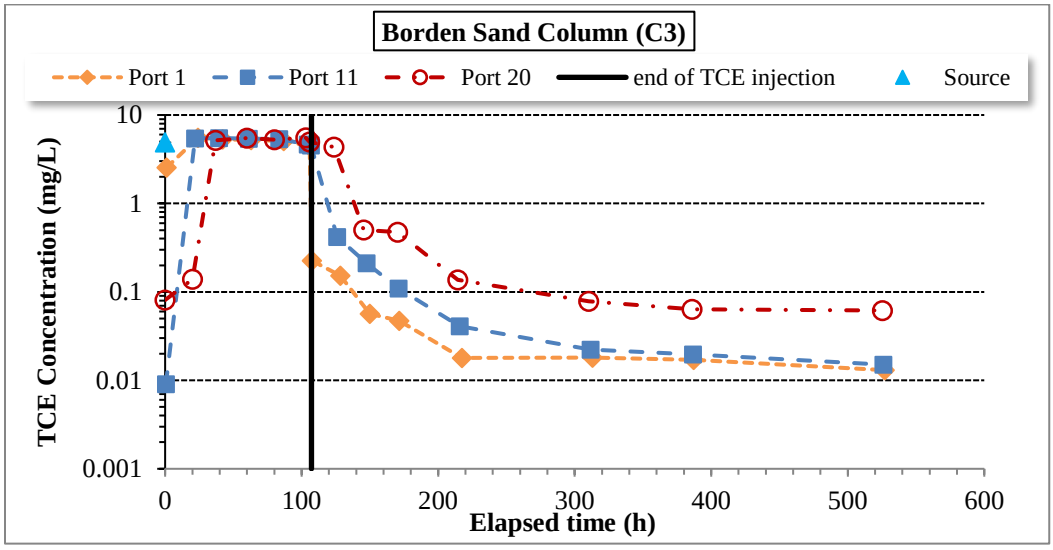

Figure 2-27 TCE concentrations of the samples taken from different ports (port 1 is the closest to the source and port 20 is the furthest); the uncertainty of the analytical method is ±10 %

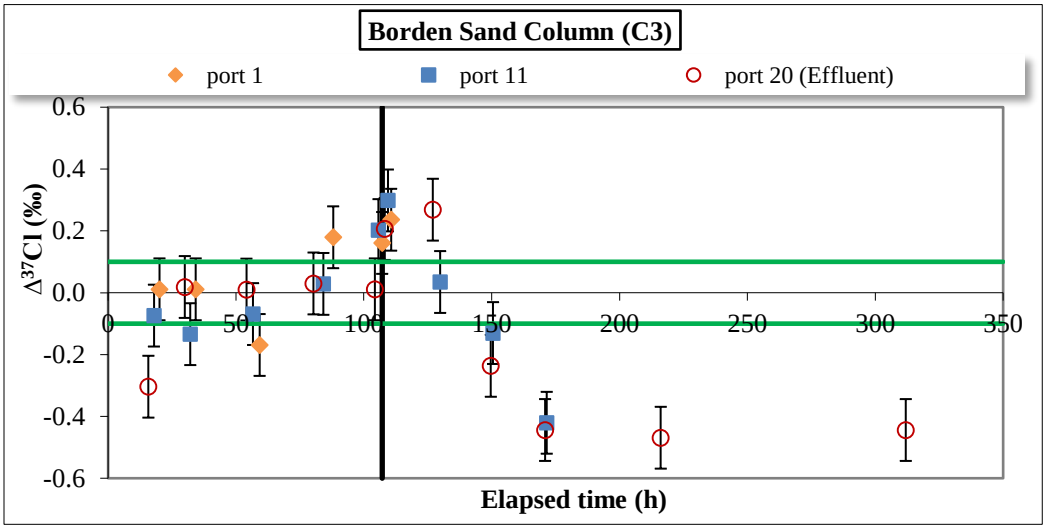

Figure 2-28 Stable chlorine isotope separations of TCE in the samples collected from different ports on Borden sand column (port 1 is the closest to the source and port 20 is the furthest); the uncertainty of the analytical methods for Cl isotope is ±0.1 ‰

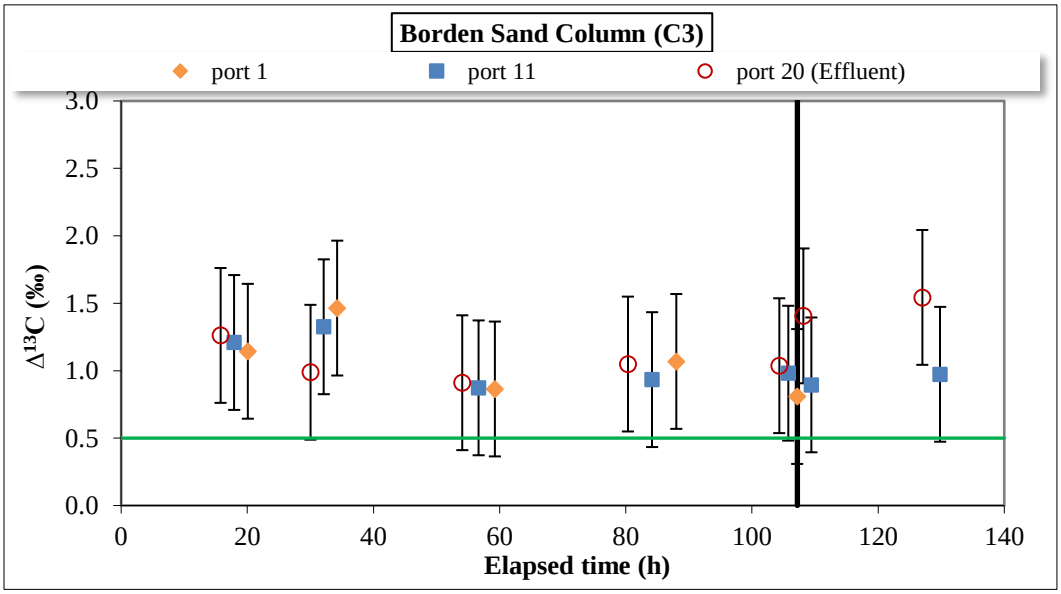

Figure 2-29 Stable carbon isotope separations of TCE in the samples collected from different ports on Borden sand column (port 1 is the closest to the source and port 20 is the furthest); the uncertainty of the analytical methods for C isotope is ±0.5 ‰

2.3.2.2 Borden Sand and Granular Activated Carbon Column (C6)

In order to increase the amount of sorption in the system, a mixture of Borden sand and 1% (by volume) granular activated carbon (GAC) was utilized. Since the sorption capacity of GAC is very high, a TCE solution at concentration of 900 mg/L was used. Samples were collected from the source solution and three different ports along the column. Port 1 was the closest to the source solution and port 5 was the column effluent which was the furthermost (Figure 2-2). The flow rate was set at about one pore volume per day. The effluent TCE concentration reached the concentration of source solution after injecting 9 pore volumes of TCE solution. Once the contaminant source was replaced with clean water and the solution in the pores are flushed out, concentration dropped rapidly. After t = 380 h, concentration dropped at a slower rate as the sorbed TCE molecules were being released slowly (Figure 2-30).

The isotopic ratios of the TCE source solution did not change over time, hence, the isotope results of the samples collected from the ports were plotted relative to the source solution (Δ values). Cl isotope results (Figure 2-31) showed that overall, samples from port 5 showed the largest isotope separation since the solution travelled a longer path and was exposed to higher amounts of sorbents. Samples from the middle port (port 3) showed smaller separations than the samples from port 5, but were still significant. Isotopic separations for the samples from port 1 were negligible as the sampling port was close to the source solution and the collected samples were exposed to the least amount of sorbents. A significant Cl isotope separation was observed for samples from port 5 with the maximum Δ^{37}Cl of 1.67 ‰. Samples from port 3 and 5 showed an enrichment during the early stages of the experiment as lighter isotopologues were being sorbed first. As the sorption sites were being occupied and less of the light isotopologues were being sorbed, the isotopic ratios of the collected samples from ports 3 and 5 shifted toward the isotopic ratios of the TCE source solution; which occurred faster for port 3 as expected. After the contaminant source was switched with ultra-pure water, the isotopic ratios of the samples from ports 3 and 5 showed a small depletion due to desorption of previously sorbed light isotopologues. The isotopic ratios of the effluent became positive relative to isotopic ratios of the source solution after flushing the system for about 190 hours. The reason for this phenomenon is that as the lighter isotopologues were desorbed and left the system, relatively heavier isotopologues were being desorbed. Stable C isotope results (Figure 2-32) showed that isotopic separations of the samples collected from ports 1 and 3 were negligible and within the uncertainty of

analytical method. Samples from port 5 which underwent the highest amount of sorption also showed very small carbon isotope separations.

The effluent samples from this column experiment were analyzed for stable H isotope as well. As seen in Figure 2-33, hydrogen isotope ratios became significantly depleted relative to the source solution due to sorption, which is in agreement with the results from sorption batch experiments. The H isotope separation reached -226 ‰ by the end of the sorption part of the experiment (before switching the contaminant source with clean water). After flushing the system with clean water, depletion of ^{2}H in the effluent samples sustained at a slower rate compared with the sorption part, but was still significant. The H isotope separation reached to -360 ‰ by the end of the experiment (after flushing the system with ultra-pure water for 18 days. Once the source of contamination was disconnected and the system was no longer fed with fresh contaminant, the contaminant solution inside the pores, which was already depleted, underwent further adsorption. This process resulted in further depletion of the solution in heavy isotopologues. The concentration results (Figure 2-30) show that TCE concentration in the effluent samples was still high (58 mg/L) after 476 hours of flushing the column with ultra-pure water. Based on the flow rate (450 mL/day), average TCE concentration of the inflow solution (900 mg/L), and the effluent concentrations, it was estimated that during 193 hours of injecting the TCE solution, about 3289 mg of TCE entered the column. About 2575 mg left the column throughout the experiment, and about 713 mg remained in the column by the end of the experiment (which was about 27% of the total TCE entered the system). It would have been beneficial to run ultra-pure water into the column for a longer period of time to observe the evolution of H isotopes ratios. Overall, from our results, it appears that heavy H isotopologues were attached to GAC strongly.

The results from the sorption part of this experiment are in agreement with the results from shale and dolostone sorption batch experiments as all of the experiments showed significant depletion of the solution in ^{2}H. However, the results do not conform to the results for the batch experiment with a mixture of Borden sand and GAC which showed a small enrichment of ^{2}H in the solution throughout the experiment. The difference between the column and the batch experiment results could be due to the way in which contaminant solution was added to the medium. For the column experiment the contaminant was injected slowly into the column and the molecules had a chance to be adsorbed preferentially. For the batch experiments, TCE solution was added to the medium instantaneously.

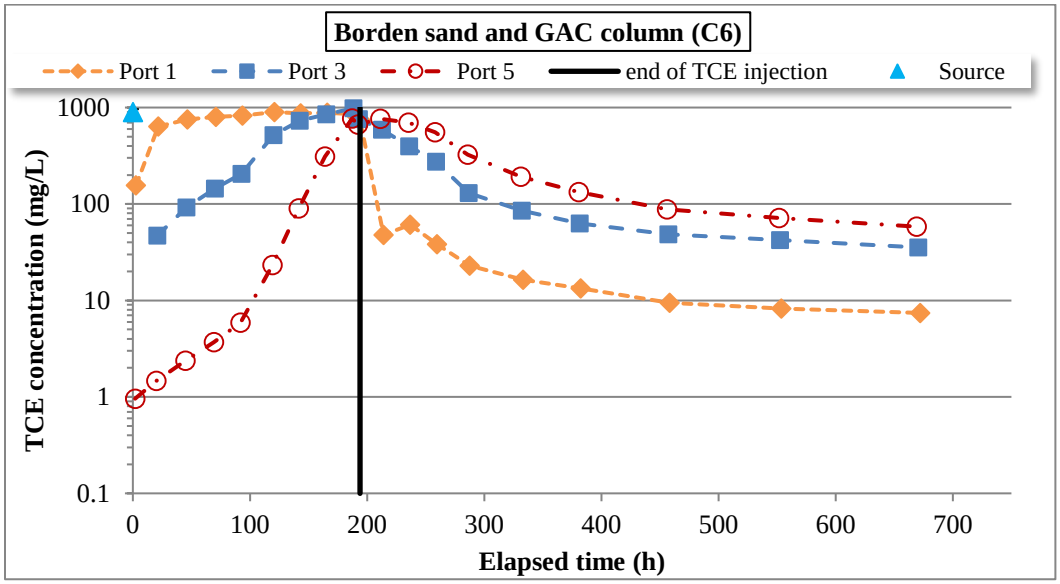

Figure 2-30 TCE concentrations of the samples taken from different ports on Borden sand and GAC column (port 1 is the closest to the source and port 5 is the furthest); the uncertainty of the analytical method is ±10 %

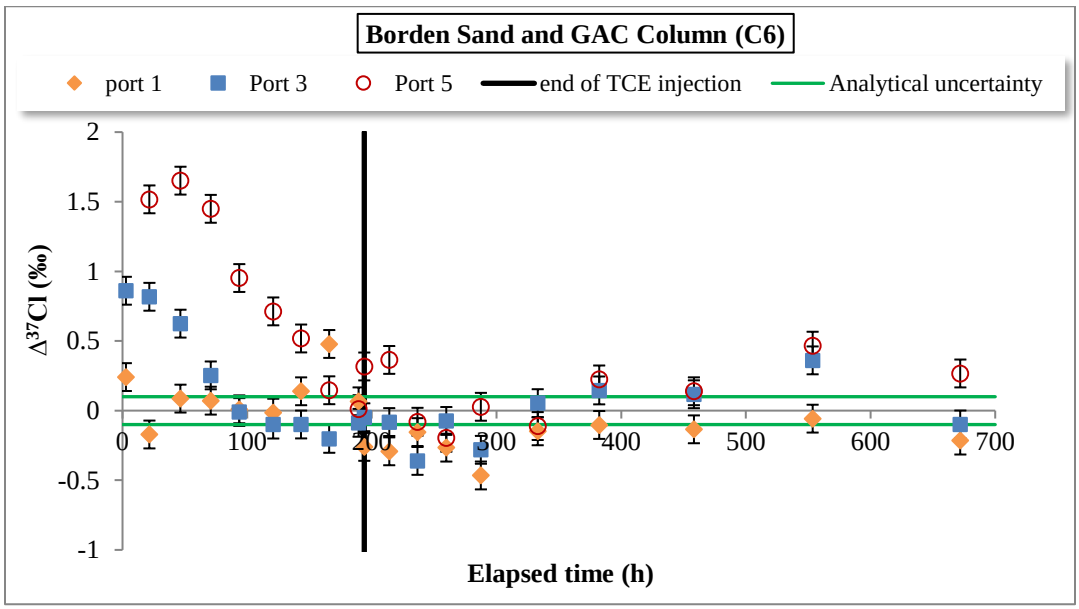

Figure 2-31 Stable chlorine isotope separations of TCE in the samples collected from different ports of Borden sand and GAC column (port 1 is closest to the source and port 5 is the furthest); the uncertainty of the analytical methods for Cl isotope is ±0.1 ‰

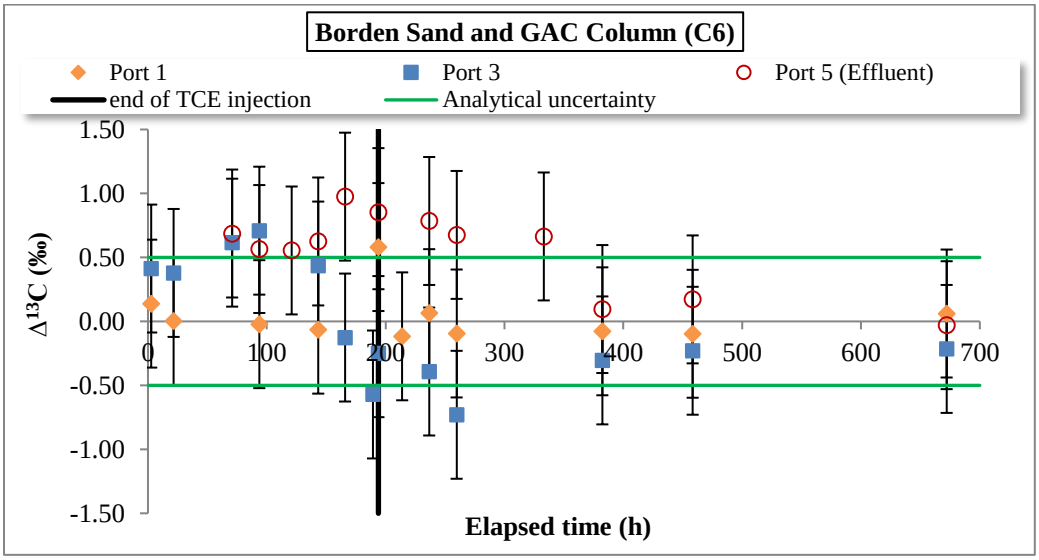

Figure 2-32 Stable carbon isotope separations of TCE in the samples collected from different ports on Borden sand and GAC column (port 1 is the closest to the source and port 5 is the furthest); the uncertainty of the analytical methods for C isotope is ±0.5 ‰

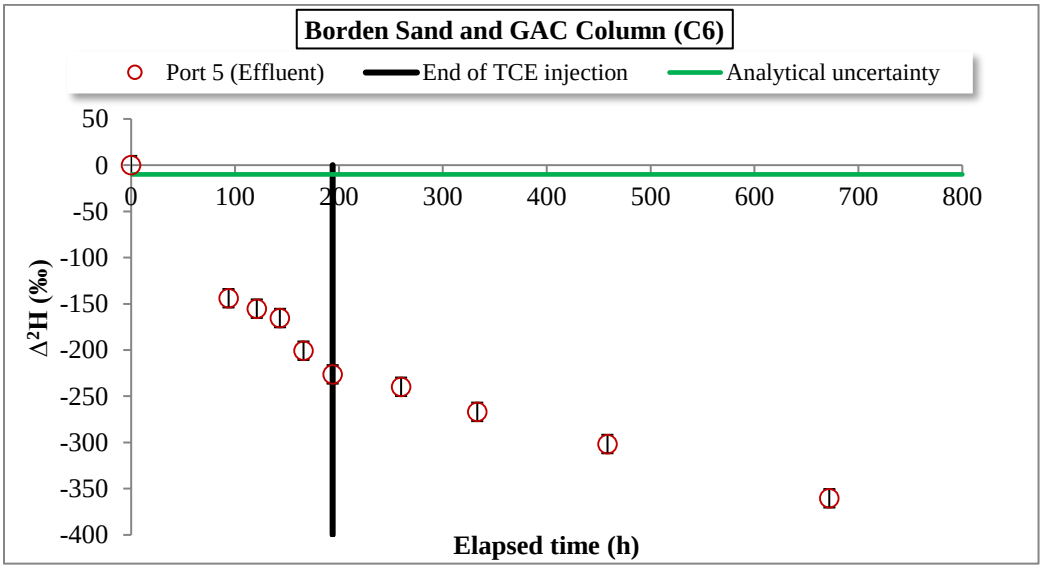

Figure 2-33 Stable hydrogen isotope separation of TCE in the samples collected from the effluent of Borden sand and GAC column; the uncertainty of the analytical methods for H isotope is ±0.10 ‰

GAC is a strong sorbent and adsorbs organic compounds rapidly. Therefore, a possible explanation for the behavior of H isotope in the batch experiment is that GAC adsorbed both light and heavy isotoplogues of TCE at the same time and therefore, did not show a significant fractionation.

2.4 Summary and Conclusion

A series of controlled batch and column experiments were conducted to investigate changes in behavior of C, Cl, and H stable isotopes of chlorinated ethenes during sorption and desorption processes under static and dynamic conditions. Overall, the findings showed that sorption had negligible effect on carbon isotope ratios under both static and dynamic conditions even in the presence of a strong sorbent such as granular activated carbon (GAC). Sorption had a relatively small effect on Cl isotope ratios, and had a significant effect on H isotopic ratios. Moreover, our results showed that during the sorption process, chlorine and hydrogen isotopes ratios evolved in opposite trends.

The concentration results from shale and dolostone batch experiments showed an early stage of rapid sorption followed by a stage of slow sorption. Chlorine isotope results of TCE and *cis*-DCE from most of the sorption batch experiments showed that the liquid phase became enriched in ^{37}Cl during the time when the rate of sorption was high. Once the system reached steady state in terms of concentration, the isotopic ratios shifted toward the original ratios. Therefore, when the system is in steady state condition such as for stationary old plumes, Cl isotope fractionation is not detectable, while in an expanding young plume where sorption is still taking place, small Cl isotope fractionations might be observed. The exception for Cl isotope results were for shale and TCE (2 mg/L solution) which showed enrichment to the end of the experiment, and dolostone and *cis*-DCE which showed negligible isotope separations and the isotopic ratios were within the uncertainty of analytical methods.

Hydrogen isotope results showed that the solution became depleted in ^{2}H significantly which is a counterintuitive phenomenon. It is generally accepted that sorption favors lighter isotopes (Caimi and Brenna. 1997; Poulson, et al. 1997; Kopinke, et al. 2005) and heavier isotopes prefer to stay in the solution since the heavier isotopes tend to have weaker interactions with the solid phase (Caimi and Brenna. 1997). The reason for sorption of heavy H isotopologues is not clear. Calculation of vibrational energies for different isotopologues using computational chemistry might help to explain this phenomenon (Schauble, et al. 2001; Schauble, et al. 2004; Black, et al. 2011).

The concentration results from the batch experiments showed that less amounts of *cis*-DCE were sorbed compared to TCE, which was due to the smaller K_{oc} value of cis-DCE than TCE. The isotope results from the batch experiments with TCE and *cis*-DCE also revealed that H and Cl isotopic fractionations of *cis*-DCE were smaller than the ones of TCE.

The effect of sorption and desorption processes on isotopic ratios of TCE was investigated through laboratory batch and column experiments using different media containing different amounts of sorbents. The isotope results of the Borden sand and GAC batch experiment showed that Cl and H isotopes did not fractionate significantly. Cl isotopes showed a small enrichment during sorption which is in line with the results from shale and dolostone batch experiments. H isotopes also showed a small enrichment throughout the experiment which is in contrast with the results from shale and dolostone batch experiments. An explanation for this behavior might be the instantaneous adsorption of molecules with heavy and light isotopes to GAC.

The isotope results from the column experiments showed that sorption causes very small C isotope fractionations of TCE, even in the presence of activated carbon, which can be neglected compared with isotope fractionations due to transformation processes (Lollar, et al. 1999b; Bloom, et al. 2000b; Slater, et al. 2001; Hunkeler, et al. 2002; Cichocka, et al. 2007; Lee, et al. 2007; Cretnik, et al. 2013; Kuder, et al. 2013). Chlorine isotope separation of TCE was small for the samples from the US Ottawa Silica sand column (C2) and Borden sand column (C3). Maximum Cl isotope separations of +0.49 ‰ and +0.47 ‰ were observed for effluent samples from C2 and C3, respectively. Chlorine isotope separation of TCE from the effluent samples of Borden sand and GAC column (C6) was high. A maximum chlorine isotope separation of +1.65 ‰ was observed from the effluent samples of C6. However, granular activated carbon is a strong sorbent and does not exist naturally in the sediments. Therefore, in the subsurface, sorption of TCE in sediments with naturally occurring organic carbon does not cause significant Cl isotope fractionations and can be neglected compared with isotope fractionations due to transformation processes (Cretnik, et al. 2013; Kuder, et al. 2013). The effluent samples from the column experiment with a mixture of Borden sand and GAC was analyzed also for H isotopes, which revealed a significant depletion with a maximum separation of -360 ‰. The results are consistent with the results from shale and dolostone sorption batch experiments.

Based on the fractionation factors calculated from shale and dolostone batch experiments, Cl isotope fractionations due to sorption can be neglected when compared with Cl isotope fractionations

during biotic and abiotic degradation of chlorinated solvents (Abe, et al. 2009; Cretnik, et al. 2013; Kuder, et al. 2013). The effect of biodegradation on H isotope fractionations of chlorinated ethenes has been investigated by Kuder et al. (2013). The authors reported an enrichment factor of ε_H = +34 ± 11 ‰ for TCE. The enrichment factors estimated for ^2H from our experimental results were within the range of +32 ± 2.7 ‰ and +149 ± 31 ‰ (Table 2-2), which were mostly higher than the reported value by Kuder et al. (2013). Furthermore, hydrogen isotope results of TCE by KB-1 culture (SiREM, Guelph, Ontario, Canada) showed that the shift in δ^2H values of TCE and cis-DCE due to biodegradation was very small (Appendix C) and either within or slightly above the uncertainty of the analytical method for H isotope analysis. Therefore, it can be concluded that the shifts in δ^2H isotope values of chlorinated solvents and especially TCE in the subsurface are related to physical processes such as sorption rather than biodegradation. Nonetheless, a definite conclusion cannot be made based on limited studies on H isotope fractionations of chlorinated ethenes due to biodegradation. Hydrogen CSIA of chlorinated ethenes is a new topic and further investigations are needed to fully understand the behavior of H isotopes of chlorinated ethenes during physical, chemical, and biologically mediated processes.

Chapter 3

The Effect of Diffusion and Back-diffusion on Chlorine and Hydrogen Stable Isotopes of TCE and *cis*-DCE

3.1 Introduction

Chlorinated solvents are denser than water and can migrate under the water table (Pankow and Cherry. 1996). If there are low permeability lenses in the subsurface, chlorinated solvents may accumulate on top of them. Due to dissolution, part of the contaminant spreads in the aquifer through advection and dispersion to form the contaminant plumes, while molecular diffusion can cause long-term storage of chlorinated solvents in low permeability zones and act as a continued source of contamination over time. In the subsurface, processes such as biodegradation and sorption also affect contaminant transport (Schwartz and Zhang. 2003). Hence, characterizing the processes that affect contaminant plumes is beneficial to design appropriate remediation strategies. During the last decade, compound-specific isotope analysis (CSIA) has emerged as one of the most useful techniques in fingerprinting the sources of organic contaminants and understanding the transformation mechanisms of these contaminants in the subsurface (Aelion, et al. 2009).

A previous study on the effect of diffusion on carbon isotope fractionation of MTBE using a simulated stratified aquifer-aquitard system showed that aquitard units are depleted in heavy isotopes (LaBolle, et al. 2008). Stable isotope fractionation of ethylbenzene as a result of diffusion, dispersion, and biological reactions was investigated by Rolle, et al. 2010 and they concluded that physical processes also need to be considered for a better interpretation of isotopic data. Wanner and Hunkeler. 2015, investigated carbon and chlorine isotopes fractionation of TCE and 1,2-DCA during diffusion in aqueous phase. Their results revealed that diffusion-related isotope fractionation is small compared with reactive processes, but it should be considered when the diffusion periods are short and isotope shifts due to reactive processes are small. Nonetheless, the effect of diffusion and back-diffusion on stable isotopic ratios (especially H isotopes) of chlorinated ethenes has not been widely investigated. In this study, we performed several laboratory batch experiments using shale and dolostone to investigate how Cl and H isotopes ratios of TCE and *cis*-DCE evolved during the back-diffusion of contaminants from a low permeability zone into the aquifer. Furthermore, a laboratory box experiment was conducted in a simulated aquitard – aquifer system to evaluate the behavior of H and Cl isotopes of TCE and *cis*-DCE during diffusion and back-diffusion of the contaminants.

3.2 Method and Materials

3.2.1 Laboratory Batch Experiments

The evolution of Cl and H isotopic ratios during back-diffusion of TCE and *cis*-DCE from a low permeability zone into stagnant water was examined through a series of laboratory batch experiments. The experiments were conducted using two different porous media including shale from the Rochester Formation (Smithville, Ontario, Canada), and dolostone from the Eramosa Formation (Smithville, Ontario, Canada). Samples of the shale and dolostone were submitted to Agriculture and Food Laboratory at the University of Guelph, Guelph, Ontario, Canada, for organic carbon analysis. The organic carbon content of shale and dolostone was 0.6 (% dry) and 0.4 (% dry), respectively.

Ground shale and dolostone were used for the batch experiments. Shale and dolostone were ground using Planetary Ball Mill Pulverisette 5 (Fritsch manufacturer). Then, 1200 ± 10 g of dry ground shale was put into a 1L glass bottle and 330 ± 5 g of TCE solution (concentration of 14 mg/L) was added. The bottle was covered with a Teflon-faced septa-cap and the mixture was shaken very well by hand. This procedure was repeated to make shale and cis-DCE, dolostone and TCE, and dolostone and cis-DCE mixtures. The initial concentration of TCE solution used for the dolostone was 30.7 mg/L and the initial concentration of cis-DCE solution for both shale and dolostone experiments was 8 mg/L. The experiments were conducted using wide-mouth 250 ml clear glass bottles that were purchased from VWR. The height of the bottles was 13.8 cm, the bottom outer diameter was 7 cm, and the glass wall thickness was 0.3 cm (Figure 3-1). The bottles were soaked in 10% nitric acid bath overnight and washed with deionized water very well before use. Once the mixture was homogenized, 50 mL of the mixture was poured into the 250 mL bottles which covered 1.6 cm of the bottom of the bottles. The mixture was covered with 100 mL (3.2 cm) of dry Ottawa silica sand (F-85). The bottle was slowly filled with ultra-pure water (no head-space) using a clean funnel with the funnel neck pointed toward the glass wall to prevent disturbance of the sand layer. The bottles were covered with a septa-cap (Figure 3-1) and kept upright and stationary until the sampling time arrived. Aqueous samples were collected at 1, 72, 168, 336, 504, 840, 1176, 1512, 1848, and 2184 hours. One bottle was dedicated for each sampling time. The experiments were conducted at room temperature (22 ± 1°C). The collected samples were kept in the refrigerator at 4°C until analyzed. The samples were analyzed for VOC concentration, and Cl and H stable isotope ratios.

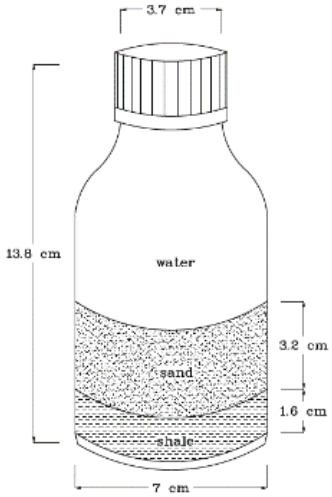

Figure 3-1 Schematic and real set up of the back-diffusion batch experiments. The bottles were kept upright and stationary for the duration of the experiment. Aqueous samples were collected from the water on top of the bottles.

3.2.2 Laboratory Box Experiment

This experiment was conducted using a Plexiglas box with dimensions of 100 cm x 20cm x 10 cm. The thickness of the Plexiglas sheet was ¼". The box was built at the Science Machine Shop, University of Waterloo, Waterloo, Ontario, Canada. Methylene chloride which is the typical glue for Plexiglas was used to weld the parts. The top part was removable and was screwed to the external rim at the top of the box. A groove was made on the cover and a Viton O-ring was inserted in the groove to provide a perfect seal when the cover was screwed to the main part. Both side panels (influent and effluent end caps) of the box were screened over the sand layer (Figure 3-2). Kaolin clay powder and U.S. Ottawa silica sand (F-85) were used as the porous media. Kaolin was obtained from Debro Chemicals, Brampton, Ontario Canada (originally from Sandersville, Georgia, USA) and Ottawa silica sand was obtained from U.S. Silica Company, Ottawa, IL, USA. Kaolin contained organic carbon content of 0.0346 % dry (analyzed by Agriculture and Food Laboratory at the University of Guelph, Guelph, Ontario, Canada) and Ottawa silica sand had negligible amount of organic carbon. Prior to packing the box, the clay was mixed with ultra-pure water to make saturated clay. The ultra-pure water contained 0.1 % sodium azide to prevent bacterial activity in the clay units. In order to pack the box, first a saturated layer of clay with a thickness of 8.5 cm was poured into the box and the surface was evened out. Then, a layer of dry Ottawa silica sand with a thickness of 3 cm was put on top of the clay layer, and the sand was covered by another layer of saturated clay (8.5 cm thick). Ultra-pure water was injected at a flow rate of 200 mL/day into the box from the left side of the box through the sand layer for 63 days in order to make sure the sand layer was fully saturated. A mixture of TCE (initial concentration of 67 mg/L) and *cis*-DCE (initial concentration of 100 mg/L) solution was used as the source of contamination. Sodium bromide (J.T.Baker® Chemicals, PA, USA), and sodium chloride (BDH Chemicals, VWR International, PA, USA) were added to the source solution as conservative tracers. The aqueous concentrations of sodium bromide and sodium chloride in the source solution were 98 mg/L and 90 mg/L, respectively. The contaminant solution was transferred to a collapsible Teflon bag (Figure 3-4) to eliminate the creation of head-space due to pumping the solution into the box over time. The contaminant was injected into the box, through the sand layer, at a flow rate of 200 ± 10 mL/day using a peristaltic pump. Effluent samples were collected in four 20 mL flow-through amber vials. The effluent overflowed to a waste container (Figure 3-3 and Figure 3-4). After 45 days of contaminant injection, the contaminant source was switched to ultra-pure water

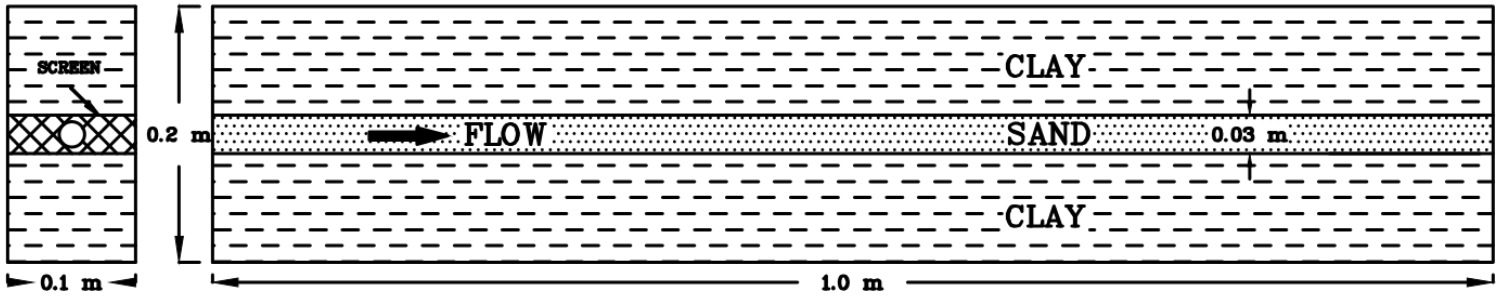

Figure 3-2 Schematic views of the box from the side (left) and the front (right)

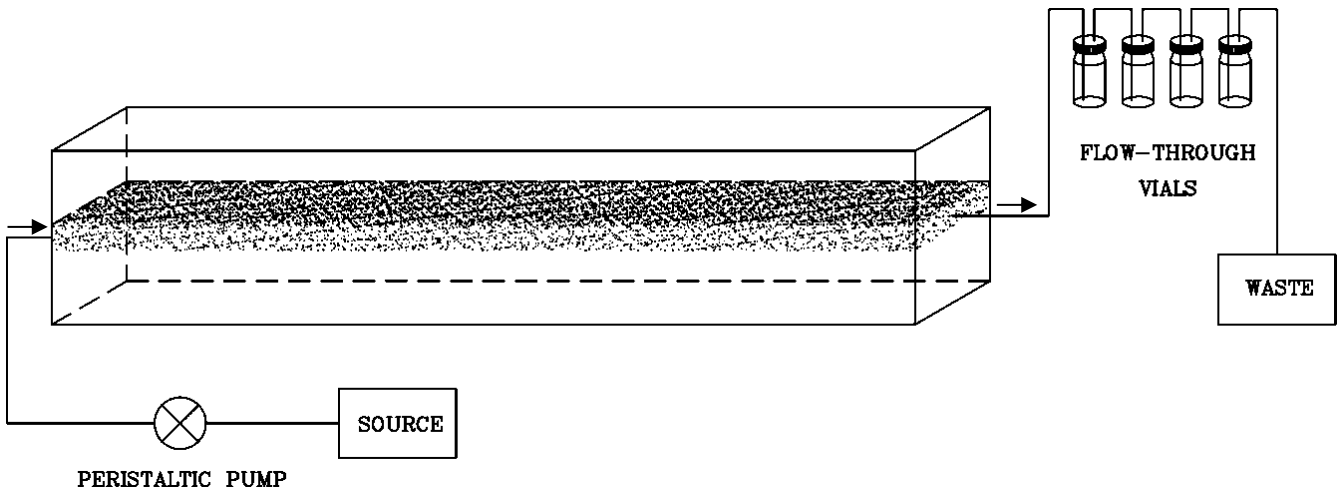

Figure 3-3 Schematic of the box experiment setup. The flow-through vials are enlarged to show the details.

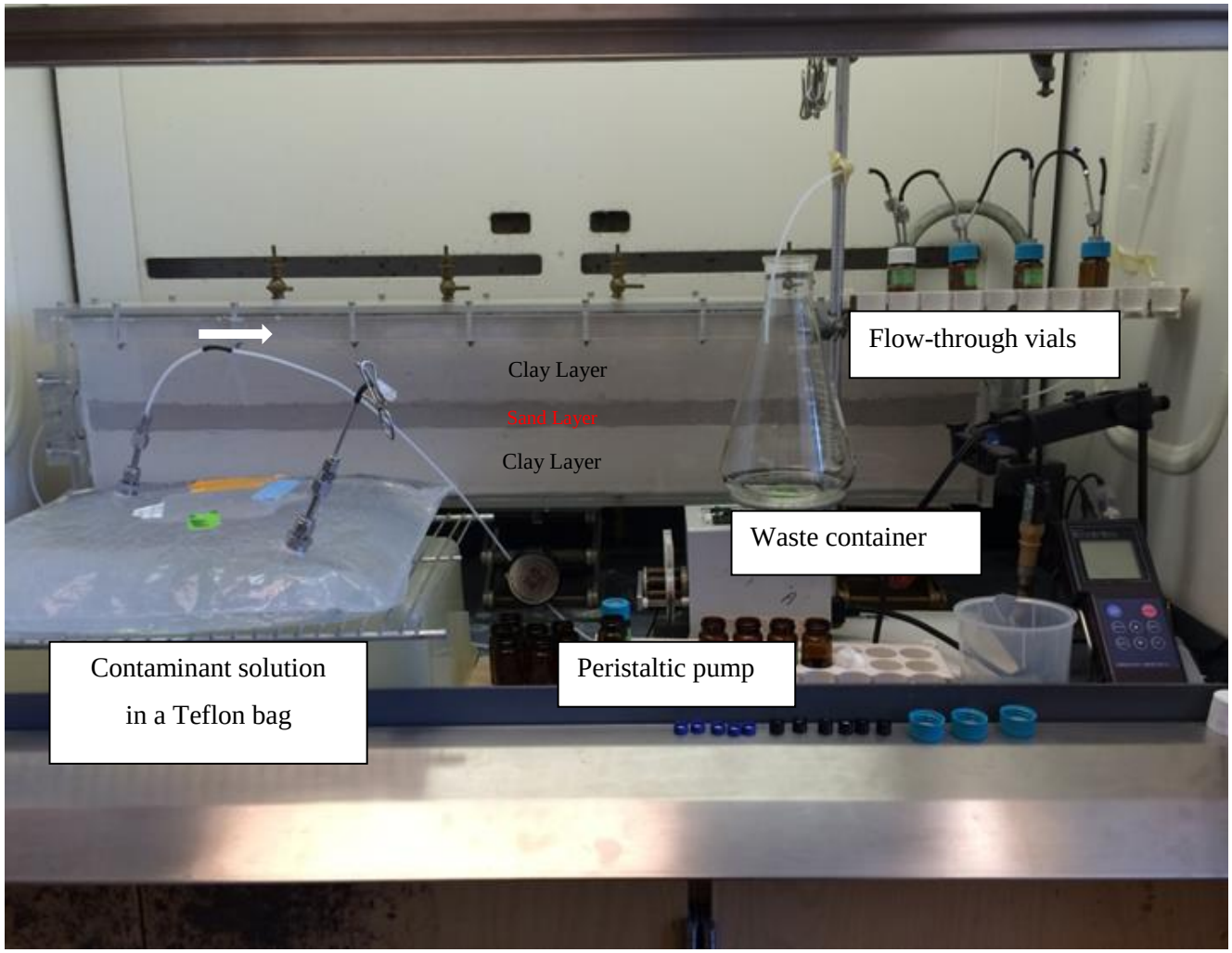

Figure 3-4 Diffusion box experiment setup

to investigate the behavior of Cl and H isotopes of TCE and *cis*-DCE during the back-diffusion process. Aqueous samples were collected frequently from the source solution and the flow-through vials and analyzed for TCE and *cis*-DCE concentration, Br^- and Cl^- concentrations, and ^{37}Cl and ^{2}H isotopic ratios. The samples were capped using Teflon-faced septa caps immediately upon sampling and stored in the refrigerator at 4°C until being analyzed. Electrical conductivity and temperature of the effluent was measured throughout the experiment using a Horiba ES-12E conductivity meter. The temperature of the effluent water was also monitored using the conductivity meter and it was 22 ± 1 °C throughout the experiment. The pH of the effluent was 7.4 ± 0.2. The pH was measured using a Thermo Orion 910600 gel filled electrode.

There was a leak at the lower right corner of the box (close to the effluent line) on day 61. An epoxy putty was applied on the area and a Ratchet Tie-Down strap was placed around the box to stop the leak. The leak was decreased over time and stopped at day 69.

3.3 Analytical Procedure

The analytical procedure for VOC and stable isotope analyses are described in Appendix A.

3.4 Results and Discussion

Chlorine and hydrogen isotopic ratios were calculated based on the following equation and the values were reported in δ notation.

$$\boldsymbol{\delta R_{sample}} = \left(\frac{\boldsymbol{R_{sample} - R_{reference}}}{\boldsymbol{R_{reference}}}\right) \cdot \mathbf{1000}\ ‰ \qquad 3\text{-}1$$

where R is $^{37}Cl/^{35}Cl$-ratio or $^{2}H/^{1}H$-ratio. The reference for chlorine isotope is Standard Mean Ocean Chloride (SMOC); and the reference for hydrogen isotope is a hydrogen gas calibrated to Vienna Standard Mean Ocean Water (VSMOW). The δ-values are expressed as parts per thousand or permil (‰).

For some of the experiments, the isotope results are plotted based on isotope separation (Δ) which is the difference between the δ-values of the isotopes of the contaminant at time zero and δ-values after a certain time has elapsed. The lines labeled as "analytical uncertainty" on the plots indicate the upper and lower limit for the uncertainty of the analytical methods for the stable isotopes analyses. For example, on the plot with C, Cl, and H isotope data, the lines intercept the $\Delta^{2}H$ vertical

axis at +10 ‰ and -10 ‰, the $\Delta^{37}Cl$ vertical axis at +0.1 ‰ and -0.1 ‰, and the $\Delta^{13}C$ vertical axis at +0.5 ‰ and -0.5 ‰.

3.4.1 Laboratory Batch Experiments

3.4.1.1 Shale and TCE/*cis*-DCE Back-diffusion Batch Experiments

Relative concentrations and stable isotopes results for shale and TCE, and shale and *cis*-DCE experiments are shown in Figure 3-5 to Figure 3-8. The concentration results (Figure 3-5) showed that TCE back-diffused at a faster rate at the beginning of the experiment (up to t = 840 h) when the concentration gradient between the contaminated shale and water at the top was still high. The back-diffusion rate became constant after 840 hours. As seen in Figure 3-5, about 4.2% of the initial mass back-diffused in 90 days.

Diffusive isotope fractionations (α_{diff}) are mass dependent and follow a general power law:

$$\boldsymbol{\alpha_{diff} = \frac{D_H}{D_L} = \left(\frac{m_L}{m_H}\right)^{\beta}} \qquad 3\text{-}2$$

where D_H and D_L are the diffusion coefficients of heavy and light isotopologues, respectively; m_L and m_H are molecular masses of light and heavy isotopologues, respectively; and β is the power law exponent (Appelo and Postma. 2005; Richter, et al. 2006; Tempest and Emerson. 2013; Jin, et al. 2014; Wanner and Hunkeler. 2015; Clark and Fritz. 1997). Therefore, it is expected that light isotopologues diffuse faster. Stable Cl isotope results for shale and TCE experiment (Figure 3-6) showed that TCE molecules with light Cl isotope back-diffused first as expected and the isotopic ratios of the back-diffused TCE gradually shifted toward the original isotopic ratio of the source. A maximum isotope separation ($\Delta^{37}Cl$) that was observed for this experiment was -1.2 ‰.

Similarly, hydrogen isotope results (Figure 3-6) indicated that molecules with light H isotope back-diffused first; however, H isotope ratios at the end of the experiment were still significantly negative compare to the original isotope ratio of TCE. This can be due to the strong sorption of heavy H isotopologues to the solid phase in the source material (i.e. shale). A maximum $\Delta^{2}H$ of -286 ‰ was observed for this experiment. It should be mentioned that hydrogen isotope ratios of the first few samples are missing because TCE concentration was below 100 µg/L which is the minimum concentration required for compound-specific H isotope analysis.

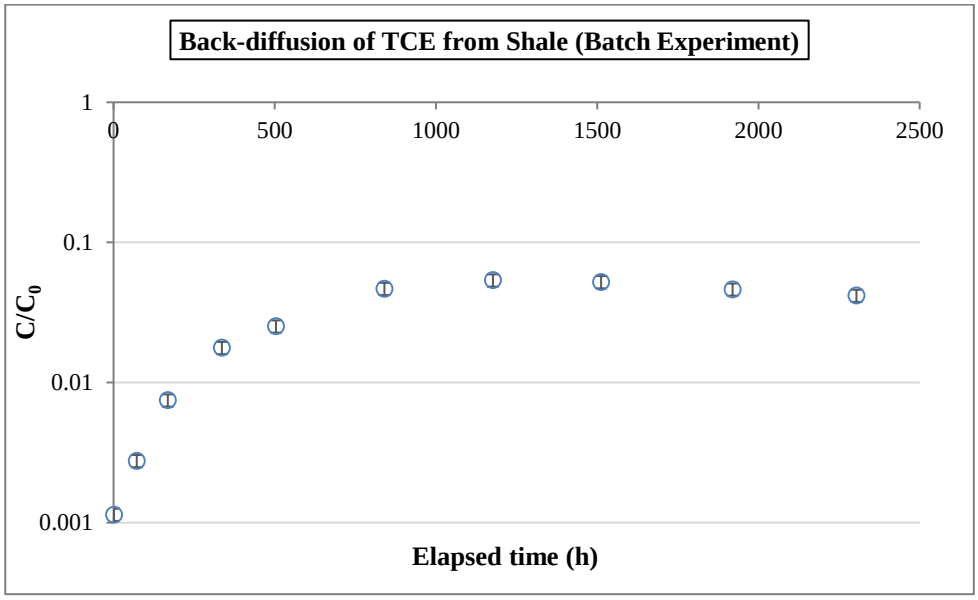

Figure 3-5 Relative concentration of back-diffused TCE from shale vs time; the uncertainty of the analytical method is ±10 %

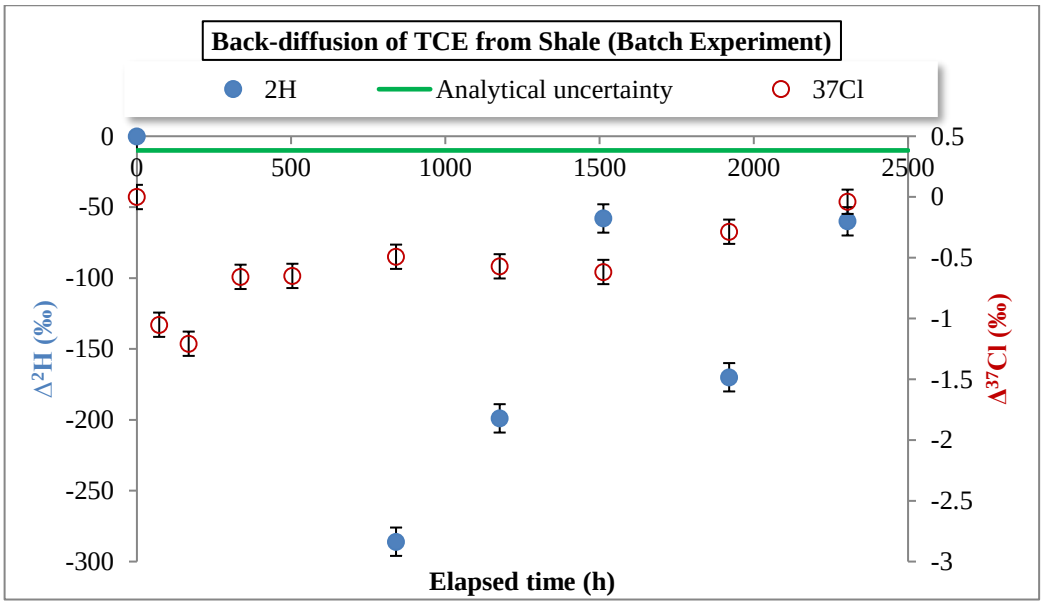

Figure 3-6 Stable hydrogen and chlorine isotopes separations of back-diffused TCE from shale vs time; the uncertainty of the analytical methods for Cl and H isotopes are ±0.1 ‰ and ±10 ‰, respectively

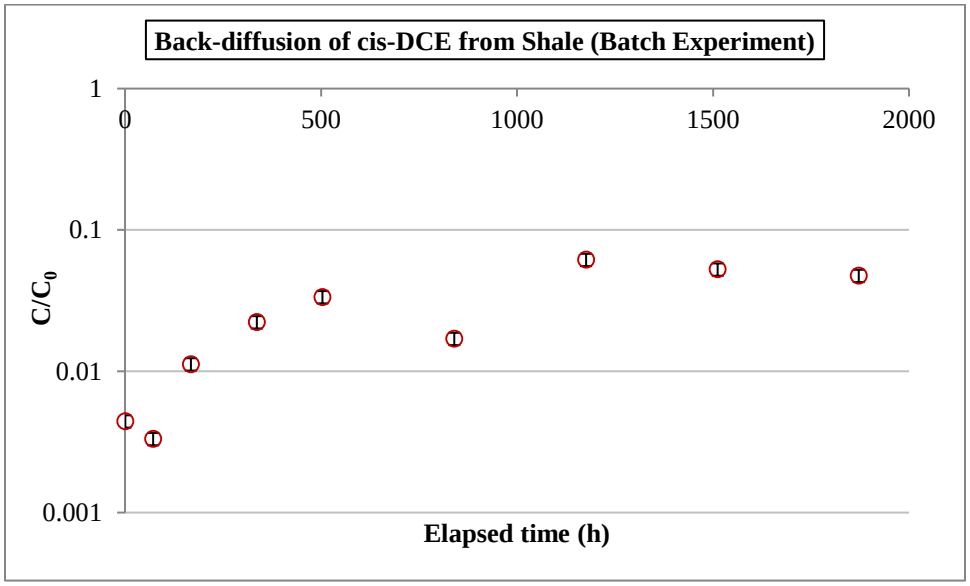

Figure 3-7 Relative concentration of back-diffused *cis*-DCE from shale vs time; the uncertainty of the analytical method is ±10 %

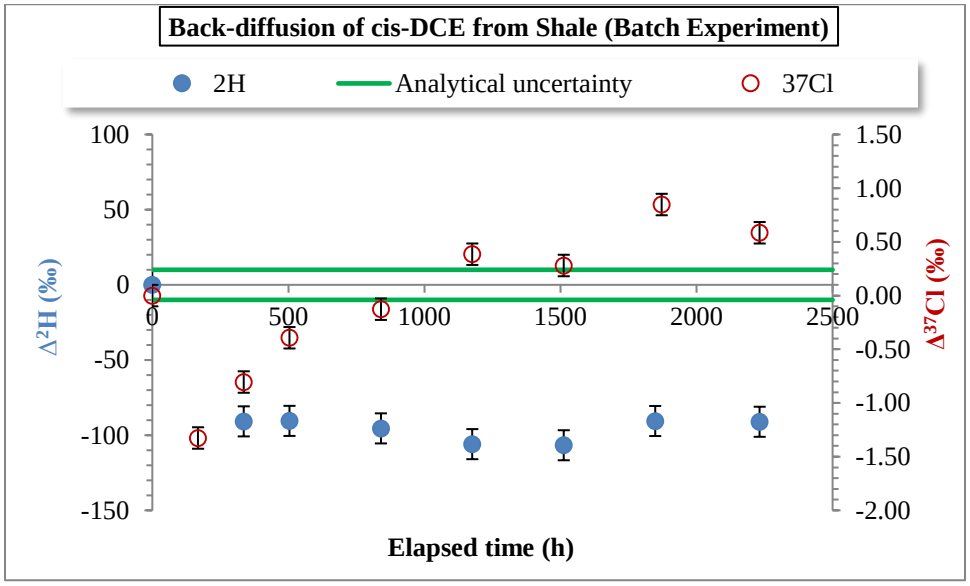

Figure 3-8 Stable hydrogen and chlorine isotopes separations of back-diffused *cis*-DCE from shale vs time; the uncertainty of the analytical methods for Cl and H isotopes are ±0.1 ‰ and ±10 ‰, respectively

The amount of back-diffused *cis*-DCE by the end of the experiment was about 4.8% of the original mass (Figure 3-7), which is slightly higher compared with back-diffused TCE which was 4.2% (Figure 3-5). The reason is the smaller molecular mass of *cis*-DCE (96.9 g/mol) compared to TCE (131.4 g/mol), and also smaller molar volume of *cis*-DCE (75.7 cm^3/mol) compared to TCE (90.2 cm^3/mol) as both properties have an inverse relationship with molecular diffusivities (Schwarzenbach, et al. 1993). The isotope results (Figure 3-8) showed that *cis*-DCE molecules with light chlorine isotopes back-diffused first with a maximum $\Delta^{37}Cl$ of -1.33 ‰. Half-way through the experiment, Cl isotope ratios of the back-diffused *cis*-DCE reached the original *cis*-DCE isotopic signature and then the isotopic ratios became more positive than isotopic ratios of the original *cis*-DCE. The reason for observing more positive isotopic ratios than the original *cis*-DCE is that light isotopologues were lost in the system which could be either due to the sorption of the light isotopologues to the sand, and/or diffusion of light isotopologues through the septum that covers the bottle. Hydrogen isotope ratios of back-diffused *cis*-DCE (Figure 3-8) were depleted compared with the isotope ratios of the original *cis*-DCE. A maximum $\Delta^{2}H$ of -106 ‰ was observed for this experiment. The isotope ratios stayed negative throughout the experiment, which indicated that heavy H isotopologues were strongly attached to organic carbon in shale (Figure 3-8).

3.4.1.2 Dolostone and TCE/*cis*-DCE Back-diffusion Batch Experiments

Stable isotopes and concentration results for dolostone and TCE, and dolostone and *cis*-DCE batch experiments are shown in Figure 3-9 to Figure 3-12. TCE relative concentration results (Figure 3-9) showed that 2.8% of TCE from dolostone back-diffused to the water above the sand layer by the end of the experiment. The isotope results (Figure 3-10) revealed that TCE molecules with lighter chlorine isotopes back-diffused faster as expected and then the isotopic signature of the solution shifted toward the original isotopic signature of TCE. A maximum $\Delta^{37}Cl$ of -0.63 ‰ was observed for this experiment. Hydrogen isotopes of TCE did not show a specific trend throughout the experiment (Figure 3-10). However, most of the diffused isotopes had lower isotopic ratios than the original isotopic ratio of TCE, meaning that the lighter H isotopologues back-diffused first. The first few samples could not be analyzed for H isotope ratios because the concentrations were below the minimum concentration needed for H isotope analysis which is 100 µg/L.

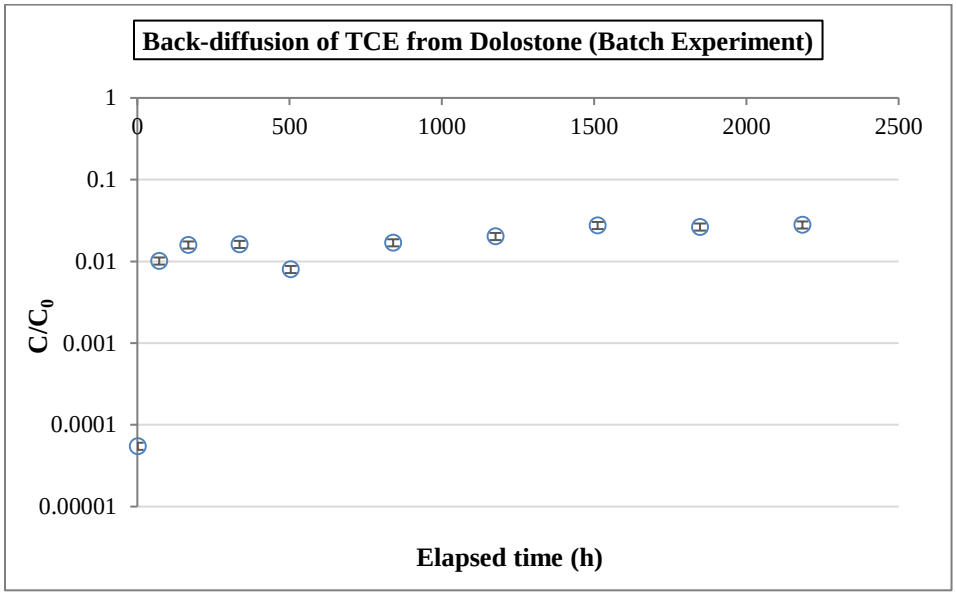

Figure 3-9 Relative concentration of back-diffused TCE from dolostone and vs time; the uncertainty of the analytical method is ±10 %

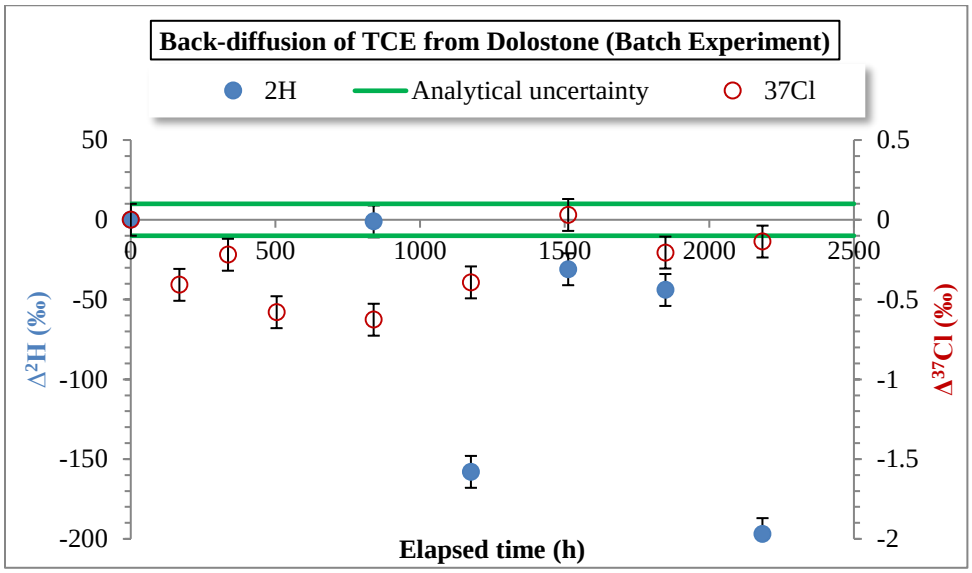

Figure 3-10 Stable hydrogen and chlorine isotopes separations of back-diffused TCE from dolostone vs time; the uncertainty of the analytical methods for Cl and H isotopes are ±0.1 ‰ and ±10 ‰, respectively

Relative concentration results of *cis*-DCE (Figure 3-11) showed that 4.4% of the original *cis*-DCE back-diffused from dolostone into the water above the sand layer by the end of the experiment. The comparison of the relative concentration results from dolostone/TCE batch experiments and dolostone/*cis*-DCE batch experiments showed that the amount of back-diffused *cis*-DCE was higher than TCE which was due to the smaller molar mass and molar volume of *cis*-DCE as discussed in the previous section. Stable isotope results (Figure 3-12) showed that *cis*-DCE molecules with lighter chlorine isotopes back-diffused within the first 500 hours of the experiment and the isotope separation was very small ($\Delta^{37}Cl$ = -0.28 ‰). The isotopic ratio of the solution became enriched relative to the initial isotopic ratio after 500 hours were elapsed. A maximum $\Delta^{37}Cl$ of 1.66 ‰ was observed by the end of the experiment which was significant considering the total analytical uncertainty for $\delta^{37}Cl$ analyses which is ±0.1 ‰. The reason behind enrichment of the samples after 500 hours could be the diffusion of lighter isotopologues of *cis*-DCE through the septa covering the bottles, and/or sorption of lighter isotopologues to the sand grains. This is an important phenomenon and need to be further investigated as it might be mistaken with biodegradation process. The trend for Cl isotope evolution was similar to the trend for shale and *cis*-DCE back-diffusion batch experiments (Figure 3-8). The results for H isotope of *cis*-DCE (Figure 3-12) showed a maximum $\Delta^{2}H$ of -34 ‰, which was very small compared with $\Delta^{2}H$ estimated from the other batch experiments. Nonetheless, most of the back-diffused isotopologues had lower isotopic ratios relative to the original isotopic ratios of *cis*-DCE.

Concentration results from all four experiments showed that *cis*-DCE back-diffused faster than TCE due to its smaller molar mass and volume. Hydrogen isotope separations of TCE and *cis*-DCE were in the range of -34 ‰ to -286 ‰. The total analytical uncertainty for $\delta^{2}H$ analyses is typically ±10 ‰ and therefore, isotope fractionations larger than 20 ‰ must be considered when interpreting the isotope data. Chlorine isotope separations were in the range of -0.28 ‰ and -1.33 ‰ which were larger than the total analytical uncertainty for $\delta^{37}Cl$ analyses (±0.1 ‰). However, the isotope ratios were depleted in ^{37}Cl which is in contrast with the evolution of isotope ratios during biodegradation. Also, the isotope separations were small compared to the fractionations reported for degradation of TCE and *cis*-DCE (Abe, et al. 2009; Cretnik, et al. 2013; Kuder, et al. 2013). Nonetheless, the enrichment of the back-diffused *cis*-DCE in the water due to diffusion of light isotopologues out of the system should be considered as this process can be mistaken with biodegradation which causes enrichment of the remaining solution in heavy isotopologues of *cis*-DCE.

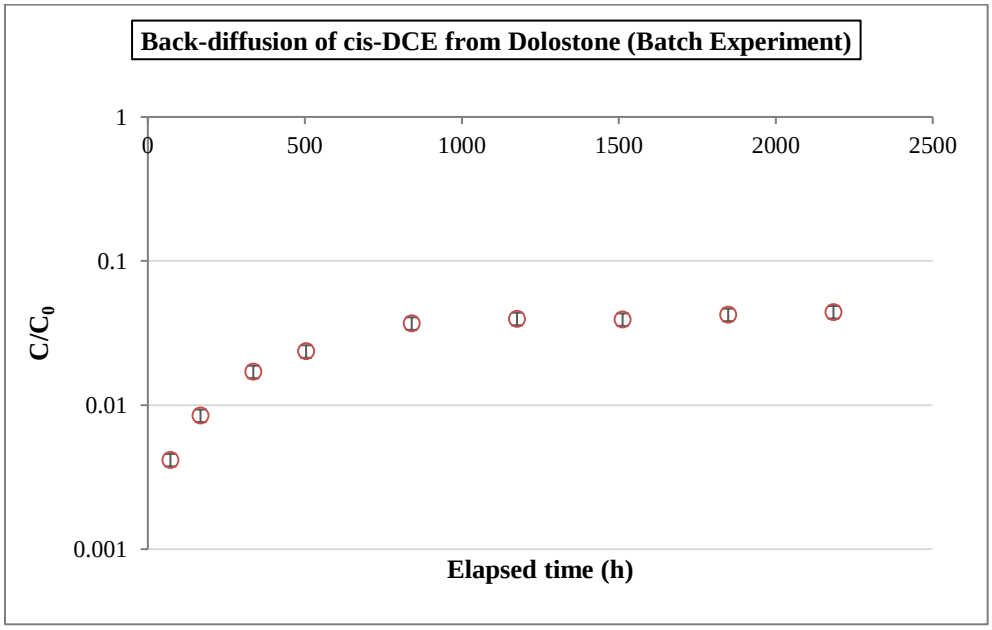

Figure 3-11 Relative concentration of back-diffused *cis*-DCE from dolostone vs time; the uncertainty of the analytical method is ±10 %

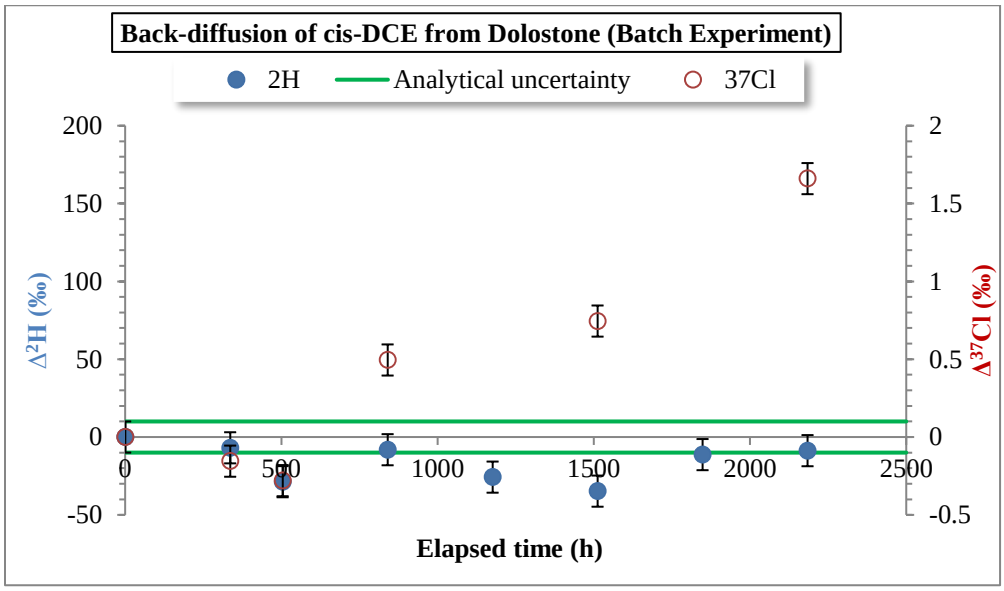

Figure 3-12 Stable hydrogen and chlorine isotopes separations of back-diffused *cis*-DCE from dolostone vs time; the uncertainty of the analytical methods for Cl and H isotopes are ±0.1 ‰ and ±10 ‰, respectively

3.4.2 Laboratory Box Experiment

3.4.2.1 Concentration Results

Aqueous samples were collected from the source solution and the effluent for TCE and *cis*-DCE concentration, Br^- and Cl^- concentration, and stable isotope analyses while the contaminant was injected into the box. Once the contaminant source was switched with clean water, samples were only collected from the effluent. The initial TCE and *cis*-DCE concentrations in the source solution were 68 mg/L and 101 mg/L, respectively. The source solution was transferred to a collapsible Teflon bag to prevent the creation of headspace when the solution was injected into the box. Aqueous samples were collected from the source solution during 45 days of contaminant injection. The concentration results of TCE and *cis*-DCE in the source solution (Figure 3-13) showed that there was a contaminant mass loss during the experiment, which was due to the diffusion of the contaminants into the air through the Teflon bag. The concentrations results of TCE and *cis*-DCE as well as the nonreactive tracers (Cl^- and Br^-) are shown in Figure 3-14 and Figure 3-15.

Figure 3-16 shows the comparison of the measured breakthrough of the nonreactive tracers, and the case that the mass loss due to diffusion is absent. The data for the first 45 days of the experiments were shown during which the contaminants were injected into the box. The case with no diffusive loss was simulated using an analytical solution for one-dimensional solute transport with a type I (Dirichlet) boundary condition (ONED_1) developed by Neville (2001). More information on the analytical solution and the parameters used for the simulation can be found in Appendix D. As seen in Figure 3-16, the results showed a delay in breakthrough of the nonreactive tracers, which was due to transverse molecular diffusion.

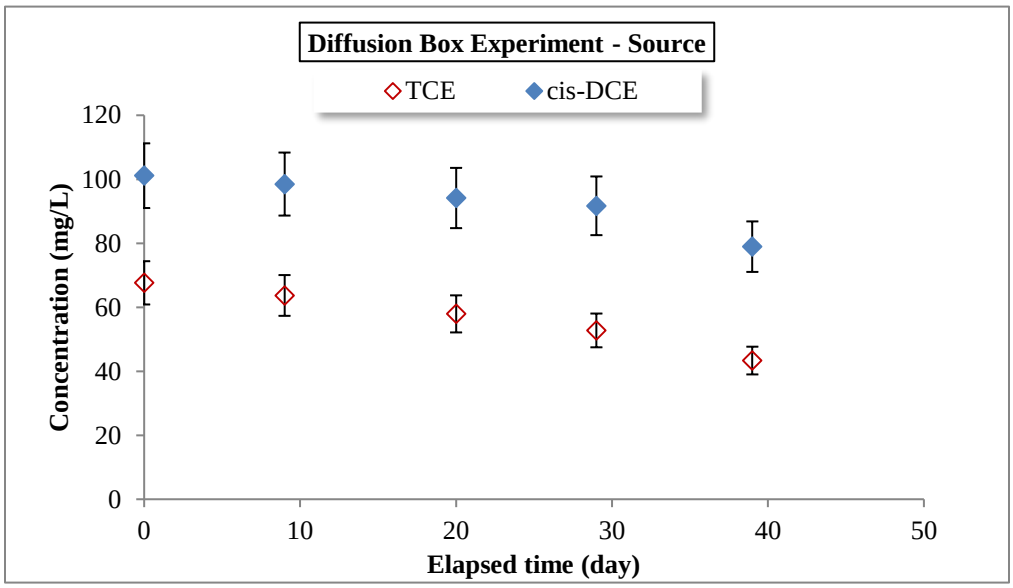

Figure 3-13: Concentration results of TCE and *cis*-DCE in the source solution; the uncertainty of the analytical method is ±10 %

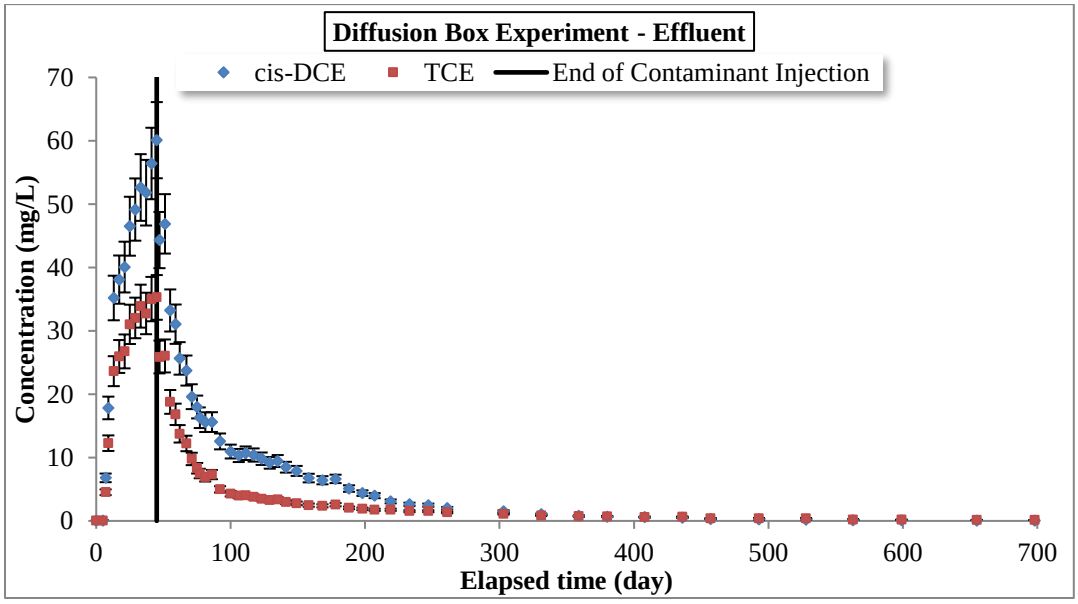

Figure 3-14 TCE and *cis*-DCE concentrations of the effluent from the sand layer; the uncertainty of the analytical method is ±10 %

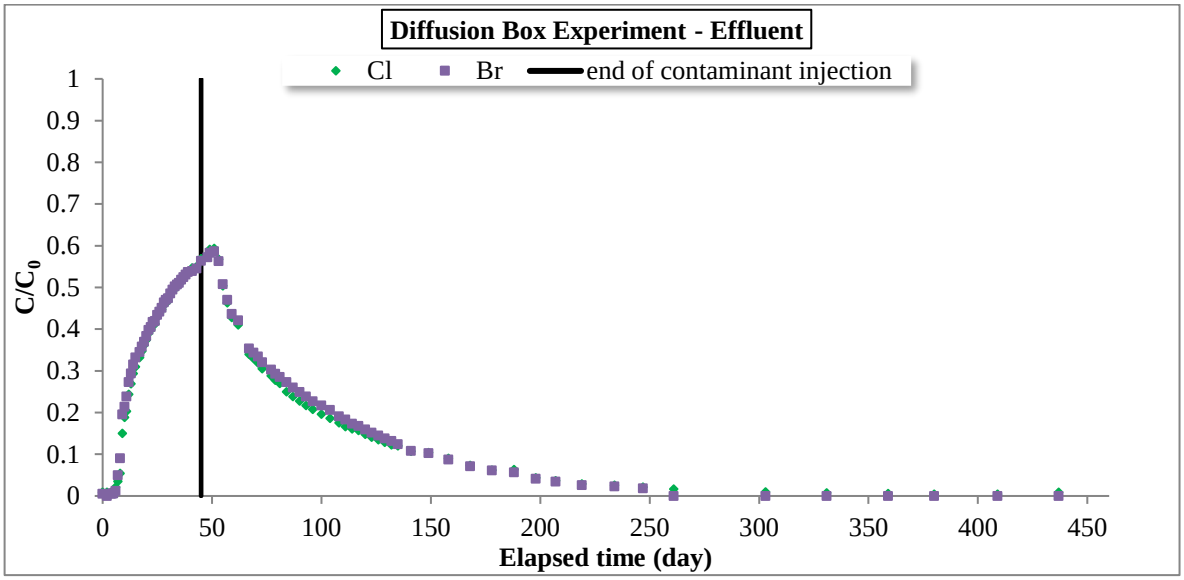

Figure 3-15 Relative concentrations of nonreactive tracers in the effluent of the sand layer

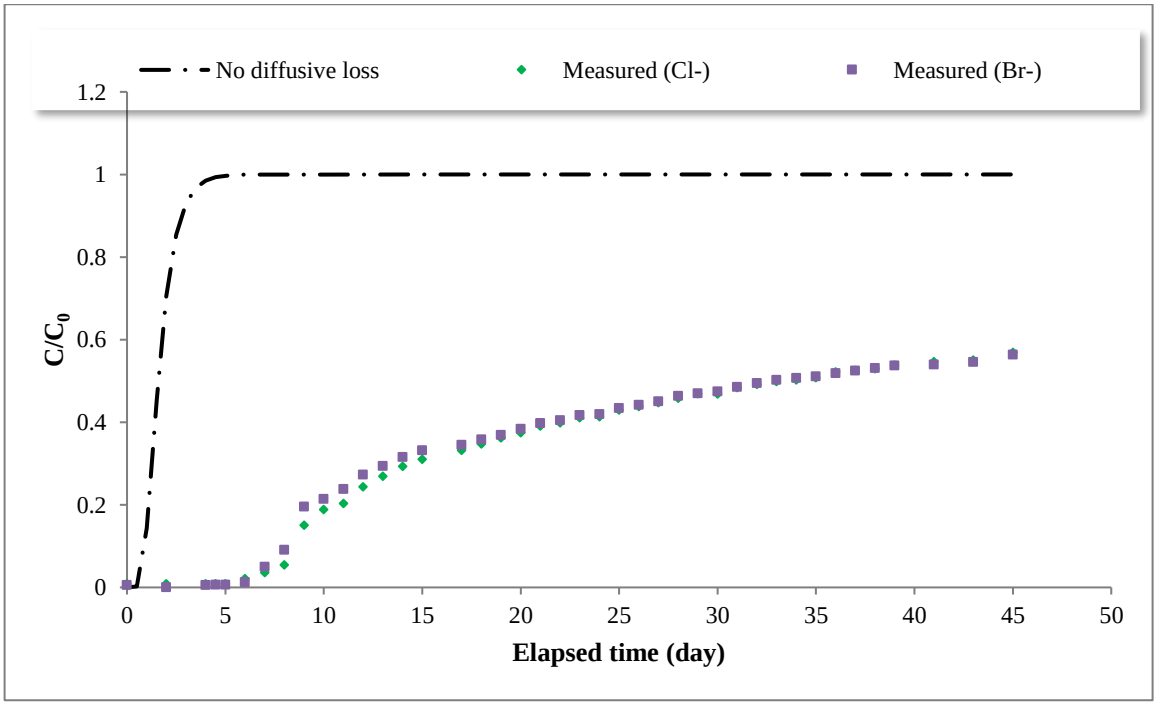

Figure 3-16 Comparison between the measurements and simulated no diffusive loss

The kaolin that was used for this experiment contained 0.0346% dry organic carbon (Agriculture and Food Laboratory at the University of Guelph, Guelph, Ontario, Canada). Therefore, adsorption of contaminants onto the organic carbon, as well as diffusion of contaminant into the clay layers was expected to take place. The total amount of TCE and *cis*-DCE adsorbed to sand/clay, diffused into the clay, and desorbed/back-diffused from sand/clay was estimated through the following steps:

1) Estimation of the total mass of TCE and *cis*-DCE entering the box during 45 days, M(in), using the following equation:

$$\boldsymbol{M(in)[mg] = \sum_{i=1}^{45} Q\ [L/day] \times C(in)_i[mg/L]} \qquad 3\text{-}3$$

where Q is the flow rate and $C(in)_i$ is the contaminants concentration during days 1 to 45 of contaminant injection

2) Estimation of the mass discharged from the box during 50 days (45 days of contaminant injection plus the residence time for removing one pore volume, which was 5 days), M(out), using the following equation:

$$\boldsymbol{M(out)[mg] = \sum_{i=1}^{45} Q\ [L/day] \times C(out)_i[mg/L]} \qquad 3\text{-}4$$

3) Estimation of the mass that was remained in the box (i.e. mass diffused and sorbed) after 45 days of contaminant injection by subtracting the values obtained in step 2 from the values obtained in step 1.

4) Estimation of the mass discharged from the box during 664 days of flushing the system with clean water (i.e. the mass back-diffused from the clay layers, desorbed from clay and sand, and flushed from the pores in the sand layer) through the following equation:

$$\boldsymbol{M(out)[mg] = \sum_{i=46}^{669} Q\ [L/day] \times C(out)_i[mg/L]} \qquad 3\text{-}5$$

5) The amount of TCE and *cis*-DCE remained in the box at the end of experiment can be estimated by subtracting the mass discharged during the 664 days of flushing the system with clean water (step 4) from the mass remained in the box after 50 days (step 3).

The flow rate (Q) was 0.2 L/day throughout the experiment. The values obtained for each step are summarized in Table 3-1. The mass units are reported in mmol to facilitate the comparison of the

Table 3-1 Summary of the mass balance during 45 days of contaminant injection and 669 days of flushing the system with clean water

Compound	Initial concentration (mmol/L)	Mass in (mmol)	Mass out (mmol)	Mass sorbed/diffused (mmol)	Mass desorbed/back-diffused (mmol)	Mass remained in the box (mmol)
TCE	0.52	3.87	1.87	1.99	1.71	0.29
cis-DCE	1.04	8.67	3.98	4.69	4.58	0.10

results for TCE and *cis*-DCE. The results indicate that approximately 60% of the *cis*-DCE mass entered the box diffused/sorbed, and around 57% of the TCE mass entered the box diffused/sorbed. It appears that *cis*-DCE diffused slightly more than TCE due to its smaller molar volume and mass. However, around 98% of the diffused/sorbed *cis*-DCE back-diffused/desorbed during 669 days of flushing the system with clean water, while 87% of the diffused/sorbed TCE back-diffused/desorbed. This is an indication of the higher rate of back-diffusion of *cis*-DCE molecules relative to TCE molecules. The reason behind this phenomenon is the smaller molar mass and volume of *cis*-DCE molecules.

3.4.2.2 Stable Isotope Results

Stable Isotope Results of the Source: The isotope results of the samples collected from the source solution during 41 days showed that TCE and *cis*-DCE in the source solution became gradually enriched in ^{2}H and ^{37}Cl (Figure 3-17 and Figure 3-18). The overall change in H isotope ratios of TCE and cis-DCE was +74 ‰ and +67 ‰, respectively (Figure 3-17). The shift in chlorine isotope ratios of TCE and *cis*-DCE was within the uncertainty of analytical method for $\delta^{37}Cl$ analyses (±0.1 ‰) for the first 30 days. However, TCE and *cis*-DCE in the source solution became enriched in ^{37}Cl by +0.73 ‰ and +0.31 ‰, respectively, on day 41 (Figure 3-18). As discussed in the previous section, concentration results showed that there was a diffusive mass loss of TCE and *cis*-DCE in the source solution. Therefore, the enrichment of ^{37}Cl and ^{2}H in the source solution can be explained by diffusion of the light isotopologues out of the Teflon bag.

Hydrogen Isotope Results of TCE: The isotope results of the effluent samples from the sand layer are shown in Figure 3-19. In order to plot the data based on isotope separation (Δ), the average δ-values of the source solution was subtracted from δ-values of the effluent. As seen in Figure 3-19, the effluent samples were depleted in ^{2}H relative to the source solution for the first 21 days of the experiment. As discussed in the previous chapter, the results from the sorption experiments revealed that heavier H isotopologues adsorbed to the solid phase and the liquid phase became depleted in heavier H isotopologues. Therefore, the depletion of the effluent in ^{2}H indicates that the system was dominated by sorption during the early stages of the experiment and molecules with heavy H isotopes were being sorbed onto the sand and clay surfaces (Figure 3-19). The difference between the H

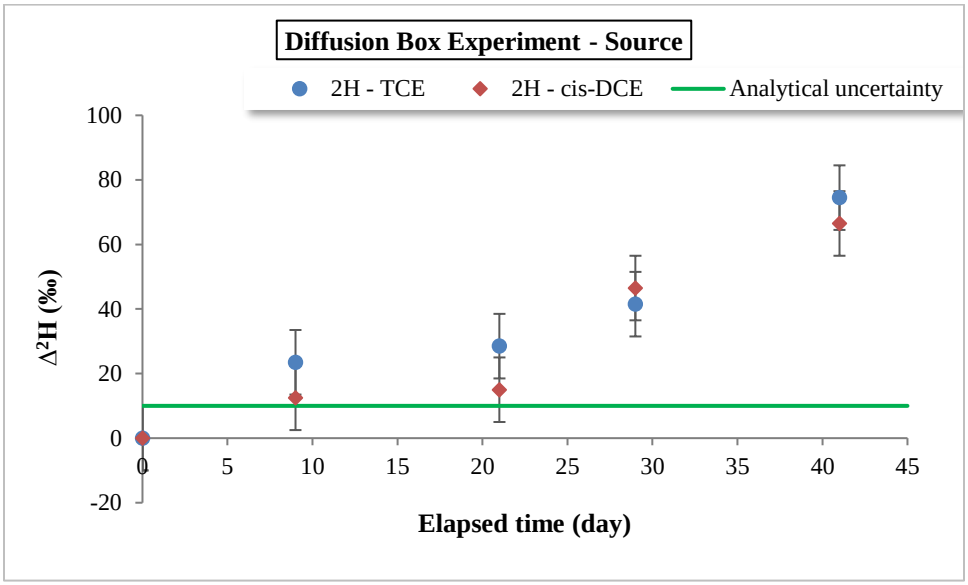

Figure 3-17 Evolution of hydrogen isotopic ratios of TCE and *cis*-DCE in the source solution

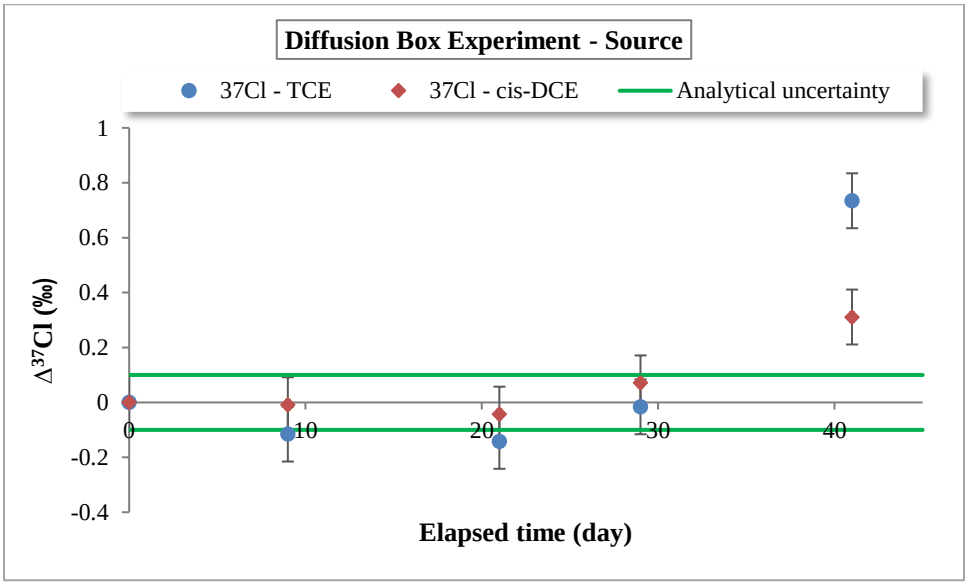

Figure 3-18 Evolution of chlorine isotopic ratios of TCE and *cis*-DCE in the source solution

isotope ratios of the source solution and the effluent became similar around day 29, indicating that diffusion process became the dominant process since diffusion causes the enrichment of heavy isotopologues in the liquid phase (LaBolle, et al. 2008). The H isotope ratios of the effluent became enriched compared with the ones of the source solution increasingly and reached a maximum isotope separation of 123 ‰ on day 62 (which was 17 days after the contaminant source was replaced with clean water). The maximum value was observed one day after the leakage occurred in the box. However, the rise in the isotopic ratios had started before the leakage was happening and therefore, the possibility of the effect of leakage on isotopic ratios is low. Furthermore, there was no abnormality in concentration results (Figure 3-14) and electrical conductivity results (Appendix D) during the leakage period. The peak can be explained by desorption of previously sorbed heavy isotopologues and also further diffusion of light isotopologues into the clay layers which enhanced the isotope enrichment. From day 62 to day 168, the isotopic ratios of the effluent started to decrease but were still highly enriched compared with the source, which indicated that desorption of heavy H isotopologues was still a dominant process. Around day 168, the isotopic ratios of the effluent shifted toward the isotopic ratios of the source solution and remained more or less constant up to day 600. This can be an indication of simultaneous occurrence of back-diffusion of the light H isotopologues and desorption of heavy H isotopologues that kept the isotope ratios of the effluent close to the isotope ratios of the source. The isotopic ratios became slightly enriched after day 600 which might be an indication of back-diffusion of relatively heavier isotopologues from the clay layers or diffusive loss of light isotopologues during the sampling. TCE concentration in the effluent after day 600 was very low (around 0.15 mg/L) and therefore, even small diffusive loss of light isotopologues can result in a pronounced isotope fractionation.

Based on the H isotope results of the effluent samples, the following stages can be defined for transport of TCE molecules: 1) sorption dominated stage from day 1 to 29; 2) sorption and diffusion dominated stage from day 29 to day 45; 3) desorption and diffusion dominated stage from day 45 to 62; 4) desorption dominated stage from day 62 to 168; 5) back-diffusion and desorption dominated stage from day 168 to the end of the experiment. As seen from the results, H isotope showed significant fractionation, and therefore, can provide great details about the physical processes that affect the contaminant transport in the subsurface.

Chlorine Isotope Results of TCE: Figure 3-20 illustrates the isotopic ratios of TCE in the effluent. The data were plotted based on the average Cl isotope ratios of TCE in the source solution. The effluent samples were significantly enriched in ^{37}Cl relative to the source solution at the beginning of the experiment. For example, at day 9 of the experiment, the Cl isotope separation between the effluent and the source solution was +1.68 ‰. The enrichment of the effluent relative to the source solution indicated that either sorption, diffusion, or both processes occurred at the same time since both processes result in the enrichment of ^{37}Cl in the liquid phase. Once the source solution was switched with clean water on day 45, the isotopic ratios of the effluent started to decrease and reached the average isotopic signature of the source solution around day 59. The low isotopic ratios of the effluent could be due to the desorption of the previously sorbed light isotopologues as clean water passed through the system. The isotope enrichment after day 59 might be an indication that desorbed light isotopes were being sorbed again (Figure 3-20). After day 71, the general trend for the isotopic ratios of the effluent is continuous depletion of ^{37}Cl which was related to desorption and back-diffusion of lighter isotopologues.

Based on the Cl isotope results of the effluent samples, the following stages can be defined for TCE molecules: 1) sorption and/or diffusion dominated stage from day 0 to day 45; 2) desorption dominated stage from day 45 to day 59; 3) desorption and back-diffusion dominated stage from day 59 to the end of the experiment.

Both Cl and H isotopes can be used to identify the effect of physical processes affecting the transport of TCE and *cis*-DCE where transformation processes are absent in the subsurface. However, since H isotope fractionation is larger compared with Cl isotope fractionation, compound-specific H isotope analysis provides higher resolution information about the physical processes that affect the contaminant.

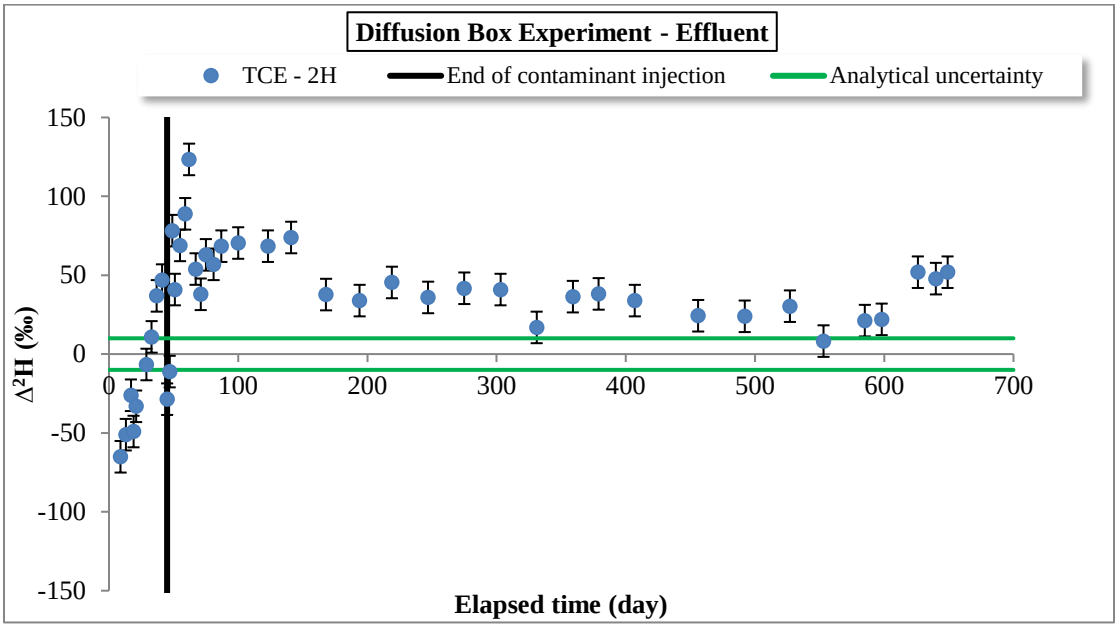

Figure 3-19 Hydrogen isotope separations of TCE in the effluent of sand layer vs time

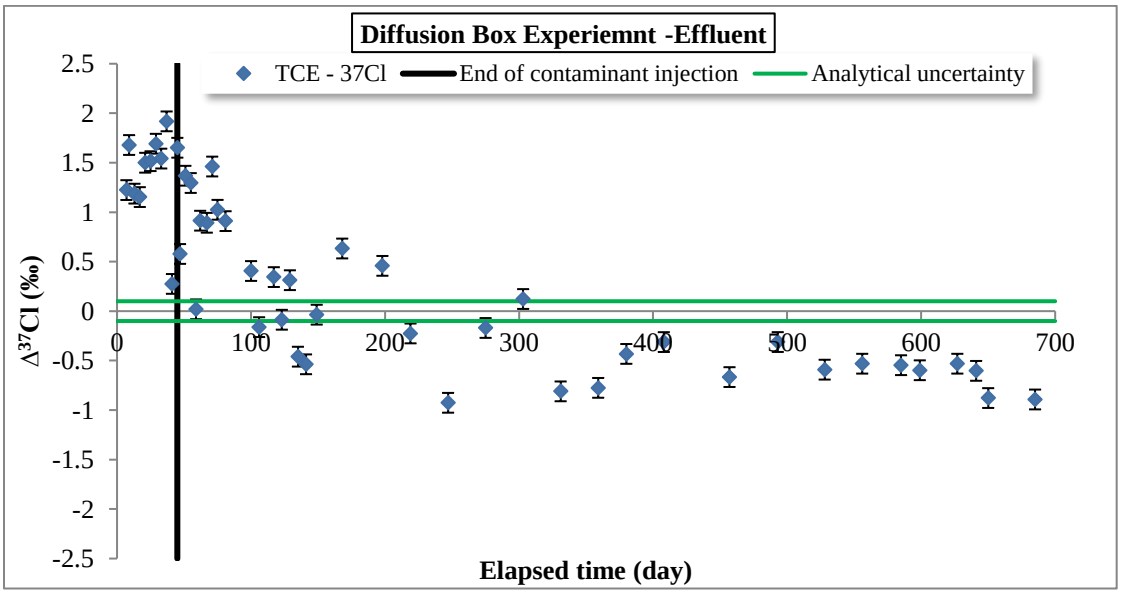

Figure 3-20 Chlorine isotope separations of TCE in the effluent of sand layer vs time

Hydrogen Isotope Results of *cis*-DCE: The isotopic ratios of the effluent during the early times of the experiment is depleted in ^{2}H relative to the isotopic ratios of the source solution (Figure 3-21). As discussed in the previous chapter, sorption caused the depletion of ^{2}H in the aqueous phase, and therefore, depletion of ^{2}H in the effluent was most likely due to the sorption of heavy H isotopologues at the early stages of the experiment. The isotopic ratios of the source solution and effluent samples became similar around day 25 suggesting that diffusion became the dominant process since diffusion causes enrichment of ^{2}H in the aqueous phase and acts against the sorption process in which the aqueous phase becomes depleted in ^{2}H. The H isotopic ratios of the effluent gradually increased and reached a maximum isotope separation of 144 ‰ on day 59 (which was 14 days after the contaminant source was replaced with clean water). The reason behind this phenomenon could be desorption of previously sorbed heavy H isotopologues and also diffusion of light H isotopologues into the clay layer, which enhanced the enrichment of ^{2}H in the aqueous phase. After day 59, the isotopic ratios started to decrease and reached the average isotopic ratios of the source solution around day 168. During that time period, the isotopic ratios of the effluent were still higher compared with the ones of the source solution which could be an indication of desorption of previously sorbed heavier H isotopologues of *cis*-DCE. The isotopic ratios of the effluent started to increase after day 168 and diverged from the isotopic signature of the source solution significantly around day 380 ($\Delta^{2}H$ = +82 ‰) and stayed enriched to the end of the experiment. The isotope enrichment can be explained by the following two scenarios: 1) if the diffused *cis*-DCE in the clay is considered as a secondary source of contamination, the light isotopologues back-diffused first; and as the back-diffusion process advanced and the source became depleted in light isotopologues, the heavy isotopologues started to diffuse back into the water inside the sand layer; 2) diffusive loss of light isotopologues from the system while the samples were collected. The results from the source solution also showed that the solution inside the Teflon bag became enriched in ^{2}H over time, therefore, the possibility of light isotoplogues loss in the system existed. This experiment can be divided into the following stages based on the H isotope results: 1) sorption dominated stage from day 1 to 25; 2) sorption and diffusion dominated stage from day 25 to 45; 3) desorption and diffusion dominated stage from day 45 to 59; 4) desorption dominated stage from day 59 to 168; 5) back-diffusion dominated stage from day 168 to the end of the

experiment. The stages identified based on the H isotopes of *cis*-DCE are matching with the stages identified for TCE.

Chlorine Isotope Results of *cis*-DCE: The effluent samples (Figure 3-22) at the beginning of the experiment showed a significant enrichment in ^{37}Cl (with a maximum Δ value of +2 ‰ at day 9), which could be an indication that either sorption, diffusion, or both processes were taking place. Sorption favors molecules with light Cl isotope, which results in enrichment of the aqueous phase in ^{37}Cl. Similarly, molecules with light Cl isotope diffuse into the low permeability zone, which result in enrichment of the aqueous phase in heavy Cl isotopologues. The isotope ratios of the effluent dropped gradually and reached the isotopic ratios of *cis*-DCE in the source solution around day 59. The drop in isotopic ratios can be related to desorption of previously sorbed light isotopologues. However, during this time period, the isotopic ratios of the effluent were still higher relative to the source solution indicating that diffusion of light isotopologues was still taking place. The isotope separation of the effluent reached a minimum value of -0.84 ‰ around day 100. This is an indication of desorption of light isotopologues from the clay minerals and sand, and back-diffusion of light isotopologues from the clay layers into the water flow. After day 100, the Cl isotopic ratios gradually increased and shifted toward more positive values. The reason behind enrichment of the effluent samples in ^{37}Cl could be back-diffusion of heavier isotopologues from the clay layers as the clay layers became depleted in lighter isotopologues. However, a possibility that light Cl isotopologues escaped while samples were collected was also existed. Since the concentrations of *cis*-DCE in the effluent samples from day 380 onward were low (between 0.72 mg/L on day 380 and 0.16 mg/L on day 714), a small concentration loss resulted in pronounced isotope fractionations.

Based on the Cl isotope results of *cis*-DCE in the effluent samples from the sand layer, the following stages can be defined: 1) sorption and/or diffusion dominated stage from day 1 to 45; 2) desorption and diffusion dominated stage from day 45 to 59; 3) desorption and back-diffusion dominated stage from day 59 to 200; 4) back-diffusion dominated stage from day 200 to the end of the experiment.

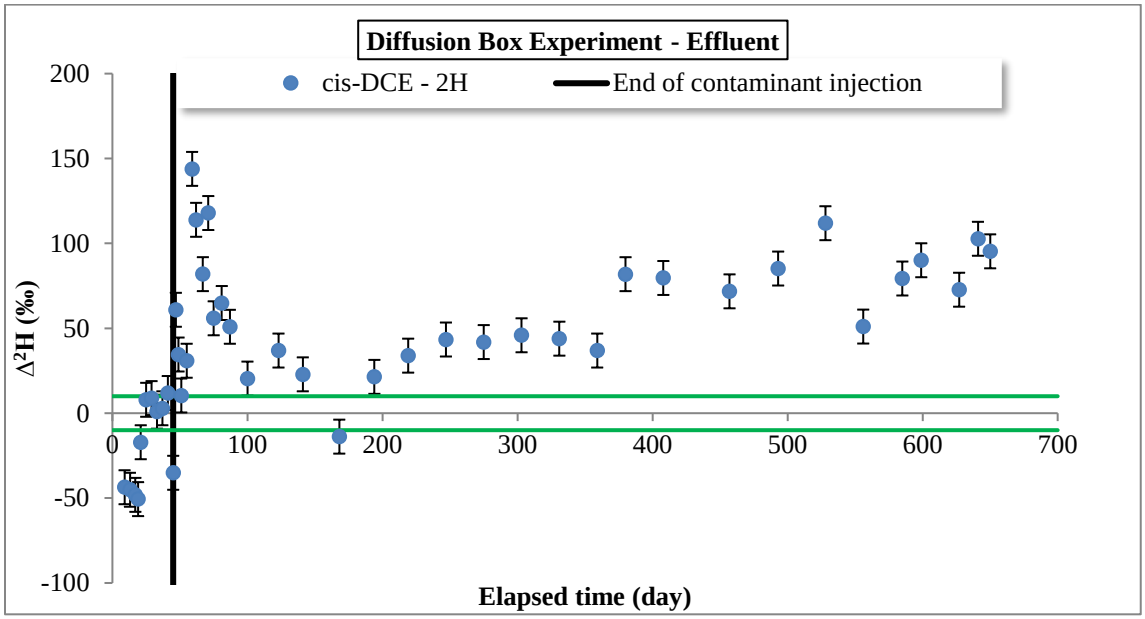

Figure 3-21 Hydrogen isotope separations of *cis*-DCE in the effluent of sand layer vs time

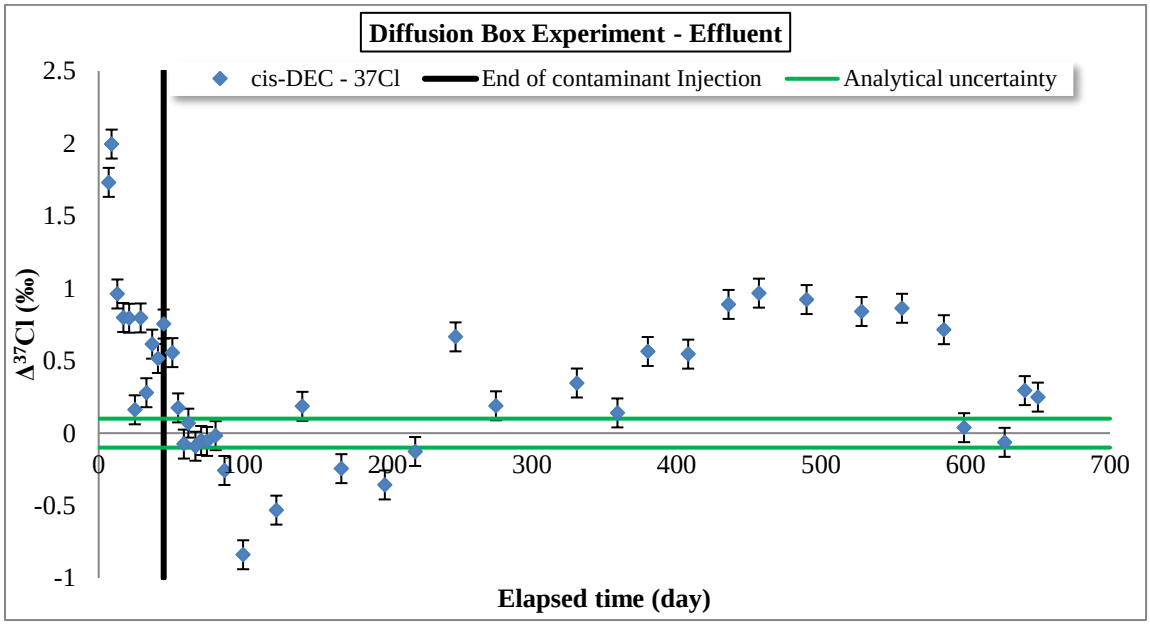

Figure 3-22 Chlorine isotope separations of *cis*-DCE in the effluent of sand layer vs time

3.5 Summary and Conclusion

A series of laboratory batch and column experiments was performed to evaluate the effect of diffusion and back-diffusion on Cl and H stable isotopes of TCE and *cis*-DCE under static and dynamic conditions. Ground shale and dolostone with organic carbon content of 0.6 % dry and 0.4 % dry, respectively, were used for the back-diffusion batch experiments. The batch experiments results showed that back-diffusion of TCE and *cis*-DCE from shale and dolostone caused observable Cl isotope fractionations and significant H isotope fractionations. Chlorine isotope separation ($\Delta^{37}Cl$) ranged between -0.28 ‰ (maximum separation for dolostone and *cis*-DCE experiment) and -1.33 ‰ (maximum separation for shale and *cis*-DCE experiment). Hydrogen isotope separation ($\Delta^{2}H$) was in a range of -35 ‰ (maximum separation for dolostone and *cis*-DCE experiment) and -286 ‰ (maximum separation for shale and TCE experiment).

Chlorine isotope results of TCE for both experiments using shale and dolostone indicated that light isotopologues back-diffused first, followed by the back-diffusion of heavier isotopologues until isotopic signature of the solution reached the isotopic signature of the source. However, chlorine isotopes of *cis*-DCE for both experiments with shale and dolostone showed a different behavior. At the beginning of the experiment, the isotopic ratios of the back-diffused *cis*-DCE was depleted compared with the original isotopic ratios of *cis*-DCE indicating that light Cl isotopologues back-diffused faster as expected. However, halfway through the experiment, isotopic ratios of the back-diffused *cis*-DCE became enriched compared with the original isotopic ratios of *cis*-DCE. The enrichment was significant (a maximum isotope separation of +0.85 ‰ for shale and *cis*-DCE experiment and a maximum isotope separation of +1.66 ‰ for dolostone and *cis*-DCE experiment) when compared with the uncertainty of analytical methods for $\delta^{37}Cl$ analyses which is ±0.1 ‰. A possible explanation for this behavior is that back-diffused *cis*-DCE molecules with light Cl isotopes diffused into the air through the septum that was covering the bottle. Since the concentrations of back-diffused *cis*-DCE in the water was very low even a small diffusive loss of light Cl isotopologues could result in a pronounced isotope fractionation. Another possible explanation for isotope enrichment could be sorption of the molecules with light Cl isotopes to the sand could have occurred as they moved upward.

In terms of H isotopes, most of the back-diffused TCE and *cis*-DCE molecules had lower isotopic ratios compared to the original isotopic ratios of TCE and *cis*-DCE. However, the isotopic ratios did

not reach the original isotopic ratios of TCE and *cis*-DCE during the time period of our experiments suggesting that the heavier H isotopologues were strongly sorbed to the organic carbon in shale and dolostone.

The effect of diffusion and back-diffusion processes on isotope fractionation of TCE and cis-DCE was investigated using a simulated stratified aquifer – aquitard system such that a thin layer of Ottawa silica sand (thickness of 3 cm) was placed between two layers of kaolin (thickness of 8.5 cm). Hydrogen isotopes showed significant fractionations and chlorine isotopes showed noticeable fractionations throughout the experiment. Since sorption and diffusion had an opposite effect on H isotope fractionation (i.e. sorption caused depletion of ^{2}H in the aqueous phase while diffusion caused enrichment of ^{2}H in the aqueous phase), compound-specific H isotope analysis can be used to distinguish between those two processes in the field. The extent of H isotope fractionation of TCE and cis-DCE during diffusion and back-diffusion was larger than the one observed for biodegradation of TCE (Kuder, et al. 2013). Furthermore, our results from biodegradation of TCE by KB-1® revealed small H isotope fractionation of TCE and cis-DCE (Appendix C) which were either within or slightly above the uncertainty of analytical method for $\delta^{2}H$ analyses (±10 ‰). Therefore, shifts in H isotopic ratios of chlorinated ethenes in the subsurface indicate that physical processes are affecting the contaminants movement. Chlorine isotopes results from the box experiment revealed remarkable enrichments for TCE and *cis*-DCE, specifically at the early stages of the experiment during which both sorption and diffusion processes were dominant (both processes result in enrichment of aqueous phase in ^{37}Cl). Maximum ^{37}Cl enrichments of +1.9 ‰ and +2‰ were observed for TCE and *cis*-DCE, respectively during the early stages of the experiment when the contaminant solution was introduced to the system. Therefore, for the expanding young contaminant plumes in the subsurface with a high possibility of sorption and diffusion of chlorinated ethenes, enrichment of chlorine isotope can be mistaken with enrichment due to biodegradation.

The isotope results from the back-diffusion batch experiments and the box experiment showed that the back-diffused *cis*-DCE molecules were enriched in ^{37}Cl compared with the original *cis*-DCE. We believe that this phenomenon was related to the diffusive loss of light isotopologues of *cis*-DCE out of the system. This hypothesis can be supported by the enrichment of the source solution in heavy Cl isotopologues of *cis*-DCE inside the Teflon bag for the box experiment. Therefore, in the subsurface

where the diffusive loss of *cis*-DCE into the unsaturated zone is taking place, one need to be careful when interpreting the enrichment of Cl isotope.

Chapter 4
Conclusions and Recommendations

4.1 Conclusions

A series of laboratory batch, column, and box experiments were performed using different porous media to investigate the effect of sorption, diffusion, and back-diffusion processes on stable carbon, chlorine, and hydrogen isotopes fractionation of TCE and *cis*-DCE. To our knowledge, this is the first study on chlorine and hydrogen CSIA of TCE and *cis*-DCE undergoing sorption and diffusion processes. Previous studies on C isotope fractionation of chlorinated ethenes (Slater, et al. 2000; Schuth, et al. 2003b) revealed that sorption has negligible effect on C isotopes of TCE. This study revealed that sorption caused noticeable enrichment of ^{37}Cl in the aqueous phase and significant depletion of ^{2}H in the aqueous phase. The results for Cl isotopes were consistent with previous studies that found sorption causes enrichment of heavy isotopes in the solution (Caimi and Brenna. 1997; Poulson, et al. 1997; Kopinke, et al. 2005). The counterintuitive behavior of H isotope might be due to different vibrational energies for molecules with different isotopes. Further investigations using theoretical and computational chemistry is needed to better understand sorption mechanisms of chlorinated ethenes to soil organic carbon. By means of computational chemistry, the molecules can be modeled to find out the sorption energies for different isotopologues of a given compound, and therefore, understand the behavior of different isotopologues during sorption (Schauble, et al. 2001; Schauble, et al. 2004; Black, et al. 2011).

Chlorine and carbon enrichment factors of *cis*-DCE and TCE obtained for sorption experiments (Table 2-2) were very small compared with the values listed in Table 1-1 for degradation. Therefore, at field sites with biodegradation as a dominant process, the effect of sorption on Cl and C isotope fractionations can be neglected. Hydrogen isotope results revealed that fractionations due to sorption were substantial. However, H isotope fractionations of chlorinated ethenes due to biodegradation have not been widely investigated yet and we cannot comment on utilizing compound-specific hydrogen analysis to distinguish between different processes in the field. Nonetheless, in the absence of biodegradation process, compound-specific hydrogen analysis can be as a tool to confirm whether sorption affects contaminant transport in the subsurface.

During the back-diffusion process, TCE and *cis*-DCE molecules with lighter chlorine and hydrogen isotopes diffused faster as expected and isotopic signature of the solution gradually reached the

isotopic signature of the original solution. Chlorine isotopes ratios of *cis*-DCE reached the original isotopic ratios halfway through the experiments and became remarkably enriched compared to the initial isotopic ratios. The reason could be either diffusion of *cis*-DCE molecules with light Cl isotope into the air through septa covering the bottles and/or sorption of *cis*-DCE with light chlorine isotope to the sand surface. This phenomenon need to be considered when interpreting the isotope data from contaminant plumes which have the possibility of diffusive mass loss.

A laboratory box experiment was performed to investigate the effect of sorption, diffusion, desorption, and back-diffusion processes on H and Cl isotope ratios of TCE and *cis*-DCE under dynamic conditions. In general, as a contaminant plume is expanding in the subsurface on top of a low permeability zone, part of the contaminant is adsorbed to the material in the aquifer and aquitard and part of the contaminant diffuses into the low permeable zone. Once the contaminant concentration in the aquifer decreases, the sorbed contaminant is becoming desorbed and the diffused contaminant re-enters the aquifer. The isotopic results (especially H isotope) from the box experiment clearly showed the processes that the contaminants went through. At the beginning of the experiment, H isotope ratios of TCE and *cis*-DCE in the effluent sample was lower relative to the source solution, which showed that sorption was the dominant process and molecules with heavy H isotopes were adsorbed. The isotope ratios of the effluent gradually increased and became similar to the isotope ratios of the source solution indicating that molecules with light H isotope started to diffuse. Approximately 10 days after the contaminant source was switched with clean water, a peak in H isotope results was observed which could be an indication of desorption of previously sorbed heavy H isotopologues and further diffusion of light H isotoplogues since the concentration was still high during that period. As the contaminant concentration decreased, back-diffusion of previously light isotopologues occurred, which was followed by back-diffusion of heavier isotopologues. The results for Cl isotopes of TCE and *cis*-DCE also showed the sequence of processes affecting the movement of contaminants. A significant enrichment of ^{37}Cl in the effluent samples at the beginning of the experiment was related to the sorption and diffusion of light isotopologues. Once the contaminant source was disconnected and desorption of light isotopologues took place, the isotopic ratios of the solution started to drop. As the contaminant concentration decreased further and back-diffusion became the dominant process, the isotopic ratios reached the lowest value. The isotopic ratios gradually rose as the back-diffusion proceeded and heavier isotopologues diffused back. The main findings of this research are:

- Physical processes such as sorption, diffusion, and back-diffusion processes can alter Cl and H isotopic signatures of TCE and *cis*-DCE.
- Sorption caused significant depletion of ^{2}H and measureable enrichment of ^{37}Cl in the solution indicating that sorption favored heavy H isotope and light Cl isotope.
- The extent of Cl and H isotope fractionations due to sorption was higher for TCE molecules than *cis*-DCE molecules.
- Diffusive mass loss had a pronounced effect on the chlorine isotope fractionation of *cis*-DCE.
- Compound-specific hydrogen isotope analysis can be a promising tool to distinguish between sorption and diffusion processes as those processes have an opposite effect on H isotope fractionations of TCE and *cis*-DCE.
- Carbon isotope fractionation of TCE and *cis*-DCE due to physical processes was small compared with the isotope fractionation reported due to biodegradation, and therefore, can be neglected where biodegradation is the dominant process.
- Chlorine isotope data should be interpreted with caution, specifically when both sorption and diffusion are dominant as both processes result in enrichment of aqueous phase in ^{37}Cl, which might be misinterpreted as biodegradation.
- Hydrogen isotope fractionation of TCE and *cis*-DCE due to physical processes was significant compared with the isotope fractionation due to biodegradation. Hence, shifts in H isotope ratios of TCE and *cis*-DCE indicating that physical processes are affecting the movement of the contaminants plumes.

4.2 Recommendations for Future Research

This study focused on the experimental aspects of the effect of sorption, desorption, diffusion, and back-diffusion processes on Cl and H stable isotope ratios of chlorinated ethenes through controlled laboratory batch, column, and box experiments. While important results were obtained on Cl and H isotope fractionations which helps to better interpret the processes affecting the chlorinated ethenes plumes in the subsurface, some questions arose during the course of this study.

Previous studies on sorption of VOCs revealed that sorption favors the lighter isotopes of organic compounds (Caimi and Brenna. 1997; Aelion, et al. 2009). However, the H isotope results of TCE and *cis*-DCE from shale and dolostone batch experiments and the column experiments showed the opposite behavior. This behavior might be due to different vibrational energies for the molecules with different isotopes. Calculation of the vibrational energies requires the knowledge of the exact molecular shape of the compounds of interest, and how their coordination changes when they are sorbed. Therefore, calculation of vibrational energies for H isotopes of chlorinated ethenes using theoretical and computational chemistry can be an interesting topic for a future research. The behavior of H isotope in sorption batch experiment with Borden sand and GAC was different from the other batch experiments and the column experiment with Borden sand and GAC. The liquid phase became slightly enriched in ^{2}H. The difference between sorption batch experiment with Borden sand and CAG and batch experiments with shale and dolostone was the type of sorbents. The sorbent in shale and dolostone was natural organic carbon of the soil, which is different than highly porous GAC. The difference between the column experiment with Borden sand and GAC and the batch experiment with GAC was the nature of the experiment. In the column experiment, TCE solution was entering the column slowly, while in the batch experiment the solution was instantaneously added to the media. It would be interesting to conduct more experiments in both static and dynamic conditions using different types of sorbents to examine the effect of the structure of the sorbents and the different conditions on H isotope fractionations of chlorinated ethenes.

Hydrogen CSIA has been recently developed for chlorinated ethenes (Kuder and Philp. 2013; Shouakar-Stash and Drimmie. 2013). To our knowledge, this is the first study to investigate the effect of physical processes such as sorption, desorption, diffusion, and back-diffusion on H isotope ratios of TCE and *cis*-DCE. Therefore, further experimental investigations are required to fully understand the behavior of H isotope during physical processes as well as transformation processes (i.e. biotic and abiotic degradation).

The results of the back-diffusion batch experiments showed that back-diffused cis-DCE molecules was enriched in ^{37}Cl isotope compare with the isotope ratio of the original cis-DCE. In order to fully understand the reason behind this phenomenon, batch experiments should be repeated with cis-DCE solution only, at the same concentrations as the back-diffused cis-DCE, under the same condition as

the batch experiments (i.e. in the fume hood at 22°C) and analyze the samples for Cl isotope ratios over time.

A new modeling tool needs to be developed that incorporates the effect of sorption and diffusion on isotope fractionations in order to quantitatively evaluate the isotope data from sorption column experiment and diffusion box experiment. A few studies have been conducted on modeling of diffusion-induced isotope fractionation of organic compounds (LaBolle, et al. 2008; Van Breukelen and Rolle. 2012; Rolle, et al. 2010). However, sorption-induced isotope fractionation has not been quantitatively investigated so far. The PHREEQC-2 code (Parkhurst and Appelo. 1999) is a one-dimensional (1D) model capable of simulating reactive transport, diffusion, sorption, and dispersion in one dimension. For simulation of the columns and box experiments results, PHREEQC-2 can be used. For 2D and 3D simulations, the PHT3D code can be used which couples MODFLOW/MT3DMS and PHREEQC-2 (Prommer, et al. 2003). Furthermore, the multiphase flow multispecies transport model COMPFLOW with degradation and isotope fractionation which was developed by Hwang and others (Hwang, et al. 2013) can be used to simulate the results.

All of the experiments were conducted in the laboratory under controlled conditions to distinguish the processes that might affect isotopic signatures. As for the box experiment, both diffusion and sorption processes were involved, however, the thin aquifer – thick aquitard system was not realistic. The subsurface might be highly heterogeneous and several processes such as sorption, diffusion, and biodegradation might happen simultaneously. Therefore, it will be beneficial to perform a laboratory sandbox experiment with heterogeneous packing with natural sediments such as Borden sand and clay to resemble more realistic field conditions. Biodegradation of chlorinated solvents occurs by anaerobic dechlorinating bacteria. Although it would be difficult to maintain anaerobic conditions in the lab, it would be interesting to add dechlorinating bacteria such as KB-1 culture to the system to investigate the effect of all processes (i.e. biodegradation, sorption, and diffusion) on stable isotope fractionations at the same time.

References

Abe, Y., Aravena, R., Zopfi, J., Shouakar-Stash, O., Cox, E., Roberts, J. D., Hunkeler, D., 2009. Carbon and Chlorine Isotope Fractionation during Aerobic Oxidation and Reductive Dechlorination of Vinyl Chloride and cis-1,2-Dichloroethene. Environmental Science & Technology. 43, 101-107.

Aelion, C.M., Aravena, R., Hunkeler, D., Höhener, P. (Eds.), 2009. Environmental Isotopes in Biodegradation and Bioremediation. CRC Press, 450. AllenKing, R., McKay, L., Trudell, M., 1997. Organic carbon dominated trichloroethene sorption in a clay-rich glacial deposit. Ground Water. 35, 124-130.

Appelo, C.A.J., Postma, D., 2005. Geochemistry, groundwater and pollution. CRC Press, London.

Audi-Miro, C., Cretnik, S., Otero, N., Palau, J., Shouakar-Stash, O., Soler, A., Elsner, M., 2013. Cl and C isotope analysis to assess the effectiveness of chlorinated ethene degradation by zero-valent iron: Evidence from dual element and product isotope values. Applied Geochemistry. 32, 175-183.

Barth, J. A. C., Slater, G., Schuth, C., Bill, M., Downey, A., Larkin, M., Kalin, R. M., 2002. Carbon isotope fractionation during aerobic biodegradation of trichloroethene by Burkholderia cepacia G4: a tool to map degradation mechanisms. Applied and Environmental Microbiology. 68, 1728-1734.

Barth, J. A. C., Slater, G., Schuth, C., Bill, M., Downey, A., Larkin, M., Kalin, R. M., 2002. Carbon isotope fractionation during aerobic biodegradation of trichloroethene by Burkholderia cepacia G4: a tool to map degradation mechanisms. Applied and Environmental Microbiology. 68, 1728-1734.

Beneteau, K. M., Aravena, R., Frape, S. K., 1999. Isotopic characterization of chlorinated solvents-laboratory and field results. Organic Geochemistry. 30, 739-753.

Black, J. R., Kavner, A., Schauble, E. A., 2011. Calculation of equilibrium stable isotope partition function ratios for aqueous zinc complexes and metallic zinc. Geochimica Et Cosmochimica Acta. 75, 769-783.

Blessing, M., Schmidt, T. C., Dinkel, R., Haderlein, S. B., 2009. Delineation of Multiple Chlorinated Ethene Sources in an Industrialized Area-A Forensic Field Study Using. Environmental Science & Technology. 43, 2701-2707.

Bloom, Y., Aravena, R., Hunkeler, D., Edwards, E., Frape, S. K., 2000. Carbon isotope fractionation during microbial dechlorination of trichloroethene, cis-1,2-dichloroethene, and vinyl chloride: Implications for assessment of natural attenuation. Environmental Science & Technology. 34, .

Caimi, R. J. and Brenna, J. T., 1997. Quantitative evaluation of carbon isotopic fractionation during reversed-phase high-performance liquid chromatography. Journal of Chromatography a. 757, 307-310.

Chartrand, M. M. G., Morrill, P. L., Lacrampe-Couloume, G., Lollar, B. S., 2005. Stable isotope evidence for biodegradation of chlorinated ethenes at a fractured bedrock site. Environmental Science & Technology. 39, 4848-4856.

Chu, K. H., Mahendra, S., Song, D. L., Conrad, M. E., Alvarez-Cohen, L., 2004. Stable carbon isotope fractionation during aerobic biodegradation of chlorinated ethenes. Environmental Science & Technology. 38, 3126-3130.

Cichocka, D., Imfeld, G., Richnow, H., Nijenhuis, I., 2008. Variability in microbial carbon isotope fractionation of tetra- and trichloroethene upon reductive dechlorination. Chemosphere. 71, 639-648.

Cichocka, D., Siegert, M., Imfeld, G., Andert, J., Beck, K., Diekert, G., Richnow, H., Nijenhuis, I., 2007. Factors controlling the carbon isotope fractionation of tetra- and trichloroethene during reductive dechlorination by Sulfurospirillum ssp and Desulfitobacterium sp strain PCE-S. FEMS Microbiology Ecology. 62, 98-107.

Clark, I.D., Fritz, P., 1997. Environmental isotopes in hydrogeology. Lewis Publishers, Boca Raton.

Cretnik, S., Thoreson, K. A., Bernstein, A., Ebert, K., Buchner, D., Laskov, C., Haderlein, S., Shouakar-Stash, O., Kliegman, S., McNeill, K., Elsner, M., 2013. Reductive Dechlorination of TCE by Chemical Model Systems in Comparison to Dehalogenating Bacteria: Insights from Dual Element Isotope Analysis (C-13/C-12, Cl-37/Cl-35). Environmental Science & Technology. 47, 6855-6863.

Dayan, H., Abrajano, T., Sturchio, N. C., Winsor, L., 1999. Carbon isotopic fractionation during reductive dehalogenation of chlorinated ethenes by metallic iron. Organic Geochemistry. 30, 755-763.

Duhamel, M., Mo, K., Edwards, E., 2004. Characterization of a highly enriched Dehalococcoides-containing culture that grows on vinyl chloride and trichloroethene. Applied and Environmental Microbiology. 70, 5538-5545.

Duhamel, M., Wehr, S. D., Yu, L., Rizvi, H., Seepersad, D., Dworatzek, S., Cox, E. E., Edwards, E. A., 2002. Comparison of anaerobic dechlorinating enrichment cultures maintained on tetrachloroethene, trichloroethene, cis-dichloroethene and vinyl chloride. Water Research. 36, 4193-4202.

Eggenkamp, H. G. M. and Coleman, M. L., 2009. The effect of aqueous diffusion on the fractionation of chlorine and bromine stable isotopes. Geochimica Et Cosmochimica Acta. 73, 3539-3548.

Elsner, M., Couloume, G. L., Mancini, S., Burns, L., Lollar, B. S., 2010. Carbon Isotope Analysis to Evaluate Nanoscale Fe(O) Treatment at a Chlorohydrocarbon Contaminated Site. Ground Water Monitoring and Remediation. 30, 79-95.

Elsner, M., Cwiertny, D. M., Roberts, A. L., Sherwood Lollar, B., 2007. 1,1,2,2-tetrachloroethane reactions with OH-, Cr(II), granular iron, and a copper-iron bimetal: Insights from product formation and associated carbon isotope fractionation. Environmental Science & Technology. 41, 4111-4117.

Elsner, M., Zwank, L., Hunkeler, D., Schwarzenbach, R. P., 2005. A new concept linking observable stable isotope fractionation to transformation pathways of organic pollutants. Environmental Science & Technology. 39, 6896-6916.

EPA, 2011. Toxicological Review of Trichloroethylene. Integrated Risk Information System, Office of Research and Development, Washington, DC. CAS No. 79-01-6, .

EPA, 2014. TSCA Work Plan Chemical Risk Assessment. Trichloroethylene: Degreasing, Spot Cleaning and Arts & Crafts Uses. Office of Chemical Safety and Pollution Prevention, Washington, DC. CASRN: 79-01-6, .

Fletcher, K. E., Nijenhuis, I., Richnow, H., Loeffler, F. E., 2011. Stable Carbon Isotope Enrichment Factors for cis-1,2-Dichloroethene and Vinyl Chloride Reductive Dechlorination by Dehalococcoides. Environmental Science & Technology. 45, 2951-2957.

Freeze, R.A., Cherry, J.A., 1979. Groundwater. Prentice-Hall, Englewood Cliffs, N.J.

Harrington, R. R., Poulson, S. R., Drever, J. I., Colberg, P. J. S., Kelly, E. F., 1999. Carbon isotope systematics of monoaromatic hydrocarbons: vaporization and adsorption experiments. Organic Geochemistry. 30, 765-775.

Hirschorn, S. K., Grostern, A., Lacrampe-Couloume, G., Edwards, E. A., MacKinnon, L., Repta, C., Major, D. W., Lollar, B. S., 2007. Quantification of biotransformation of chlorinated hydrocarbons in a biostimulation study: Added value via stable carbon isotope analysis. Journal of Contaminant Hydrology. 94, 249-260.

Huang, L., Sturchio, N. C., Abrajano, T., Heraty, L. J., Holt, B. D., 1999. Carbon and chlorine isotope fractionation of chlorinated aliphatic hydrocarbons by evaporation. Organic Geochemistry. 30, 777-785.

Hunkeler, D. and Aravena, R., 2000. Determination of compound-specific carbon isotope ratios of chlorinated methanes, ethanes, and ethenes in aqueous samples. Environmental Science & Technology. 34, 2839-2844.

Hunkeler, D., Abe, Y., Broholm, M. M., Jeannottat, S., Westergaard, C., Jacobsen, C. S., Aravena, R., Bjerg, P. L., 2011. Assessing chlorinated ethene degradation in a large scale contaminant plume by dual carbon-chlorine isotope analysis and quantitative PCR. Journal of Contaminant Hydrology. 119, 69-79.

Hunkeler, D., Aravena, R., Butler, B. J., 1999. Monitoring microbial dechlorination of tetrachloroethene (PCE) in groundwater using compound-specific stable carbon isotope ratios: Microcosm and field studies. Environmental Science & Technology. 33, 2733-2738.

Hunkeler, D., Aravena, R., Cox, E., 2002. Carbon isotopes as a tool to evaluate the origin and fate of vinyl chloride: Laboratory experiments and modeling of isotope evolution. Environmental Science & Technology. 36, 3378-3384.

Hunkeler, D., Aravena, R., Shouakar-Stash, O., Weisbrod, N., Nasser, A., Netzer, L., Ronen, D., 2011. Carbon and Chlorine Isotope Ratios of Chlorinated Ethenes Migrating through a Thick Unsaturated Zone of a Sandy Aquifer. Environmental Science & Technology. 45, 8247-8253.

Hunkeler, D., Chollet, N., Pittet, X., Aravena, R., Cherry, J., Parker, B., 2004. Effect of source variability and transport processes on carbon isotope ratios of TCE and PCE in two sandy aquifers. Journal of Contaminant Hydrology. 74, 265-282.

Hunkeler, D., Chollet, N., Pittet, X., Aravena, R., Cherry, J., Parker, B., 2004. Effect of source variability and transport processes on carbon isotope ratios of TCE and PCE in two sandy aquifers. Journal of Contaminant Hydrology. 74, 265-282.

Hwang, H. -., Park, Y. -., Sudicky, E. A., Unger, A. J. A., Illman, W. A., Frape, S. K., Shouakar-Stash, O., 2013. A multiphase flow and multispecies reactive transport model for DNAPL-involved Compound Specific Isotope Analysis. Advances in Water Resources. 59, 111-122.

Imfeld, G., Kopinke, F. -., Fischer, A., Richnow, H. -., 2014. Carbon and hydrogen isotope fractionation of benzene and toluene during hydrophobic sorption in multistep batch experiments. Chemosphere. 107, 454-461.

Jeannottat, S. and Hunkeler, D., 2012. Chlorine and Carbon Isotopes Fractionation during Volatilization and Diffusive Transport of Trichloroethene in the Unsaturated Zone. Environmental Science & Technology. 46, 3169-3176.

Jendrzejewski, N., Eggenkamp, H., Coleman, M., 2001. Characterisation of chlorinated hydrocarbons from chlorine and carbon isotopic compositions: scope of application to environmental problems. Applied Geochemistry. 16, 1021-1031.

Jin, B., Rolle, M., Li, T., Haderlein, S. B., 2014. Diffusive Fractionation of BTEX and Chlorinated Ethenes in Aqueous Solution: Quantification of Spatial Isotope Gradients. Environmental Science & Technology. 48, 6141-6150.

Karickhoff, S. W., Brown, D. S., Scott, T. A., 1979. Sorption of Hydrophobic Pollutants on Natural Sediments. Water Research. 13, 241-248.

Kopinke, F. D., Georgi, A., Voskamp, M., Richnow, H. H., 2005. Carbon isotope fractionation of organic contaminants due to retardation on humic substances: Implications for natural attenuation studies in aquifers. Environmental Science & Technology. 39, 6052-6062.

Kuder, T., van Breukelen, B. M., Vanderford, M., Philp, P., 2013. 3D-CSIA: Carbon, Chlorine, and Hydrogen Isotope Fractionation in Transformation of ICE to Ethene by a Dehalococcoides Culture. Environmental Science & Technology. 47, 9668-9677.

Kuder, T., van Breukelen, B. M., Vanderford, M., Philp, P., 2013. 3D-CSIA: Carbon, Chlorine, and Hydrogen Isotope Fractionation in Transformation of ICE to Ethene by a Dehalococcoides Culture. Environmental Science & Technology. 47, 9668-9677.

LaBolle, E. M., Fogg, G. E., Eweis, J. B., Gravner, J., Leaist, D. G., 2008. Isotopic fractionation by diffusion in groundwater. Water Resources Research. 44, W07405.

Langer, V., Novakowski, K., Woodbury, A., 1999. Sorption of trichloroethene onto stylolites. Journal of Contaminant Hydrology. 40, 1-23.

Lee, P. K. H., Conrad, M. E., Alvarez-Cohen, L., 2007. Stable carbon isotope fractionation of chloroethenes by dehalorespiring isolates. Environmental Science & Technology. 41, 4277-4285.

Liu, Y., Gan, Y., Zhou, A., Liu, C., Li, X., Yu, T., 2014. Carbon and chlorine isotope fractionation during Fenton-like degradation of trichloroethene. Chemosphere. 107, 94-100.

Lojkasek-Lima, P., Aravena, R., Shouakar-Stash, O., Frape, S. K., Marchesi, M., Fiorenza, S., Vogan, J., 2012. Evaluating TCE Abiotic and Biotic Degradation Pathways in a Permeable Reactive Barrier Using Compound Specific Isotope Analysis. Ground Water Monitoring and Remediation. 32, 53-62.

Lollar, B. S., Slater, G. F., Ahad, J., Sleep, B., Spivack, J., Brennan, M., MacKenzie, P., 1999. Contrasting carbon isotope fractionation during biodegradation of trichloroethylene and toluene: Implications for intrinsic bioremediation. Organic Geochemistry. 30, 813-820.

Lollar, B. S., Slater, G. F., Sleep, B., Witt, M., Klecka, G. M., Harkness, M., Spivack, J., 2001. Stable carbon isotope evidence for intrinsic bioremediation of tetrachloroethene and trichloroethene at area 6, Dover Air Force Base. Environmental Science & Technology. 35, 261-269.

Morrill, P. L., Lacrampe-Couloume, G., Slater, G. F., Sleep, B. E., Edwards, E. A., McMaster, M. L., Major, D. W., Lollar, B. S., 2005. Quantifying chlorinated ethene degradation during reductive dechlorination at Kelly AFB using stable carbon isotopes. Journal of Contaminant Hydrology. 76, 279-293.

Neville, C.J., 2001, ONED_1 Analytical Solution User Guide.

Palau, J., Jamin, P., Badin, A., Vanhecke, N., Haerens, B., Brouyere, S., Hunkeler, D., 2016. Use of dual carbon-chlorine isotope analysis to assess the degradation pathways of 1,1,1-trichloroethane in groundwater. Water Research. 92, 235-243.

Pankow, A., Cherry, J.A., 1996. Dense Chlorinated Solvents and Other DNAPLs in Groundwater. Waterloo Press, Waterloo, Canada.

Parkhurst, D. L. and Appelo, C. A. J., 1999. User's guid to PHREEQC (version 2)— a computer program for speciation, batch-reaction, onedimensional transport, and inverse geochemical calculations. U.S. Geological Survey: Denver, CO.

Poulson, S. R. and Drever, J. I., 1999. Stable isotope (C, Cl, and H) fractionation during vaporization of trichloroethylene. Environmental Science & Technology. 33, 3689-3694.

Poulson, S. R. and Naraoka, H., 2002. Carbon isotope fractionation during permanganate oxidation of chlorinated ethylenes (cDCE, TCE, PCE). Environmental Science & Technology. 36, 3270-3274.

Poulson, S. R., Drever, J. I., Colberg, P. J. S., 1997. Estimation of K-oc values for deuterated benzene, toluene, and ethylbenzene, and application to ground water contamination studies. Chemosphere. 35, 2215-2224.

Prommer, H., Barry, D. A., Zheng, C., 2003. MODFLOW/MT3DMS-based reactive multicomponent transport modeling. Ground Water. 41, 247-257.

Richter, F., Mendybaev, R., Christensen, J., Hutcheon, I., Williams, R., Sturchio, N., Beloso, A., 2006. Kinetic isotopic fractionation during diffusion of ionic species in water. Geochimica Et Cosmochimica Acta. 70, 277-289.

Rolle, M., Chiogna, G., Bauer, R., Griebler, C., Grathwohl, P., 2010. Isotopic Fractionation by Transverse Dispersion: Flow-through Microcosms and Reactive Transport Modeling Study. Environmental Science & Technology. 44, 6167-6173.

Sangster, J., 1997. Octanol-Water Partition Coefficients: Fundamentals and Physical Chemistry. Wiley, New York.

Schauble, E., Rossman, G., Taylor, H., 2001. Theoretical estimates of equilibrium Fe-isotope fractionations from vibrational spectroscopy. Geochimica Et Cosmochimica Acta. 65, 2487-2497.

Schauble, E., Rossman, G., Taylor, H., 2004. Theoretical estimates of equilibrium chromium-isotope fractionations. Chemical Geology. 205, 99-114.

Schmidt, T. C., Zwank, L., Elsner, M., Berg, M., Meckenstock, R. U., Haderlein, S. B., 2004. Compound-specific stable isotope analysis of organic contaminants in natural environments: a critical review of the state of the art, prospects, and future challenges. Analytical and Bioanalytical Chemistry. 378, 283-300.

Schuth, C., Bill, M., Barth, J., Slater, G., Kalin, R., 2003. Carbon isotope fractionation during reductive dechlorination of TCE in batch experiments with iron samples from reactive barriers. Journal of Contaminant Hydrology. 66, 25-37.

Schwartz, F.W., Zhang, H., 2003. Fundamentals of ground water. Wiley, New York.

Schwarzenbach, R. P. and Westall, J., 1981. Transport of nonpolar organic compounds from surface water to groundwater. Laboratory sorption studies. Environ. Sci. Technol. 15, 1300-1367.

Schwarzenbach, R.P., Gschwend, P.M., Imboden, D.M., 1993. Environmental Organic Chemistry. JOHN WILEY & SONS, INC., New York.

Shouakar-Stash, O. and Drimmie, R. J., 2013. Online methodology for determining compound-specific hydrogen stable isotope ratios of trichloroethene and 1,2-cis-dichloroethene by continuous-flow isotope ratio mass spectrometry. Rapid Communications in Mass Spectrometry. 27, 1335-1344.

Shouakar-Stash, O., Drimmie, R., Zhang, M., Frape, S., 2006. Compound-specific chlorine isotope ratios of TCE, PCE and DCE isomers by direct injection using CF-IRMS. Applied Geochemistry. 21, 766-781.

Slater, G. F., Ahad, J. M. E., Lollar, B. S., Allen-King, R., Sleep, B., 2000. Carbon isotope effects resulting from equilibrium sorption of dissolved VOCs. Analytical Chemistry. 72, 5669-5672.

Slater, G. F., Lollar, B. S., Sleep, B. E., Edwards, E. A., 2001. Variability in carbon isotopic fractionation during biodegradation of chlorinated ethenes: Implications for field applications. Environmental Science & Technology. 35, 901-907.

Squillace, P. J., Moran, M. J., Lapham, W. W., Price, C. V., Clawges, R. M., Zogorski, J. S., 1999. Volatile organic compounds in untreated ambient groundwater of the United States, 1985-1995. Environmental Science & Technology. 33, 4176-4187.

Tempest, K. E. and Emerson, S., 2013. Kinetic isotopic fractionation of argon and neon during air-water gas transfer. Marine Chemistry. 153, 39-47.

Tiehm, A., Schmidt, K. R., Pfeifer, B., Heidinger, M., Ertl, S., 2008. Growth kinetics and stable carbon isotope fractionation during aerobic degradation of cis-1,2-dichloroethene and vinyl chloride. Water Research. 42, 2431-2438.

Van Breukelen, B. M. and Rolle, M., 2012. Transverse Hydrodynamic Dispersion Effects on Isotope Signals in Groundwater Chlorinated Solvents' Plumes. Environmental Science & Technology. 46, 7700-7708.

VanStone, N. A., Focht, R. M., Mabury, S. A., Lollar, B. S., 2004. Effect of iron type on kinetics and carbon isotopic enrichment of chlorinated ethylenes during abiotic reduction on Fe(0). Ground Water. 42, 268-276.

vanWarmerdam, E. M., Frape, S. K., Aravena, R., Drimmie, R. J., Flatt, H., Cherry, J. A., 1995. Stable chlorine and carbon isotope measurements of selected chlorinated organic solvents. Applied Geochemistry. 10, 547-552.

Vieth, A., Muller, J., Strauch, G., Kastner, M., Gehre, M., Meckenstock, R. U., Richnow, H. H., 2003. In-situ biodegradation of tetrachloroethene and trichloroethene in contaminated aquifers monitored by stable isotope fractionation. Isotopes in Environmental and Health Studies. 39, 113-124.

Wanner, P. and Hunkeler, D., 2015. Carbon and chlorine isotopologue fractionation of chlorinated hydrocarbons during diffusion in water and low permeability sediments. Geochimica Et Cosmochimica Acta. 157, 198-212.

Wiegert, C., Aeppli, C., Knowles, T., Holmstrand, H., Evershed, R., Pancost, R. D., Machackova, J., Gustafsson, O., 2012. Dual Carbon-Chlorine Stable Isotope Investigation of Sources and Fate of Chlorinated Ethenes in Contaminated Groundwater. Environmental Science & Technology. 46, 10918-10925.

Yeh, H. C. and Kastenberg, W. E., 1991. Health Risk Assessment of Biodegradable Volatile Organic-Chemicals - a Case-Study of Pce, Tce, Dce and Vc. Journal of Hazardous Materials. 27, 111-126.

Appendix A

Chemical Concentration and Isotope Analysis

Chemical Analyses

For TCE analysis, the aqueous samples were extracted using a pentane internal standard containing 500 µg/L of 1,2-dibromoethane at sample-pentane ratio of 1:1. The samples were placed in 5 ml glass screw-cap vials which contained pentane and then the vials were placed on a rotary shaker for 15 minutes at 300 rpm. Afterward, ~ 1 mL of the pentane was transferred to 2 mL glass crimp-top vials. Using a Hewlett Packard 7673 liquid auto-sampler, a 1 µL sample was injected onto a DB-624 capillary column in a Hewlett Packard 5890 Series II gas chromatograph, which was equipped with a ^{63}Ni electron capture detector (ECD). The detector temperature was 300 °C and the injection temperature was 200 °C. The column temperature was raised from 50 to 150 °C at a rate of 15 °C/min and then held for 1 minute. The carrier gas was pre-purified helium and the make-up gas was 5% methane and 95% argon.

Isotope Analyses

Compound-Specific Chlorine Isotope Analysis

Chlorine isotope ratios were analyzed using a continuous flow-isotope ratio mass spectrometer (CF-IRMS) which was attached to an Agilent 6890 Gas Chromatograph (GC). The GC was equipped with a CTC Analysis CombiPAL SPME auto-sampler. The auto-sampler holds 32 vials (20 mL, crimp-cap). The dissolved organic compounds were extracted using a SPME fiber (75 µm Carboxen-PDMS for Merlin Microseal™, 23 gauge needle Auto-holder from Supelco). The gas chromatographic column used for the gas separations was DB-5 MS column, 60 m × 0.320 mm, 1 µm thickness from J&W Scientific Inc. A constant flow of He gas through a 4-way Valco valve, which was installed

between GC and IRMS, directs the desired compounds to the IRMS and the rest of the compounds to a flame ionization detector (FID) to be burned. The reference gases used for this method were mixture of the desired chlorinated ethenes and He. Detailed information about analytical method can be found in Shouakar-Stash, et al. 2006. The isotopic concentrations ($\delta^{37}Cl$) are expressed as the difference between the measured ratios ($^{37}Cl/^{35}Cl$) of the sample and reference over the measured ratio of reference (Equation 2-1). The reference for chlorine isotope is Standard Mean Ocean Chloride (SMOC). The δ-values for Cl stable isotopes are calculated based on the following equation and reported in permil (‰).

$$\boldsymbol{\delta 37Cl_{sample}} = \left(\frac{(37Cl/35Cl)_{sample} - (37Cl/35Cl)_{reference}}{(37Cl/35Cl)_{reference}}\right) \cdot \mathbf{1000‰}\ \boldsymbol{SMOC} \qquad \text{A 1}$$

The accuracy of the method is ± 0.1‰.

Compound-Specific Carbon Isotope Analysis

Compound-specific carbon isotope ratios were measured using a gas chromatography-combustion-isotope ratio mass spectrometry (GC-C-IRMS) system consisted of an Agilent 6890 GC. A DB-VRX gas chromatographic column (60 m × 0.25 mm, 1 µm stationary phase from J&W Scientific) used for gas separation. The extraction of organic compounds in the aqueous phase was performed by a SPME fiber (100 µM polydimethylsiloxane (PDMS) fiber, Supelco). Further details on the methodology can be found in Hunkeler and Aravena. 2000. The δ-values for carbon stable isotopes are calculated as follows and the values are reported in permil (‰):

$$\boldsymbol{\delta 13C_{sample}} = \left(\frac{(13C/12C)_{sample} - (13C/12Cl)_{reference}}{(13C/12C)_{reference}}\right) \cdot \mathbf{1000‰}\ \boldsymbol{VPDB} \qquad \text{A 2}$$

The reference for carbon isotopes is the international standard Vienna Pee Dee Belemnite (VPDB). The uncertainty of the analytical method is ± 0.5‰.

Compound-Specific Hydrogen Isotope Analysis

Compound-specific hydrogen isotope ratios were measured using a Delta^{plus} XL CF-IRMS instrument (ThermoFinnigan, Bremen, Germany), coupled with a gas chromatograph and a chromium reduction system. The gas chromatograph (Agilent 6890, Agilent Technologies Inc., Santa Clara, CA, US) equipped with DB-5 capillary column was used to separate the organic compounds. The Cr reduction tube was heated to 1000°C during the analysis using tube furnace (Thermcraft, model XST-3-0-12-10). The extraction of organic compounds was performed using a SPME fiber (75 µm Carboxen-PDMS for Merlin Microseal^{TM}, 23 gauge needle Manual holder from Supelco). Further details on the methodology can be found in Shouakar-Stash and Drimmie. 2013.

The δ^2H values are determined using the following equation and the valued are reported in prmil (‰):

$$\boldsymbol{\delta 2H_{sample}} = \left(\frac{(2H/1H)_{sample} - (2H/1H)_{reference}}{(2H/1H)_{reference}}\right) \cdot \mathbf{1000‰}\ \boldsymbol{VSMOW} \qquad \text{A 3}$$

The reference for H isotopes is a hydrogen gas calibrated to VSMOW. The accuracy of the method is ± 10‰.

Appendix B

Rayleigh plots for Sorption Batch Experiments

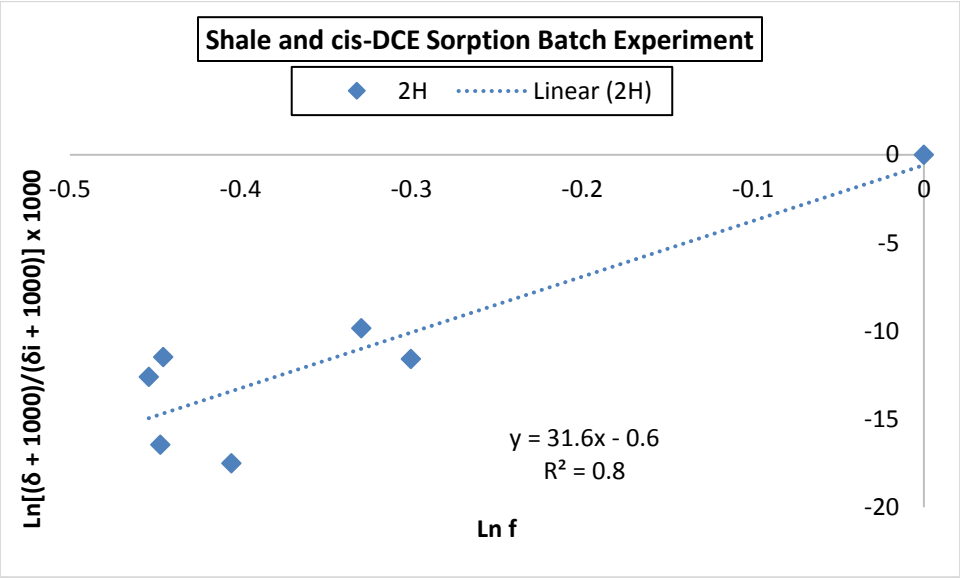

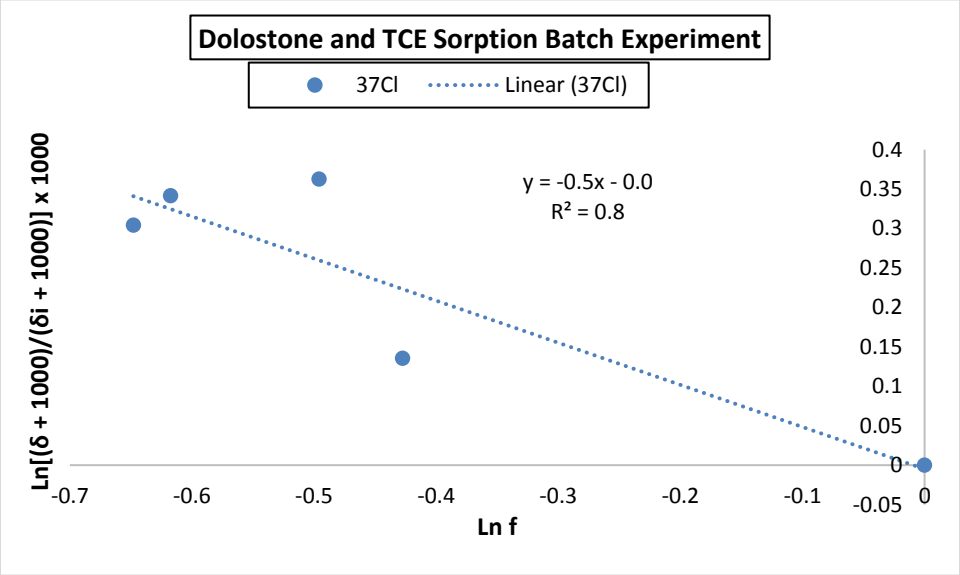

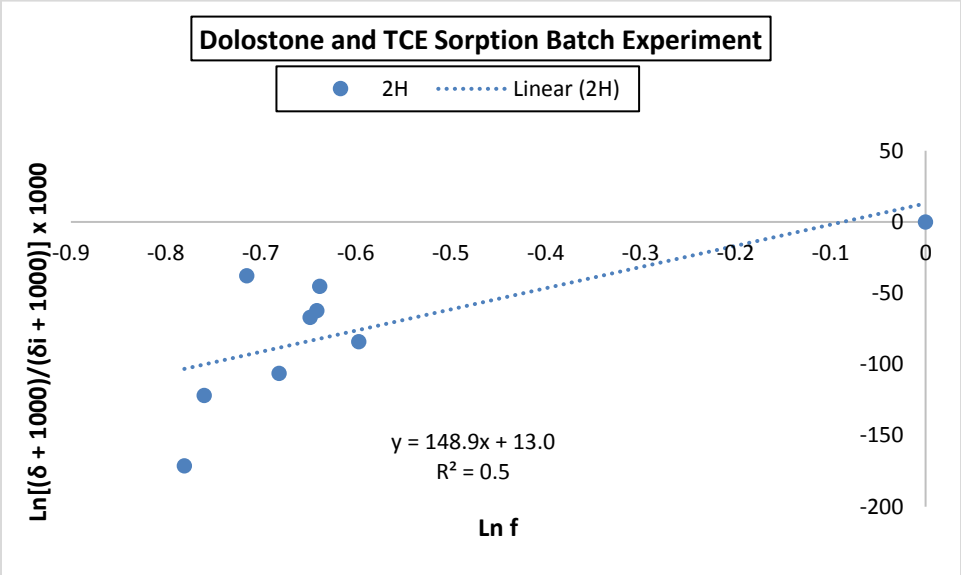
Dolostone and TCE Sorption Batch Experiment
2H
Linear (2H)
Ln[(δ + 1000)/(δi + 1000)] x 1000
Ln f
y = 148.9x + 13.0
R² = 0.5
50
0
-50
-100
-150
-200
-0.9
-0.8
-0.7
-0.6
-0.5
-0.4
-0.3
-0.2
-0.1
0

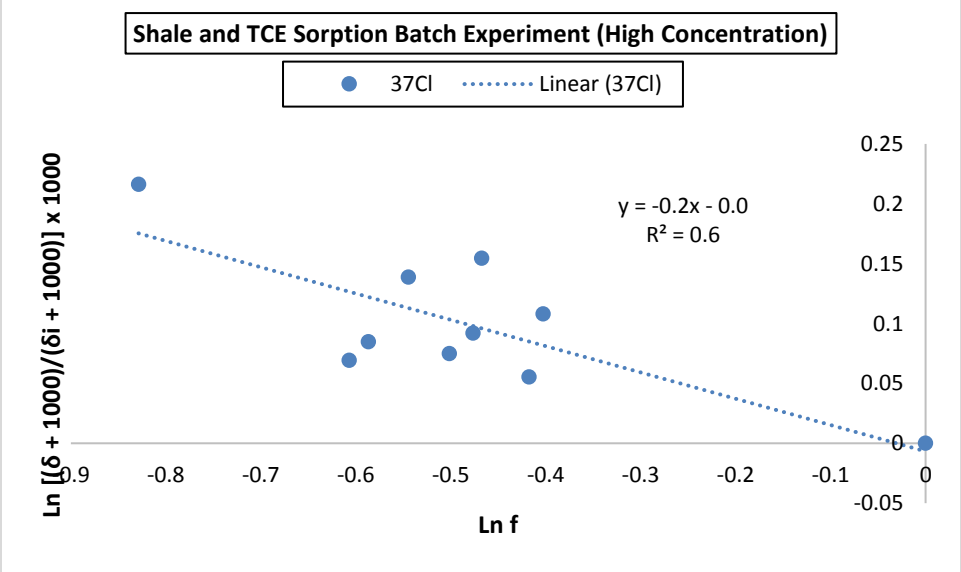
Shale and TCE Sorption Batch Experiment (High Concentration)
37Cl
Linear (37Cl)
Ln [(δ + 1000)/(δi + 1000)] x 1000
Ln f
y = -0.2x - 0.0
R² = 0.6
0.25
0.2
0.15
0.1
0.05
0
-0.05
-0.9
-0.8
-0.7
-0.6
-0.5
-0.4
-0.3
-0.2
-0.1
0

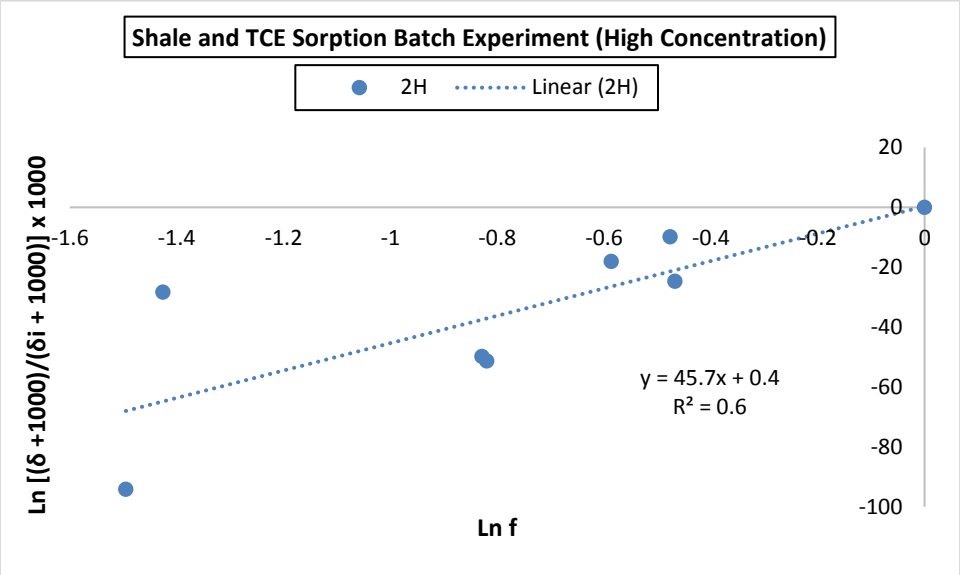
Shale and TCE Sorption Batch Experiment (High Concentration)
2H
Linear (2H)
Ln [(δ +1000)/(δi + 1000)] x 1000
Ln f
y = 45.7x + 0.4
R² = 0.6
20
0
-20
-40
-60
-80
-100
-1.6
-1.4
-1.2
-1
-0.8
-0.6
-0.4
-0.2
0

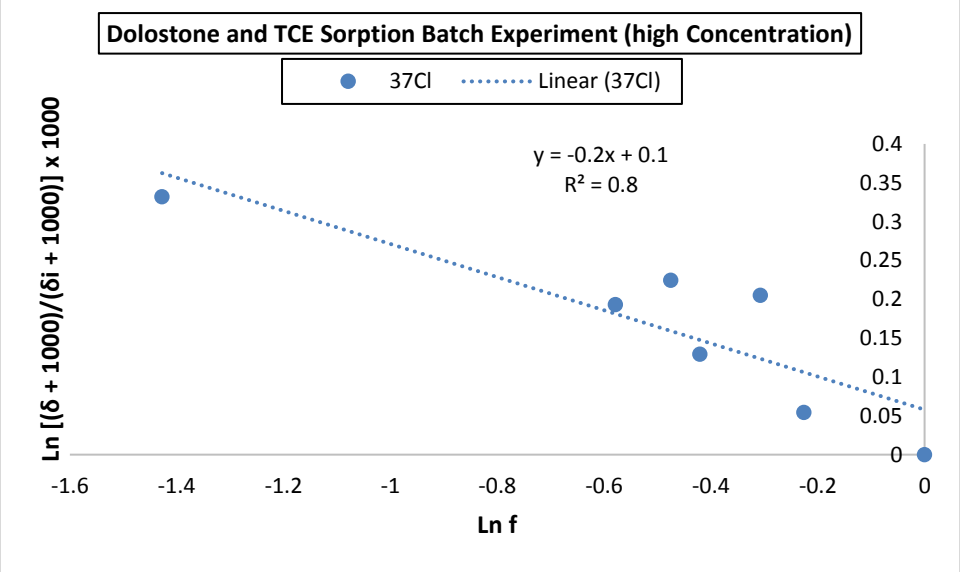
Dolostone and TCE Sorption Batch Experiment (high Concentration)
37Cl
Linear (37Cl)
Ln [(δ + 1000)/(δi + 1000)] x 1000
Ln f
y = -0.2x + 0.1
R² = 0.8
0.4
0.35
0.3
0.25
0.2
0.15
0.1
0.05
0
-1.6
-1.4
-1.2
-1
-0.8
-0.6
-0.4
-0.2
0

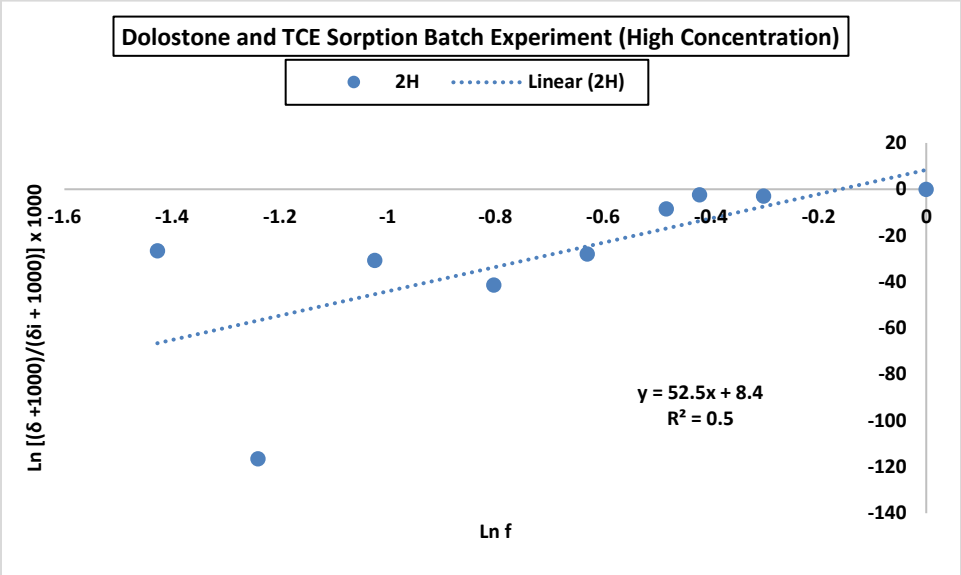
Dolostone and TCE Sorption Batch Experiment (High Concentration)
2H
Linear (2H)
Ln [(δ +1000)/(δi + 1000)] x 1000
Ln f
y = 52.5x + 8.4
R² = 0.5
20
0
-20
-40
-60
-80
-100
-120
-140
-1.6
-1.4
-1.2
-1
-0.8
-0.6
-0.4
-0.2
0

Appendix C

The Effect of Biodegradation on Chlorine and Hydrogen Stable Isotopes of TCE and *cis*-DCE

Introduction

Chlorinated ethenes are toxic volatile organic compounds and widespread groundwater contaminants in the United States (Squillace, et al. 1999). The consumption of trichloroethene (TCE) in the United States is 225 million pounds (lbs.) per year according to the U.S. Environmental Protection Agency (EPA. 2014). TCE is classified as a human carcinogen (EPA. 2011). Therefore, it is necessary to delineate the source(s) of contamination in the subsurface and the fate of the contaminant to be able to decide on appropriate remediation techniques. During the last decade, compound-specific isotope analysis has been emerged as a powerful tool in fingerprinting the contaminant source as well as understanding the processes that affect the contaminant plume in the subsurface. It is generally accepted that physical processes have a minor effect on stable isotope fractionations of organic compounds (Hunkeler, et al. 2004; Harrington, et al. 1999; Schuth, et al. 2003b; Slater, et al. 2000). However, previous studies revealed that transformation mechanisms during which bond cleavage of organic compounds occurs (i.e. biotic and abiotic degradations) are associated with significant C isotope fractionation (Lollar, et al. 1999a; Lollar, et al. 2001; Slater, et al. 2001; Barth, et al. 2002; Poulson and Naraoka. 2002; Vieth, et al. 2003; Schmidt, et al. 2004; VanStone, et al. 2004; Chartrand, et al. 2005; Elsner, et al. 2005; Morrill, et al. 2005; Hirschorn, et al. 2007; Elsner, et al. 2010; Cichocka, et al. 2008; Abe, et al. 2009; Fletcher, et al. 2011; Hunkeler, et al. 2011a; Lojkasek-Lima, et al. 2012; Wiegert, et al. 2012; Cretnik, et al. 2013; Liu, et al. 2014). There are limited number of studies on the effect of degradation on Cl isotope fractionation of chlorinated ethenes (Abe, et al. 2009; Cretnik, et al. 2013; Kuder, et al. 2013). Compound-specific hydrogen isotope

analysis of chlorinated ethenes was developed recently (Kuder and Philp. 2013; Shouakar-Stash and Drimmie. 2013) and to our knowledge, there is a single study on the effect of biodegradation on H isotope ratios of TCE to date (Kuder, et al. 2013).

In this study, carbon, chlorine, and hydrogen isotope fractionation of TCE and *cis*-DCE was investigated through microcosm experiments with KB-1® dechlorinating culture. KB-1® is a naturally occurring microbial culture containing *Dehalococcoides* strain which is capable of dechlorination of chlorinated ethenes to harmless ethane (Duhamel, et al. 2002; Duhamel, et al. 2004).

Laboratory Batch Experiments

Microcosm experiments were conducted in collaboration with SiREM, Guelph, Ontario, Canada and Isotope Tracer Technologies Inc., Waterloo, Ontario, Canada. The objective of these experiments was to evaluate the effect of biodegradation on stable carbon, chlorine, and hydrogen isotopes ratios of TCE at two initial concentrations of 40 mg/L and 150 mg/L.

Method and Materials

Two sets of duplicate treatments (containing KB-1 culture) and a set of duplicate controls (without KB-1 culture) were prepared for this study. The first set of treatments consisted of seven duplicates (total of 14 bottles) that were prepared for sampling times of 0, 2, 3, 5, 8, 11, and 14 days. The second set of the treatments consisted of six duplicates (total of 12 bottles) that were prepared for sampling times of 0, 3, 7, 21, 24, and 38 days. The controls consisted of three duplicates that were prepared for sampling times of 0, 14, and 38 days. For both treatments and controls, one duplicate was sacrificed for each sampling time. The study was started by adding 150 mL of mineral solution (for details, see Duhamel et al., 2002) and labels to the bottles (250 mL sterile glass bottles). The bottles were capped using screw cap Mininert valves (Figure C1). The first set of treatment bottles was spiked with 7.5 µL

of neat TCE to target a final TCE concentration of 50 mg/L. The second set of treatment bottles and controls were spiked with 30 µL of neat TCE to target a final TCE concentration of 200 mg/L and the bottles were allowed to equilibrate for two days. Each of the treatment bottles with initial TCE concentration of 50 mg/L and 200 mg/L were amended with 100 µL and 400 µL of lactate, respectively. Lactate was used as an electron donor. Then, 20 mL of fresh KB-1® (SiREM, Guelph, Ontario, Canada) was added to each treatment bottle. Prior to the addition of KB-1 culture to the bottles, the culture was purged with N_2 for 15 minutes in order to remove any residual volatile organic compounds (VOCs) from the medium. The control bottles were spiked with 1.0 mL of 5% mercuric chloride and 1.0 mL of 5% sodium azide to inhibit microbial activity. In order to stop degradation, the treatment bottles were acidified with phosphoric acid to a pH of 2. All experiments were conducted in an anaerobic glovebox at SiREM, Guelph, Ontario, Canada. The control and treatment bottles were shipped in a cooler to Isotope Tracer Technologies Inc. (Waterloo, Ontario, Canada) for stable isotopes analyses. Samples from the 250 mL bottles were transferred to 20 mL and 40 mL vials, capped using screw caps with Teflon faced septa, and kept in the refrigerator at 4°C until analyzed.

Figure C1: Experimental setup for microcosm study

Analytical Procedures

Concentration Analysis

The aqueous TCE and its degradation by-products concentrations were measured at SiREM using a Hewlett-Packard (Hewlett Packard 7890) gas chromatograph (GC) equipped with an auto-sampler (Hewlett Packard G1888) programmed to heat each sample vial to 75°C for 45 minutes prior to headspace injection into a GSQ Plot column (0.53 millimeters x 30 meters, J&W) and a flame ionization detector. Sample vials were heated to ensure that all VOCs in the aqueous sample would partition into the headspace. The injector temperature was 200°C, and the detector temperature was 250°C. The oven temperature was programmed as follows: 35°C for 2 minutes, increased to 100°C at 50 degrees Celsius per minute (°C/min), then increased to 185°C at 25°C/min and held at 185°C for 6.80 minutes. The carrier gas was helium at a flow rate of 11 milliliters per minute (mL/min).

After withdrawing a sample, it was injected into a 10 mL auto sampler vial containing acidified de-ionized water (pH ~2) to a final volume of 6 mL total. The water was acidified to inhibit microbial activity between microcosm sampling and GC analysis. The vial was sealed with an inert Teflon®-coated septum and aluminum crimp cap for automated injection of 3 mL of headspace onto the GC. One VOC standard was analyzed with each set of samples to verify the instrument five-point calibration curve. Calibration was performed using external standard solutions (Sigma, St Louis, MO), where known volumes of standard solutions were added to acidified water in auto-sampler vials and analyzed as described above for microcosm samples. Data were integrated using Chemstation Software (Agilent Technologies, Santa Clara, CA).

Stable Isotopes Analyses

Carbon, chlorine, and hydrogen stable isotopes ratios of TCE and *cis*-DCE were measured at Isotope Tracer Technologies Inc., Waterloo, Ontario, Canada. The analytical methods for the stable isotopes can be found in Appendix A. We were not able to perform compound-specific isotope analysis of vinyl chloride (VC) since we did not have access to a VC standard.

Results and Discussions

Controls Results

The average concentration results from duplicate control bottles are shown in Figure C2. The results showed that there was a mass loss of 0.06 mmol/bottle by the end of the experiment. The stable isotope results (Figure C3) showed that most of the isotopic ratios were between the uncertainty of the analytical methods which means that the isotopic ratios did not change during the experiment. There are 3 outliers among the isotope results which might be due to analytical errors.

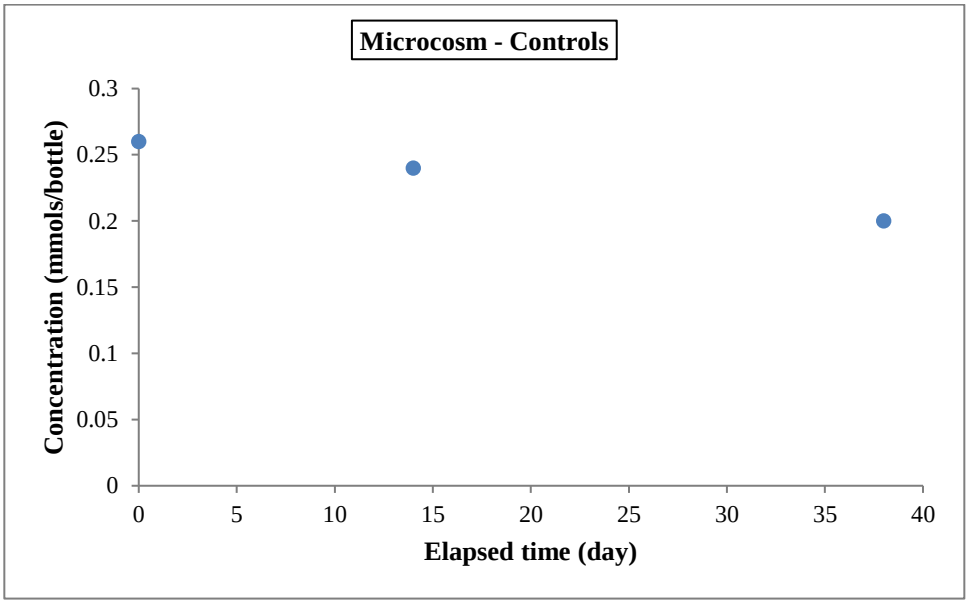

Figure C2: TCE concentration results of the control bottles versus time

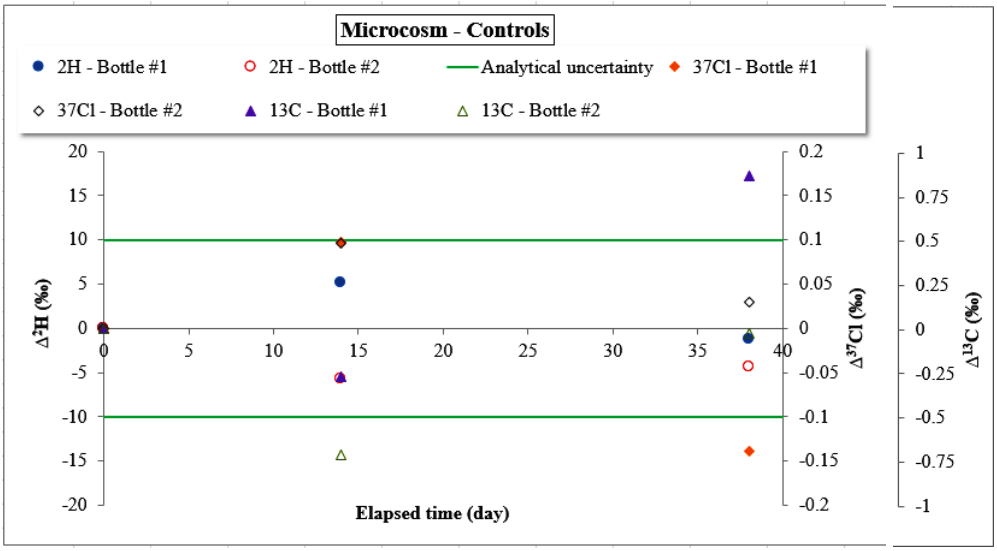

Figure C3: Chlorine, carbon, and hydrogen isotope ratios of TCE from the control bottles. The open and closed symbols represent the two replicates.

Microcosms Results

Concentration Results

In the experiment with initial TCE concentration of 50 mg/L, <95% of TCE was degraded to *cis*-DCE within 2 days and *cis*-DCE reached its maximum concentration (Figure C4) on day 2. VC and Ethene started to accumulate from the beginning of the experiment. Dechlorination of TCE to ethene was completed in 14 days for this experiment. In the experiment with initial TCE concentration of 200 mg/L, TCE was degraded to *cis*-DCE within 7 days and *cis*-DCE reached its maximum concentration (Figure C5) on day 7. VC and ethene were detected on days 2 and 11, respectively. Dechlorination of TCE to ethene was completed within 38 days. In addition to the VOCs mentioned above, small amounts of *trans*-DCE were detected (maximum concentration of 2.2 µmol/bottle on day 28) in the treatment bottles with initial TCE concentration of 200 mg/L.

Stable Isotope Results

The isotopic ratios of TCE and its degradation product *cis*-DCE from both sets of treatments are shown in Figures C6 to C11. Once $\delta^{13}C$ and $\delta^{37}Cl$ values of TCE samples from controls and treatments bottles on day 0 were compared, it was noticed that the values were different, although the same TCE was used for both control and treatments. It was expected to observe the same isotopic values for day-0 samples. For example, TCE samples from the control bottles showed $\delta^{13}C$ = -29.6 ‰, while TCE samples from the treatment bottles with initial TCE concentration of 50 mg/L showed $\delta^{13}C$ = -13.4 ‰, and samples from the treatment bottles with initial TCE concentration of 200 mg/L showed $\delta^{13}C$ = -23.2 ‰. The results indicate that TCE in the treatment bottles with initial TCE concentration of 50 mg/L was enriched in ^{13}C by 16.2 ‰ relative to the TCE in the control bottles, and TCE in the treatment bottles with initial TCE concentration of 200 mg/L was enriched in ^{13}C by

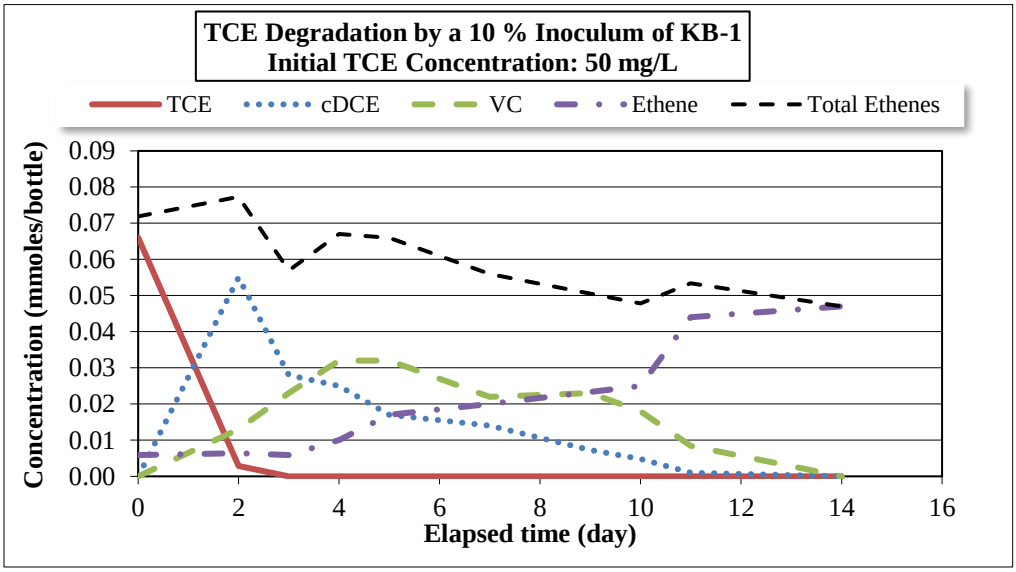

Figure C4: Concentration results of chlorinated ethenes per bottle versus time for reductive dechlorination of TCE by KB-1®

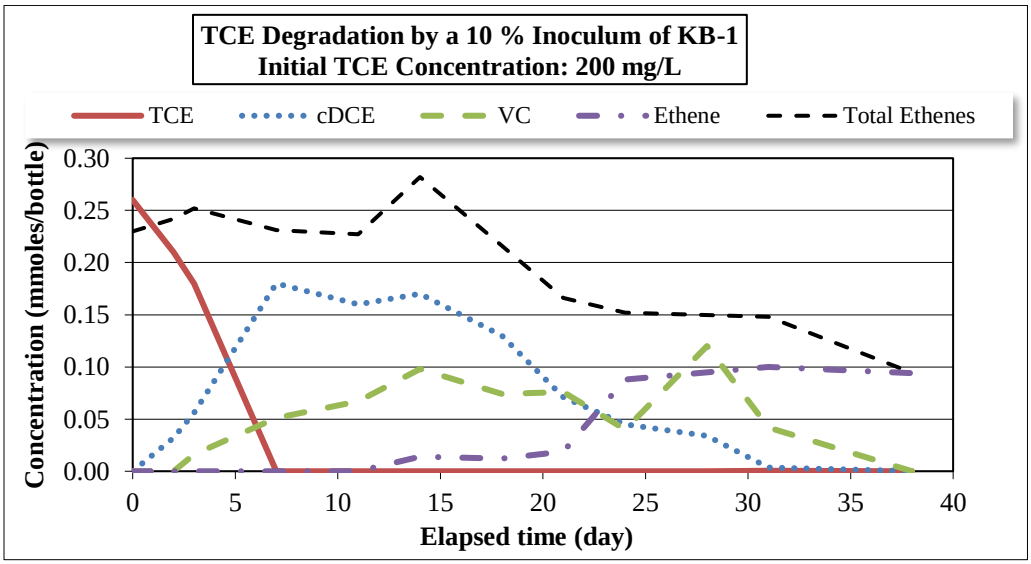

Figure C5: Concentration results of chlorinated ethenes per bottle versus time for reductive dechlorination of TCE by KB-1®

6.4 ‰ relative to the TCE in the control bottles. Similarly, day-0 TCE samples from the control bottles showed $\delta^{37}Cl$ = 1.75 ‰; while TCE samples from the treatment bottles with initial TCE concentration of 50 mg/L showed $\delta^{37}Cl$ = 3.3 ‰, and samples from the treatment bottles with initial TCE concentration of 200 mg/L showed $\delta^{37}Cl$ = 2.2 ‰. The difference between the control and treatment bottles was that the control bottles did not contain the KB-1 culture. However, the KB-1 medium that was added to the treatment bottles was purged with N_2 for 15 minutes to remove any residual chlorinated ethenes from the medium. Furthermore, in the study by Slater, et al. 2001, differences in isotopic ratios of the controls with and without the KB-1® were not reported. Hence, the difference between the isotopic ratios of TCE in the control and treatment bottles on day 0 cannot be attributed to the presence of chlorinated ethenes from the KB-1 culture medium. The enrichment of the samples in treatment bottles can be due to the fast degradation of TCE by KB-l®. TCE concentrations of the treatment bottles on day 0 was 50 mg/L and 200 mg/L as expected based on the amount of TCE that was added to the bottles. However, there is a possibility that the concentration values were not correct. It would have been beneficial to take samples for concentration and isotope analyses before addition of KB-1® as well to obtain a certain day-0 concentration and isotope ratios of TCE. Nonetheless, to plot the data, the isotopic ratios of TCE in the control bottles on day 0 were considered as isotope ratios at t = 0, and the isotopic ratios of the samples collected after addition of KB-1 culture were considered as isotope ratios at t = 5 min (assuming that it took 5 minutes between addition of KB-1® and collection of the sample for concentration analysis and stopping the experiment). For the microcosms with initial TCE concentration of 50 mg/L, the only samples that could be analyzed for C, Cl and H isotope ratios of TCE were the ones that were collected after KB-1® was added to the bottles. The next samples were taken after two days that <95% of TCE was degraded and therefore, the samples could not be analyzed for stable isotopes of TCE. Extra samples

should have been collected with a few hour intervals for isotope analysis in order to capture the shift in isotopic ratios of TCE. For the microcosms with initial TCE concentration of 200 mg/L, samples taken after addition of KB-1® and samples taken on day 3 were analyzed for C, Cl, and H isotope analyses. The next set of samples were collected on day 7 which TCE was consumed completely. Samples should have been taken with shorter time intervals in order to capture the shift in isotopic ratios of TCE.

As can be seen in Figures C6 and C7, carbon isotope fractionations were significant for *cis*-DCE in both microcosm experiments. Carbon isotope separation ($\Delta^{13}C$) of 50 mg/L (based on the values from bottle #2) was observed for the microcosms with initial TCE concentration of 50 mg/L, and $\Delta^{13}C$ of 31.45 ‰ was observed for the microcosms with initial TCE concentration and 200 mg/L (based on the average isotopic ratios of the duplicates). Chlorine isotope fractionations of *cis*-DCE were also significant (Figures C8 and C9), but smaller than carbon isotope fractionations. Microcosms with initial TCE concentration of 50 mg/L showed an average $\Delta^{37}Cl$ of 10.22 ‰ and microcosms with initial TCE concentration of 200 mg/L showed an average $\Delta^{37}Cl$ of 3.47 ‰. Similar to the carbon isotope results, the extent of Cl isotope fractionation decreased in microcosms with higher initial TCE concentration of 200 mg/L. Overall, significant Cl and C isotope fractionations were observed for TCE and *cis*-DCE, since C–Cl bonds were broken during biodegradation (primary isotope effects).

The average hydrogen isotope ratio (δ^2H) of the TCE in control bottles was 550 ‰. As can be seen in Figures C10 and C11, the TCE samples collected from treatment bottles after the addition of KB-1® showed δ^2H of 517 ‰ (treatment bottles with initial TCE concentration of 50 mg/L), 515 ‰ (treatment bottles with initial TCE concentration of 200 mg/L). The difference between δ^2H of the controls and microcosms was about 35 ‰, which is small compared to the total analytical uncertainty for δ^2H analyses (±10 ‰). The δ^2H values of the produced cis-DCE for microcosms with initial TCE

concentrations of 50 mg/L and 200 mg/L were 147 ‰ and 148 ‰, respectively, which were significantly depleted compared to the δ^2H of the parent TCE (550 ‰). In general, reductive dechlorination of chlorinated solvents take place through the following oxidation – reduction reaction:

$$H_2 + C - Cl \rightarrow C - H + H^+ + Cl^-$$

where C–Cl and C–H represent carbon–chlorine and carbon–hydrogen bonds, respectively. The H_2 required for this reaction is provided from an electron donor (lactate in this experiment). Normally, H isotopic signature of electron donors are distinct from H isotopic signature of chlorinated ethenes. The δ^2H value of the newly added hydrogen atom is calculated using the following equation (Kuder, et al. 2013):

$$\boldsymbol{\delta^2 H_{addition} = n \times \delta^2 H_{daughter} - (n-1) \times \delta^2 H_{parent}} \qquad \text{C 1}$$

where *n* is the number of hydrogen atoms in the daughter product. Based on equation C1, δ^2H of the newly added H atom is about -255 ‰ for our experiments. A maximum H isotope separation of 14 ‰ and 41 ‰ was observed for *cis*-DCE in the treatment bottles with initial TCE concentration of 50 mg/L and 200 mg/L, respectively, by the end of the experiment. The isotope separations were very small considering the total uncertainty of the analytical method for δ^2H analyses, which is ±10 ‰. During reductive dechlorination of TCE and *cis*-DEC, C–H bonds were not involved in the reaction directly and were slightly affected by the closeness to the reacting bonds, which is called secondary isotope effects (Elsner, et al. 2005).

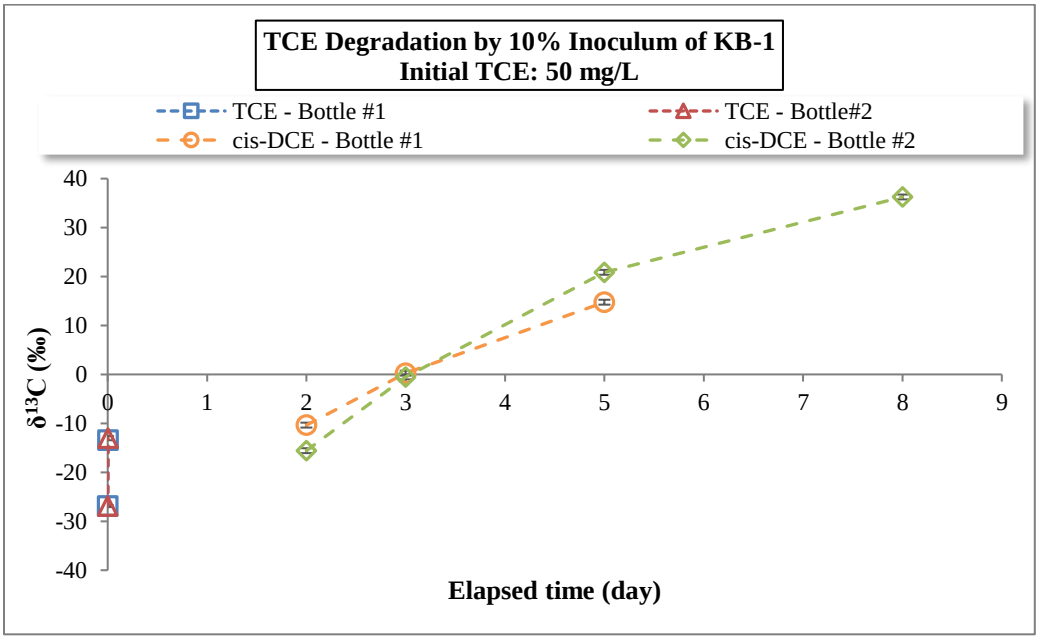

Figure C6: Carbon isotopic ratios of TCE and *cis*-DCE versus time for reductive dechlorination of TCE by KB-1®

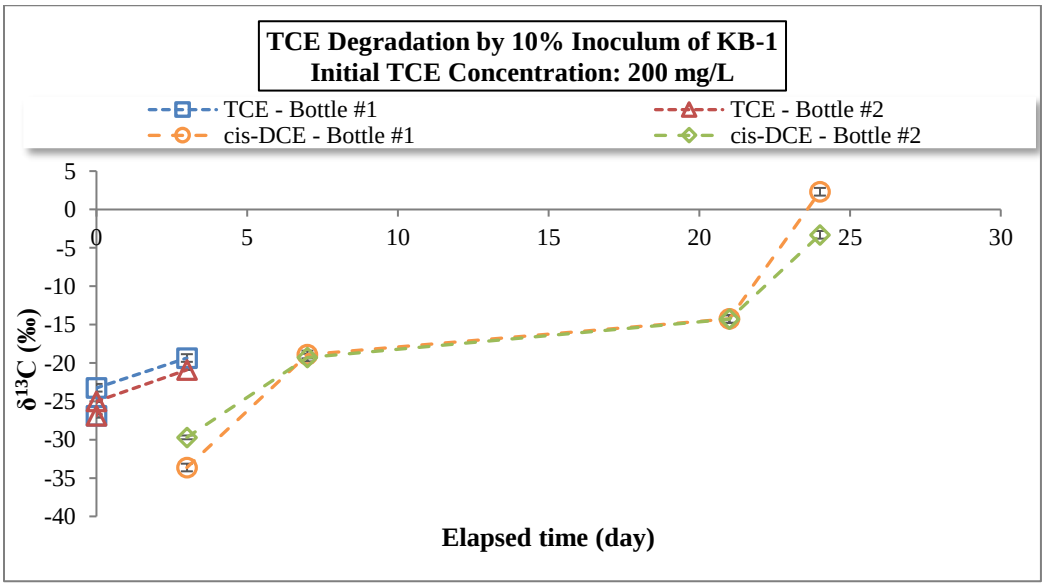

Figure C7: Carbon isotopic ratios of TCE and *cis*-DCE versus time for reductive dechlorination of TCE by KB-1®

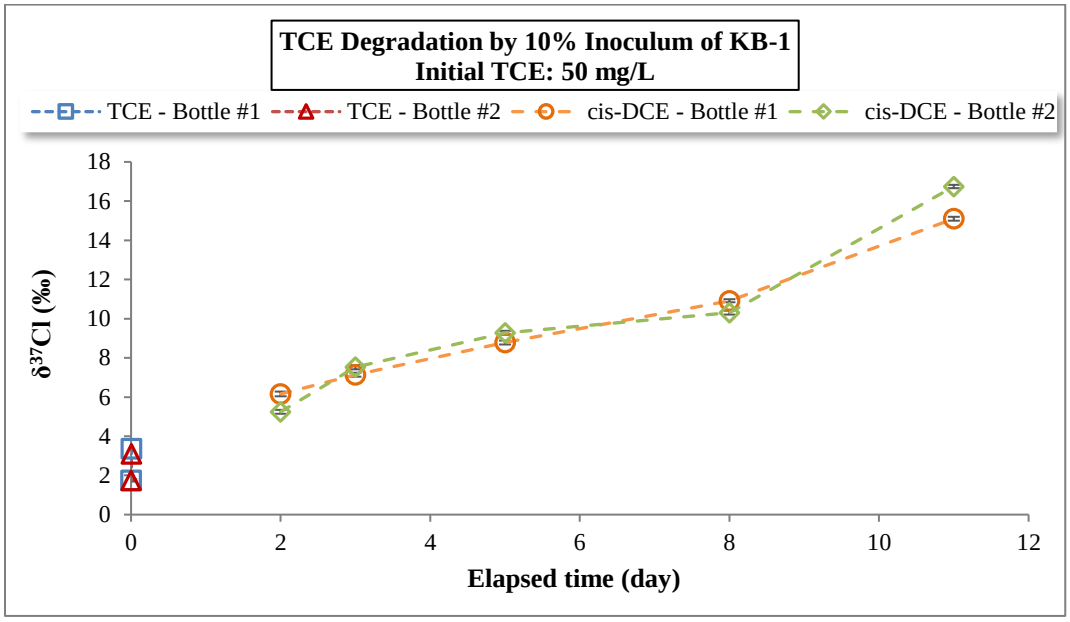

Figure C8: Chlorine isotopic ratios of TCE and *cis*-DCE versus time for reductive dechlorination of TCE by KB-1®

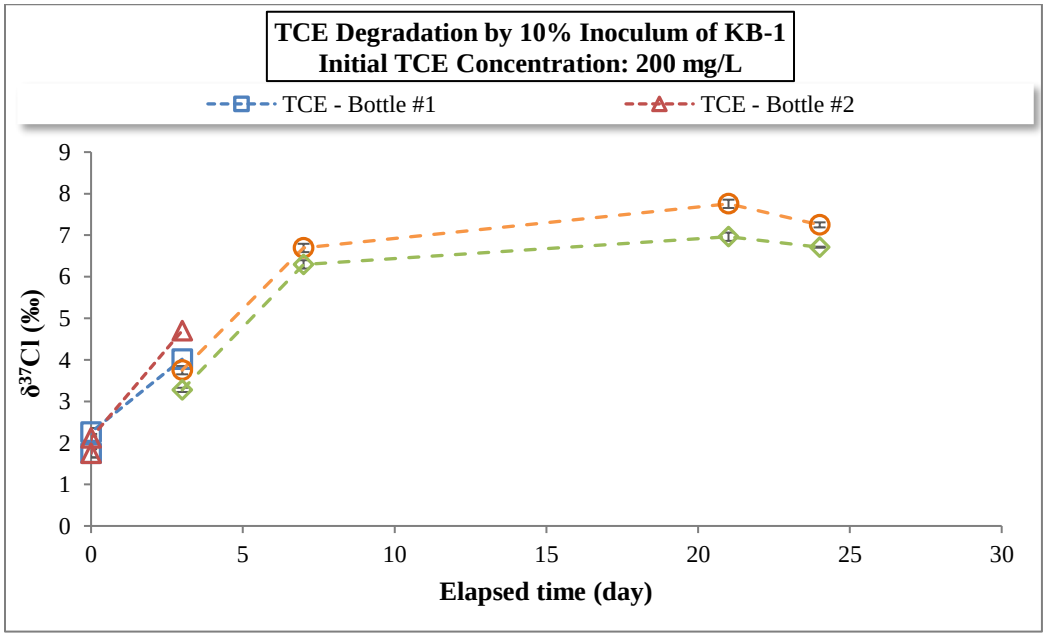

Figure C9: Chlorine isotopic ratios of TCE and *cis*-DCE versus time for reductive dechlorination of TCE by KB-1®

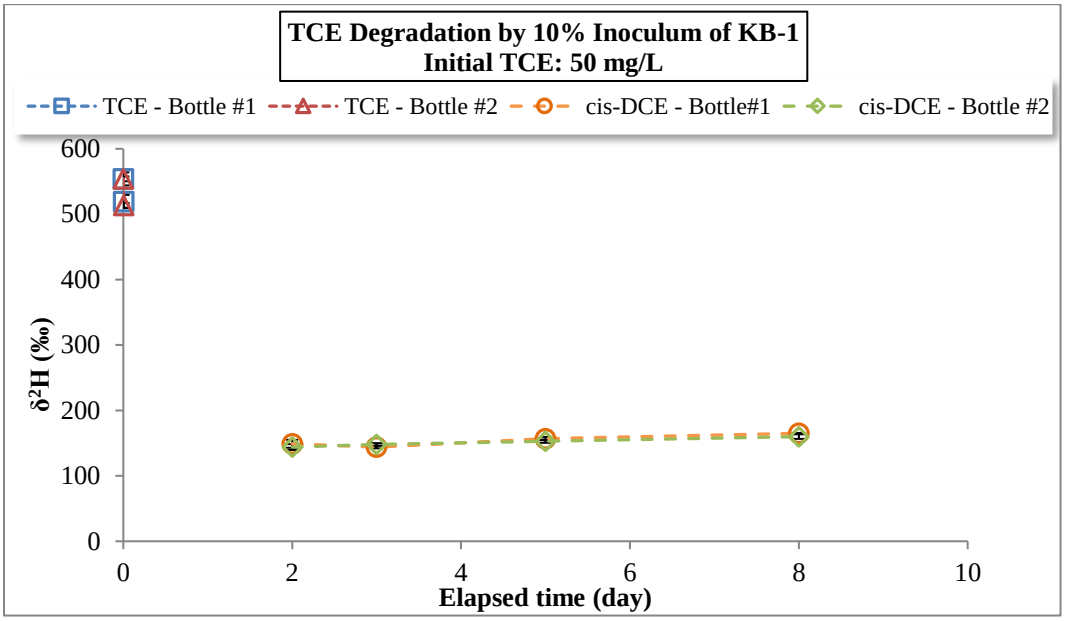

Figure C10: Hydrogen isotopic ratios of TCE and *cis*-DCE versus time for reductive dechlorination of TCE by KB-1®. The error bars are smaller than symbols.

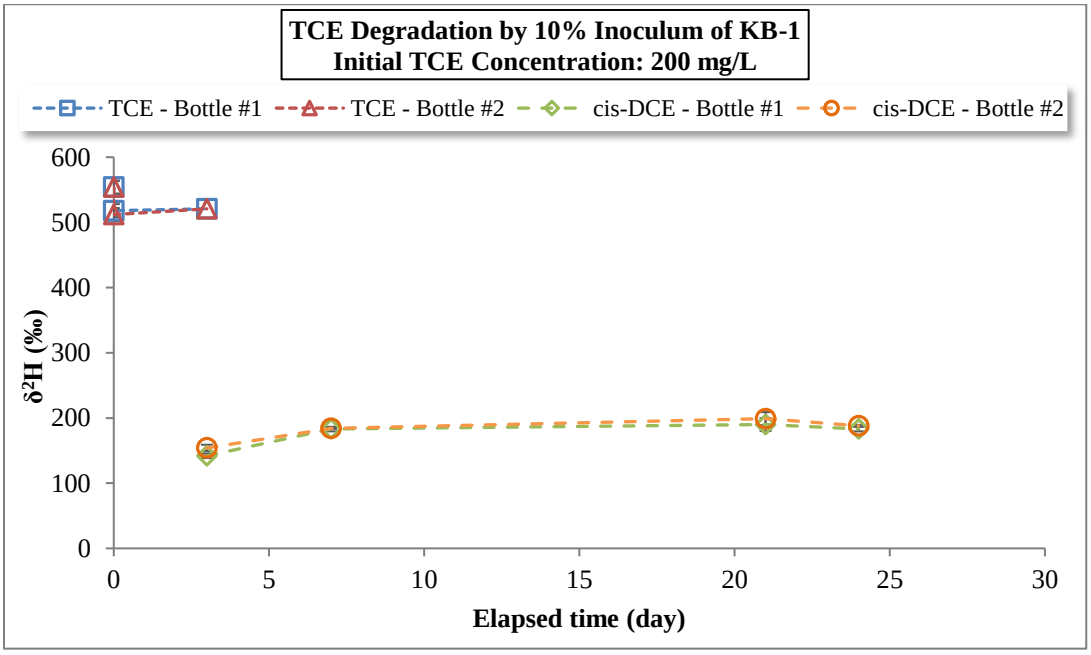

Figure C11: Hydrogen isotopic ratios of TCE and *cis*-DCE versus time for reductive dechlorination of TCE by KB-1®. The error bars are smaller than symbols.

Appendix D

Breakthrough Curve Obtained by ONED-1 Analytical Solution

The ONED_1 solution is capable of demonstrating 1D advection and dispersion, linear sorption, and first-order transformation reaction. The governing equation for the solution is:

$$R\theta\frac{\partial C}{\partial t} = -q\frac{\partial C}{\partial x} + \theta D\frac{\partial^2 C}{\partial x^2} - R\theta\lambda C \quad ; 0 \le x < \infty$$

R: retardation factor [-]

θ: porosity [-]

C: concentration [ML^{-3}]

x: distance from inflow boundary [L]

q: Darcy flux [LT^{-1}]

λ: first-order degradation coefficient [T^{-1}]

D: mechanical dispersion coefficient [L^2T^{-1}], which is calculated as:

$$D = \propto_L \left(\frac{q}{\theta}\right) + D^*$$

α_L: longitudinal dispersivity [L]

*D**: effective molecular diffusion coefficient [L^2T^{-1}], which is calculated as:

$$D^* = \tau\theta D_m$$

τ: tortuosity [-]

D_m: molecular diffusion coefficient [L^2T^{-1}]

The breakthrough curve with no diffusive loss was simulated for Br^-. The molecular diffusion coefficient (D_m) of Br^- was considered as 1.736 cm/day (Schwartz and Zhang. 2003). The porosity (θ) of sand layer was assumed to be 0.33. Tortuosity (τ) for sand was calculated as: $\tau=\theta^{1/3}$ (Schwartz and Zhang. 2003). Longitudinal dispersivity (α_L) was assumed to be 10 cm, and Darcy flux (*q*) was estimated to be 19 cm/day.

Electrical Conductivity Results from Diffusion Box Experiment

The electrical conductivity of the effluent samples was measured throughout the experiment using the Horiba ES-12E conductivity meter. The electrical conductivity of the effluent was above zero at the beginning of the experiment because of the sodium azide in the clay units. Once the contaminant solution was injected into the box, the electrical conductivity started to rise and reached a maximum value of 1.44 mS/cm on day 52. The contaminant source was switched with clean water on day 45.

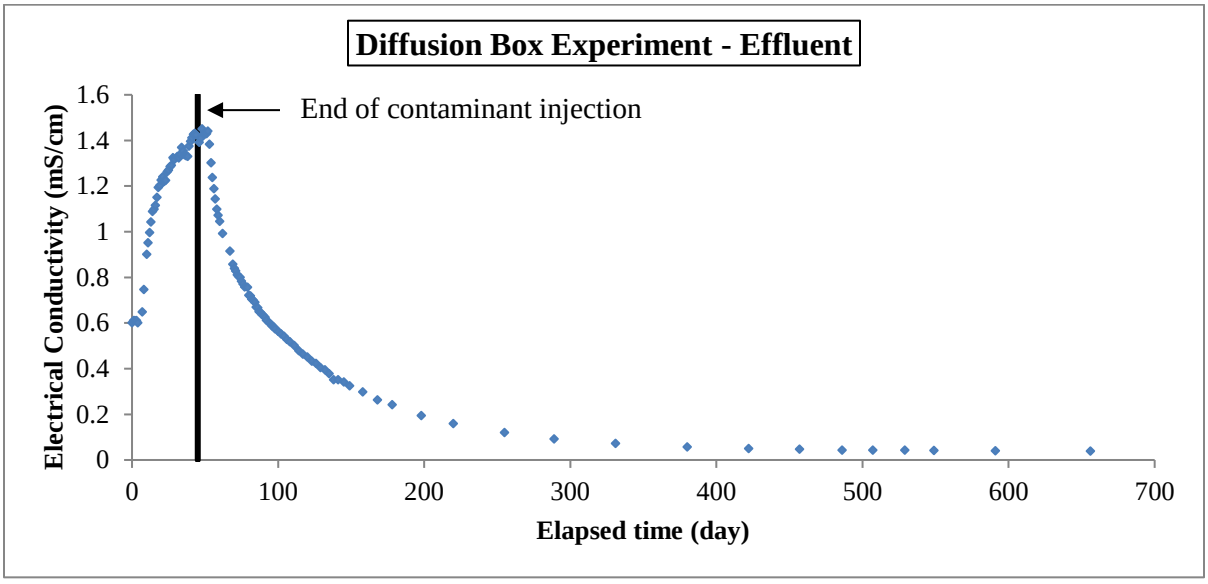

Appendix E

Data Table

Sorption Column Experiments

Borden Sand and GAC Column – Source							
Time (h)	TCE Concentration (mg/L)	Ave. $\delta^{13}C$ (‰)	STDEV	Ave. $\delta^{37}Cl$ (‰)	STDEV	Ave. $\delta^{2}H$ (‰)	STDEV
2	975.7	-31.1	0.2	-2.2	0.1	492	19
20	913.1			-2.1	0.1		
45	895.5			-1.9	0.1		
69	933.8			-2.0	0.1		
92	906.5	-31.1	0.5	-2.0	0.1	492	7
119	946.7			-2.2	0.1		
142	957.1			-2.5	0.1		
164	868.2			-2.0	0.0		
187	800.0			-2.4	0.0		
192	786.5	-31.2	0.5	-2.0	0.1	489	10

Port 1 Borden Sand and GAC Column					
Time (h)	TCE Concentration (mg/L)	Ave. $\delta^{13}C$ (‰)	STDEV	Ave. $\delta^{37}Cl$ (‰)	STDEV
3	156.0	-31.4	0.0	-1.3	0.1
22	635.4	-31.0	0.5	-1.3	0.0
47	754.8			-1.5	0.1
71	797.5			-1.9	0.0
94	827.5	-31.1	0.5	-2.1	0.1
121	897.4			-2.2	0.1
143	867.4	-31.2	0.5	-2.2	0.0
166	884.8			-2.3	0.1
189	852.0			-2.2	0.0
194	754.4	-31.2	0.5	-2.2	0.2
214	47.7	-30.6	0.0	-2.2	0.1
237	61.1			-2.5	0.1
260	38.2	-31.1	0.1	-2.2	0.1
288	22.9	-31.2	0.0	-2.4	0.1
333	16.4			-2.1	0.1
382	13.3	-31.2	0.5	-2.0	0.1

458	9.5	-31.2	0.5	-2.0	0.1
554	8.3			-1.8	0.1
672	7.4	-31.1	0.5	-2.2	0.1

Port 3 Borden Sand and GAC Column					
Time (h)	TCE Concentration (mg/L)	Ave. $\delta^{13}C$ (‰)	STDEV	Ave. $\delta^{37}Cl$ (‰)	STDEV
21	47.1			-0.8	0.0
46	91.9			-0.9	0.1
70	144.7	-30.7	0.5	-0.7	0.1
93	205.6	-30.8	0.0	-1.8	0.1
120	518.5	-30.5	0.5		
142	728.5	-30.4	0.5	-1.9	0.1
165	848.3	-30.7	0.5	-2.5	0.1
188	981.2			-2.0	0.0
193	760.3	-31.3	0.0	-1.8	0.1
213	587.5	-31.7	0.5	-1.9	0.1
236	395.9			-2.1	0.0
259	274.0	-31.5	0.5	-2.9	0.0
287	129.5			-2.2	0.0
332	85.3			-2.3	0.0
381	62.8	-31.6	0.2	-2.0	0.1
457	48.6	-31.4	0.5	-2.1	0.1
553	42.4			-1.8	0.1
671	35.5	-31.4	0.5	-2.0	0.1

Port 5 Borden Sand and GAC Column							
Time (h)	TCE Concentration (mg/L)	Ave. $\delta^{13}C$ (‰)	STDEV	Ave. $\delta^{37}Cl$ (‰)	STDEV	Ave. $\delta^{2}H$ (‰)	STDEV
2	1.0						
20	1.5			-0.6	0.1		
45	2.4			-0.5	0.1		
69	3.7	-30.5	0.5	-0.7	0.1		
92	5.9	-30.6	0.5	-1.2	0.0	359	
119	23.3	-30.6	0.4	-1.4	0.1	336	

142	89.9	-30.5	0.5	-1.6	0.1	326	
164	310.7	-30.2	0.5	-2.0	0.1	290	7
187	768.1			-2.1	0.1		
192	665.1	-30.3	0.0	-1.8	0.1	265	8
211	765.3	-30.4	0.5	-1.8	0.0		
235	699.8			-2.2	0.0	251	4
258	554.6	-30.5	0.5	-2.3	0.1		
286	325.9			-2.1	0.1	224	20
331	191.9	-30.5	0.0	-2.2	0.1	189	12
381	132.6	-31.0	0.5	-1.9	0.0		
456	88.1	-31.0	0.5	-2.0	0.1	171	13
552	71.6			-1.7	0.1		
669	58.1	-31.2	0.1	-1.9	0.1	131	5

Borden Sand and Ottawa Silica Sand Columns - Source					
Time (h)	TCE Conceentration (mg/L)	Ave. $\delta^{13}C$ (‰)	STDEV	Ave. $\delta^{37}Cl$ (‰)	STDEV
0	4.9	-28.7	0.0	1.3	0.0
20	4.4			1.2	0.1
37	5.3	-29.3	0.0	1.2	0.1
60	4.8	-29.2	0.5	1.2	0.0
80	5.2	-28.9	0.5	1.3	0.0
103	3.8	-29.0	0.5	1.4	0.1

Port 1 Borden Sand Column					
Time (h)	TCE Concentration (mg/L)	Ave. $\delta^{13}C$ (‰)	STDEV	Ave. $\delta^{37}Cl$ (‰)	STDEV
1	2.55				
24	5.55	-27.9	0.2	1.3	0.0
42	5.28	-27.5	0.5	1.3	0.1
63	5.20	-28.1	0.5	1.1	0.0
87	5.11	-27.9	0.5	1.5	0.0
106	4.46	-28.2	0.1	1.4	0.1
107	0.23	-26.8	0.5	1.5	0.1
128	0.15				
150	0.06				
171	0.05				

217	0.02				
313	0.02				
387	0.02				
527	0.01				

Port 11 Borden Sand Column					
Time (h)	TCE Concentration (mg/L)	Ave. $\delta^{13}C$ (‰)	STDEV	Ave. $\delta^{37}Cl$ (‰)	STDEV
1	0.01				
22	5.45	-27.8	0.5	1.2	0.1
40	5.50	-27.7	0.3	1.1	0.1
61	5.38	-28.1	0.5	1.2	0.2
84	5.35	-28.1	0.5	1.3	0.2
105	4.65	-28.0	0.5	1.5	0.0
107	4.51	-28.1	0.5	1.6	0.0
126	0.42	-28.0	0.5	1.3	0.1
148	0.21			1.1	0.1
171	0.11			0.9	0.1
216	0.04				
312	0.02				
387	0.02				
526	0.02				

Port 20 Borden Sand Column					
Time (h)	TCE Concentration (mg/L)	Ave. $\delta^{13}C$ (‰)	STDEV	Ave. $\delta^{37}Cl$ (‰)	STDEV
0	0.08				
20	0.14			1.0	0.1
37	5.16	-27.7	0.5	1.3	0.2
60	5.49	-28.0	0.0	1.3	0.2
80	5.26	-28.1	0.5	1.3	0.2
103	5.53	-27.9	0.5	1.3	0.2
106	4.97	-28.0	0.5	1.5	0.0
124	4.34	-27.6	0.3	1.5	0.2
145	0.50	-27.5	0.5	1.0	0.2
170	0.47			0.8	0.1
214	0.14			0.8	0.1

310	0.08			0.8	0.1
386	0.06				
525	0.06				

Borden Sand Column - Source					
Time (h)	TCE Concentration (mg/L)	Ave. $\delta^{13}C$ (‰)	STDEV	Ave. $\delta^{37}Cl$ (‰)	STDEV
0	4.9	-28.7	0.0	1.3	0.0
20	4.4			1.2	0.1
37	5.3	-29.3	0.0	1.2	0.1
60	4.8	-29.2	0.5	1.2	0.0
80	5.2	-28.9	0.5	1.3	0.0
103	3.8	-29.0	0.5	1.4	0.1

Port 1 Borden Sand Column					
Time (h)	TCE Concentration (mg/L)	Ave. $\delta^{13}C$ (‰)	STDEV	Ave. $\delta^{37}Cl$ (‰)	STDEV
1	2.55				
24	5.55	-27.9	0.2	1.3	0.0
42	5.28	-27.5	0.5	1.3	0.1
63	5.20	-28.1	0.5	1.1	0.0
87	5.11	-27.9	0.5	1.5	0.0
106	4.46	-28.2	0.1	1.4	0.1
107	0.23	-26.8	0.5	1.5	0.1
128	0.15				
150	0.06				
171	0.05				
217	0.02				
313	0.02				
387	0.02				
527	0.01				

Port 11 Borden Sand Column

Time (h)	TCE Concentration (mg/L)	Ave. $\delta^{13}C$ (‰)	STDEV	Ave. $\delta^{37}Cl$ (‰)	STDEV
1	0.01				
22	5.45	-27.8	0.5	1.2	0.1
40	5.50	-27.7	0.3	1.1	0.1
61	5.38	-28.1	0.5	1.2	0.2
84	5.35	-28.1	0.5	1.3	0.2
105	4.65	-28.0	0.5	1.5	0.0
107	4.51	-28.1	0.5	1.6	0.0
126	0.42	-28.0	0.5	1.3	0.1
148	0.21			1.1	0.1
171	0.11			0.9	0.1
216	0.04				
312	0.02				
387	0.02				
526	0.02				

Port 20 Borden Sand Column					
Time (h)	TCE Concentration (mg/L)	Ave. $\delta^{13}C$ (‰)	STDEV	Ave. $\delta^{37}Cl$ (‰)	STDEV
0	0.08				
20	0.14			1.0	0.1
37	5.16	-27.7	0.5	1.3	0.2
60	5.49	-28.0	0.0	1.3	0.2
80	5.26	-28.1	0.5	1.3	0.2
103	5.53	-27.9	0.5	1.3	0.2
106	4.97	-28.0	0.5	1.5	0.0
124	4.34	-27.6	0.3	1.5	0.2
145	0.50	-27.5	0.5	1.0	0.2
170	0.47			0.8	0.1
214	0.14			0.8	0.1
310	0.08			0.8	0.1
386	0.06				
525	0.06				

Port 1 Ottawa Silica Sand Column

Time (h)	TCE Concentration (mg/L)	Ave. $\delta^{13}C$ (‰)	STDEV	Ave. $\delta^{37}Cl$ (‰)	STDEV
24	5.20				
42	5.47	-28.9	0.1	1.4	0.0
63	5.00	-28.7	0.5	1.4	0.0
84	5.04	-28.2	0.5	1.4	0.2
102	4.42	-29.1	0.5	1.5	0.2
103	0.25			0.3	0.2
123	0.07				
144	0.05				
165	0.04				
210	0.02				
305	0.02				
379	0.02				
519	0.01				

Port 11 Ottawa Silica Sand Column					
Time (h)	TCE Concentration (mg/L)	Ave. $\delta^{13}C$ (‰)	STDEV	Ave. $\delta^{37}Cl$ (‰)	STDEV
1	0.01				
22	4.32	-28.2	0.5		
40	5.21	-28.8	0.5	1.39	0.06
61	5.18	-28.7	0.5	1.52	0.04
82	5.20	-28.3	0.5	1.27	0.20
101	4.75	-29.2	0.5		
103	4.32				
122	0.14	-29.3	0.1	0.69	0.20
142	0.12				
165	0.05				
209	0.02				
304	0.02				
379	0.01				
518	0.02				

Port 20 Ottawa Silica Sand Column					
Time (h)	TCE Concentration (mg/L)	Ave. $\delta^{13}C$ (‰)	STDEV	Ave. $\delta^{37}Cl$ (‰)	STDEV
0	0.01				
20	0.01				
37	4.21	-28.6	0.5	1.6	0.1
60	5.20	-28.3	0.0	1.1	0.2
80	5.07	-29.1	0.5	1.0	0.1
100	5.08		0.5	1.5	0.0
102	4.62	-28.9	0.5	1.0	0.1
120	2.76	-28.0	0.0	1.4	0.1
140	0.22			1.4	0.2
164	0.23				
208	0.06				
303	0.04				
378	0.03				
517	0.02				

Sorption Batch Experiments

Controls					
Time (h)	TCE Concentration (mg/L)	Ave. $\delta^{37}Cl$ (‰)	STDEV	Ave. $\delta^{2}H$(‰)	STDEV
0	1.99	3.57	0.04	501	10
240	1.86	3.57	0.20	490	10
480		3.56	0.21	489	8
720	2.03	4.32	0.17	509	10
1440	2.03	3.50	0.08	497	10

Controls			
Time (h)	cis-DCE Concentration (mg/L)	Ave. $\delta^{37}Cl$ (‰)	STDEV
0	2.19	-0.09	0.08
240	2.18	0.00	0.20
480		0.00	0.05
720	2.27	-0.13	0.20
1440	2.30	0.04	0.04

Sorption Batch Experiment (Shale and TCE)							
Time (h)	TCE Concentration (mg/L)	Ave. $\delta^{13}C$ (‰)	STDEV	Ave. $\delta^{37}Cl$ (‰)	STDEV	Ave. $\delta^{2}H$(‰)	STDEV
0	2.022	-27.6	0.5	3.9	0.1	400	1
0.5	1.529	-27.3	0.5	3.9	0.1	362	20
2	1.502	-27.3	0.0	4.0	0.0	378	7
6	1.643	-27.3	0.5	3.9	0.1	377	20
24	1.568	-27.6	0.5	3.7	0.1	376	4
48	1.642	-27.3	0.5	4.0	0.1	353	6
72	1.701	-27.4	0.5	3.9	0.1	358	2
120	1.547	-27.4	0.5	3.9	0.0	343	20
168	1.311	-27.2	0.1	4.0	0.1	375	20
240	1.016	-26.8	0.5	3.9	0.1	345	42
336	1.038	-26.3	0.5	4.1	0.1	350	20
480	0.998	-25.9	0.5	4.3	0.0	347	20
840	0.738	-26.2	0.5	4.7	0.1	309	20
1440	0.941	-26.1	0.0	4.7	0.1	313	20

Sorption Batch Experiment (Shale and TCE)					
Time (h)	TCE Concentration (mg/L)	Ave. $\delta^{37}Cl$ (‰)	STDEV	Ave. $\delta^{2}H$(‰)	STDEV
0	11.6	1.7	0.2	513	6
0.5	7.8	1.8	0.0		
2	6.3	1.7	0.0		
6	7.6	1.7	0.1		
24	7.0	1.7	0.0	499	8
48	6.7	1.8	0.2		
72	7.2	1.7	0.1	486	11
120	6.5	1.7	0.0	476	5
168	7.3	1.8	0.0		
240	2.8	1.9	0.2	471	8
336		2.0	0.1	456	10
480	5.1	1.9	0.1	440	2
720	5.1	1.7	0.0	438	10
1440	2.6	1.6	0.0	377	10

Sorption Batch Experiment (Dolostone and TCE)					
Time (h)	TCE Concentration (mg/L)	Ave. $\delta^{37}Cl$ (‰)	STDEV	Ave. $\delta^{2}H$(‰)	STDEV
0	2.7	1.6	0.1	497	11
0.5	1.7	1.8	0.0		
2	1.6	2.0	0.1		
6	1.4	2.0	0.1		
24	1.4	2.0	0.0	400	16
48	1.4	1.9	0.0		
72	1.4	2.0	0.1	431	4
120	1.4	1.8	0.0	406	20
168	1.3	1.8	0.0	441	20
240	1.5	1.7	0.0	376	16
336	1.3	1.7	0.1	346	20
480	1.2	1.6	0.1	325	20
720	1.2	1.8	0.0	261	42
1440	1.2	1.7	0.0	133	20

Sorption Batch Experiment (Dolostone and TCE)					
Time (h)	TCE Concentration (mg/L)	Ave. $\delta^{37}Cl$ (‰)	STDEV	Ave. $\delta^{2}H$(‰)	STDEV
0	11.9	1.7	0.2	524	8
0.5	8.8	1.9	0.1		
2	9.5	1.7	0.1		
6	7.4	1.9	0.0		
24	2.9	2.0	0.2	484	20
48	6.7	1.8	0.0		
72	8.8			519	20
120	7.8	1.8	0.0	520	10
168	7.4	1.8	0.0	511	12
240	4.3	1.8	0.0	477	6
336		1.7	0.1	457	20
480	6.4	1.8	0.1	482	13
720	5.4	1.7	0.2	462	18
1440	3.5	1.5	0.1	356	11

Sorption Batch Experiment (Shale and cis-DCE)							
Time (h)	cis-DCE Concentration (mg/L)	Ave. $\delta^{13}C$ (‰)	STDEV	Ave. $\delta^{37}Cl$ (‰)	STDEV	Ave. $\delta^{2}H$(‰)	STDEV
0	1.8	-21.9	0.0	0.2	0.2	757	11
0.5	1.5	-22.2	0.5	0.1	0.2		
2	1.4	-22.0	0.5	0.0	0.1		
6	1.4	-22.1	0.5	0.2	0.1		
24		-21.8	0.5	0.4	0.2		
48	1.4	-21.5	0.5	0.4	0.2	751	10
72	1.4	-21.7	0.5	0.4	0.1	744	10
120	1.3	-21.7	0.5				
168	1.2	-21.5	0.5	0.2	0.1	733	1
240	1.2	-21.6	0.5	0.3	0.1	735	10
336	1.2	-22.0	0.0				
480	1.2	-21.7	0.5	0.1	0.1	744	10
720	1.3	-21.7	0.0	0.1	0.1	745	3
1464	1.2			0.2	0.0	736	9

Sorption Batch Experiment (Dolostone and cis-DCE)					
Time (h)	cis-DCE Concentration (mg/L)	Ave. $\delta^{37}Cl$ (‰)	STDEV	Ave. $\delta^{2}H$(‰)	STDEV
0.5	1.7	0.15	0.0	728	1
2	1.6	0.11	0.0		
6	1.6	0.10	0.0		
24	1.6	0.09	0.0	740	5
48	0.0				
72	1.6	0.08	0.0	745	20
120	1.6	0.08	0.1	736	2
168	1.6	0.01	0.1	727	20
240	1.5	0.15	0.0	723	20
336	1.9	-0.02	0.1	735	0
480	1.9	-0.02	0.0	733	20
720	1.8	0.06	0.1	733	5
1440	1.7	0.05	0.0	728	20

Controls for Borden Sand and GAC Experiment					
Time (h)	TCE Concentration (mg/L)	Ave. δ37Cl (‰)	STDEV	Ave. δ2H(‰)	STDEV
0	269.9	-4.36314	0.2	536	2
69	233.8	-4.23202	0.2		
119	232.0	-4.01828	0.2	546	20
164	224.0	-4.48121	0.2	520	10
192	225.2	-4.29942	0.08371	524	13

Sorption Batch Experiment (Borden sand and GAC)					
Time (h)	TCE Concentration (mg/L)	Ave. $\delta^{37}Cl$ (‰)	STDEV	Ave. $\delta^{2}H$(‰)	STDEV
22	40.5	-3.76	0.20	563	20
48	23.1	-3.54	0.20	550	20
73	18.5	-3.56	0.24	553	0.5
92	13.7	-4.00	0.16	552	20
124	12.2	-3.88	0.09	549	20
146	8.1	-3.39	0.13	554	6
170	3.9	-4.13	0.07	550	20
196	3.3	-3.89	0.09	563	20
263	1.3	-4.29	0.07	599	20
287	0.9	-4.15	0.09	545	20
335	0.9	-4.27	0.02	562	20
408	1.6	-4.40	0.02	547	20
986	1.9	-4.37	0.02	590	20

Back-diffusion Batch Experiment

Back-diffusion Batch Experiment (Shale and TCE)					
Time (h)	TCE Concentration (mg/L)	Ave. $\delta^{37}Cl$ (‰)	STDEV	Ave. $\delta^{2}H$(‰)	STDEV
0	14.44	2.64	0.12	362	20
1	0.02	3.16	0.24		
72	0.04	1.59	0.37		
168	0.11	1.43	0.02		
336	0.26	1.98	0.09		
504	0.36	1.99	0.01		
840	0.67	2.15	0.07	76	20

1176	0.78	2.07	0.19	163	20
1512	0.75	2.02	0.01	304	20
1920	0.67	2.35	0.20	192	20
2304	0.60	2.60	0.05	302	20

Back-diffusion Batch Experiment (Shale and cis-DCE)					
Time (h)	cis-DCE Concentration (mg/L)	Ave. $\delta^{37}Cl$ (‰)	STDEV	Ave. $\delta^{2}H$(‰)	STDEV
0	7.94	-0.22	0.10	830	4
1	0.04				
72	0.03				
168	0.09	-1.54	0.12		
336	0.18	-1.02	0.14	739	1
504	0.27	-0.61	0.01	740	5
840	0.14	-0.34	0.11	735	7
1176	0.49	0.17	0.02	724	0
1512	0.42	0.06	0.03	723	20
1872	0.38	0.63	0.02	740	30
2232	0.41	0.37	0.04	739	13

Back-diffusion Batch Experiment (Dolostone and TCE)					
Time (h)	TCE Concentration (mg/L)	Ave. $\delta^{37}Cl$ (‰)	STDEV	Ave. $\delta^{2}H$(‰)	STDEV
0	30.74	2.57	0.13	370	20
1	0.00	2.73	0.46		
72	0.31	1.45	0.44		
168	0.49	2.16	0.10		
336	0.50	2.35	0.06		
504	0.25	1.99	0.03	369	20
840	0.52	1.94	0.04	212	20
1176	0.62	2.18	0.11	339	20
1512	0.85	2.60	0.09	326	20
1848	0.81	2.36	0.09	173	20
2184	0.86	2.43	0.01	259	20

Back-diffusion Batch Experiment (Dolostone and cis-CE)					
Time (h)	cis-DCE Concentration (mg/L)	Ave. $\delta^{37}Cl$ (‰)	STDEV	Ave. $\delta^{2}H$(‰)	STDEV
0	7.97	-1.87	0.08	765	18
1	0.12				
72	0.03				
168	0.07				
336	0.14	-2.02		758	20
504	0.19	-2.15	0.04	737	4
840	0.29	-1.37	0.06	757	1
1176	0.32			740	2
1512	0.31	-1.12	0.14	731	5
1848	0.34	0.44	0.04	754	3
2184	0.35	-0.21	0.12	757	11

Diffusion Box Experiment

Time (day)	cis-DCE (source) mg/L	TCE (Source) mg/L
0	101.1	67.6
9	98.5	63.7
20	94.1	57.9
29	91.7	52.8
39	78.9	43.3

Time (day)	cis-DCE (Effluent) mg/L	TCE (Effluent) mg/L
0.0	0.0	0.0
5.0	0.0	0.0
7.0	6.8	4.5
9.0	17.8	12.3
13.0	35.2	23.6
17.1	38.1	26.0
21.0	40.1	26.8

25.1	46.5	31.0
29.0	49.1	32.0
33.1	52.6	33.9
37.1	51.8	32.7
41.0	56.4	35.0
45.0	60.1	35.3
47.0	44.3	25.9
51.1	46.9	26.0
55.0	33.2	18.8
59.1	31.1	16.8
62.0	25.7	13.7
67.1	23.7	12.2
71.0	19.6	9.8
75.1	18.0	8.3
77.0	16.3	7.5
81.1	15.6	6.9
86.1	15.6	7.3
92.1	12.5	5.0
100.1	10.9	4.3
106.0	10.3	4.0
111.1	10.7	4.0
117.1	10.4	3.8
123.1	9.8	3.5
129.1	9.2	3.3
135.0	9.5	3.4
141.1	8.5	3.0
149.1	7.9	2.8
158.1	6.8	2.5
168.3	6.4	2.4
178.0	6.6	2.6
188.0	5.1	2.1
198.0	4.4	1.9
207.1	4.0	1.8
219.0	3.1	1.8
233.0	2.6	1.5
247.0	2.5	1.5
261.1	2.0	1.3
303	1.5	1.1

331.0	1.1	0.9
359.0	0.8	0.7
380.0	0.7	0.7
408	0.6	0.6
436	0.5	0.6
457	0.3	0.4
493	0.2	0.4
528	0.2	0.4
563	0.1	0.2
599	0.1	0.2
655	0.1	0.2
698	0.0	0.1
714	0.0	0.2

Time (day)	Cl^- (mg/L)	Br^- (mg/L)
0	0.8	0.5
2	0.8	0.0
4	0.8	0.5
4.5	0.8	0.6
5	0.8	0.6
6	1.9	1.2
7	3.2	4.9
8	4.9	8.9
9	13.6	19.2
10	17.0	21.0
11	18.4	23.4
12	22.0	26.8
13	24.3	28.9
14	26.5	31.0
15	28.0	32.6
17	30.0	33.9
18	31.4	35.2
19	32.7	36.3
20	33.8	37.7
21	35.3	39.1
22	36.0	39.8

23	37.1	41.0
24	37.3	41.2
25	38.8	42.7
26	39.6	43.4
27	40.4	44.3
28	41.4	45.6
29	42.4	46.2
30	42.3	46.6
31	43.7	47.7
32	44.4	48.6
33	45.0	49.4
34	45.4	49.8
35	45.9	50.2
36	47.1	51.0
37	47.5	51.6
38	47.8	52.2
39	48.6	52.8
41	49.4	53.0
43	49.7	53.6
45	51.4	55.4
48	52.3	56.2
49	53.4	57.3
51	53.7	57.7
53	51.3	55.4
55	45.6	49.9
57	41.8	46.2
59	38.7	42.9
62	37.1	41.4
67	30.7	34.7
69	29.8	33.8
71	28.8	32.9
73	27.5	31.5
77	26.0	29.8
79	25.1	28.8
81	24.4	28.0
84	22.6	26.8
87	21.5	25.6
90	20.6	24.5

93	19.6	23.4
96	18.8	22.3
100	17.8	21.3
104	16.8	20.3
108	15.8	18.7
111	15.0	18.0
114	14.6	17.1
117	14.2	16.5
120	13.3	15.7
123	12.7	14.9
126	12.2	14.2
129	11.6	13.5
132	11.1	13.0
135	10.8	12.2
141	9.7	10.6
149	9.4	10.1
158	8.2	8.6
168	6.6	7.0
178	5.6	6.0
188	5.7	5.6
198	3.9	4.1
207	3.3	3.4
219	2.6	2.5
234	2.4	2.3
247	1.9	1.8
261	1.5	0.0
303	0.9	0.0
331	0.7	0.0
359	0.5	0.0
380	0.4	0.0
409	0.4	0.0
437	0.8	0.0

	TCE (Source)	
Time (day)	$\delta^{37}Cl$ (‰)	$\delta^{37}Cl$ (Repeat) (‰)
0	-2.85	-3.05
9	-3.17	
21	-3.19	
29	-3.12	-3.02
41	-2.33	-2.30

	TCE (Source)	
Time (day)	$\delta^{2}H$ (‰)	$\delta^{2}H$ (Repeat) (‰)
0	460	467
9	479	495
21	492	
29	495	515
41	528	548

	cis-DCE (Source)	
Time (day)	$\delta^{37}Cl$ (‰)	$\delta^{37}Cl$ (Repeat) (‰)
0	0.86	
9	0.85	0.96
21	0.79	0.84
29	0.99	0.88
41	1.24	1.10

	cis-DCE (Source)	
Time (day)	$\delta^{2}H$	$\delta^{2}H$ (Repeat) (‰)
0	631	623
9	632	647
21	642	
29	671	676
41	690	697

	TCE (Effluent)	
Time (day)	$\delta^{37}Cl$ (‰)	$\delta^{37}Cl$ (Repeat) (‰)
7	-1.59	-1.84
9	-1.39	-1.13
13	-1.74	-1.76
17	-1.69	-1.88
21	-1.40	-1.48
25	-1.41	-1.43
29	-1.22	-1.27
33	-1.32	-1.47
37	-1.08	-0.96
41	-2.48	-2.84
45	-1.33	-1.24
47	-2.39	-2.33
51	-1.56	-1.58
55	-1.64	
59	-2.99	-2.84
62	-2.02	

67	-2.19	-1.90
71	-1.48	
75	-2.05	-1.78
81	-2.03	
100	-2.56	-2.50
106	-3.10	
117	-2.70	-2.49
123	-3.02	
129	-2.59	-2.66
135	-3.40	
141	-3.58	-3.37
149	-2.97	
168	-2.19	-2.42
198	-2.34	-2.62
219	-3.17	-3.15
247	-3.93	-3.80
275	-3.14	-3.08
303	-2.82	-2.81
331	-3.89	-3.60
359	-3.59	-3.83
380	-3.37	-3.37
408	-3.22	-3.28
457	-3.71	-3.49
493	-3.06	-3.44
528	-3.67	-3.39
556	-3.50	-3.44
585	-3.56	-3.41
599	-3.50	-3.57
627	-3.49	-3.45
641	-3.64	-3.44
650	-3.99	-3.64
685	-3.73	-3.93

	cis-DCE (Effluent)	
Time (day)	$\delta^{37}Cl$ (‰)	$\delta^{37}Cl$ (Repeat) (‰)
7	2.66	
9	2.98	2.88

13	1.89	
17	1.73	
21	1.71	1.74
25	1.05	1.14
29	1.68	1.77
33	1.07	1.35
37	1.55	
41	1.45	
45	1.72	1.65
47	1.42	
51	1.53	1.45
55	1.11	
59	1.01	0.70
62	1.00	
67	0.90	0.78
71	0.88	
75	0.95	0.79
81	0.91	
87	0.71	0.64
100	0.09	
123	0.34	0.46
141	1.23	1.00
168	0.69	
198	0.50	0.65
219	0.80	
247	0.66	
275	1.12	
303	1.41	
331	1.26	1.29
359	1.02	1.12
380	1.50	
408	1.48	
436	1.82	
457	1.90	
490	1.85	
528	1.77	
556	1.75	1.84
585	1.65	1.64

599	1.07	0.87
627	0.87	
641	1.41	1.04
650	1.18	

	TCE (Effluent)	
Time (day)	δ^2H (‰)	δ^2H (Repeat) (‰)
9	436	428
13	446	
17	471	
19	440	451
21	464	
25	507	552
29	483	498
33	508	
37	534	
41	544	
45	469	468
47	486	
49	561	582
51	538	
55	566	
59	586	
62	639	602
67	551	
71	535	
75	560	
81	554	
87	568	563
100	576	559
123	558	573
141	568	574
168	543	527
194	531	
219	558	527
247	541	525

275	537	541
303	538	
331	491	537
359	555	512
379	538	532
407	531	
456	521	522
492	521	527
527	527	
553	498	512
585	518	
598	519	
626	549	
640	541	549
649	549	

	cis-DCE (Effluent)	
Time (day)	δ^2H (‰)	δ^2H (Repeat) (‰)
9	626	597
13	610	
17	618	596
19	603	606
21	638	
25	663	
29	663	665
33	656	
37	658	
41	667	
45	618	622
47	716	
49	677	684
51	655	659
55	686	
59	799	
62	767	771
67	737	
71	773	

75	711	
81	720	
87	703	709
100	689	662
123	680	704
141	670	686
168	640	642
194	680	673
219	690	688
247	694	703
275	697	697
303	701	
331	708	690
359	692	
380	746	728
408	735	
457	731	723
493	740	
528	767	
556	709	704
585	734	
599	745	
627	728	
641	770	745
650	750	